THERMAL CONTACT RESISTANCE IN A VACUUM ENVIRONMENT

DEPARTMENT OF MECHANICAL AND INDUSTRIAL ENGINEERING
URBANA, IL

1963

ENGINEERING EXPERIMENT STATION
DEPARTMENT OF MECHANICAL
AND INDUSTRIAL ENGINEERING
ME-T -242-1

THERMAL CONTACT RESISTANCE IN A VACUUM ENVIRONMENT

by
A. M. CLAUSING and B. T. CHAO

Research Sponsored by
NATIONAL AERONAUTICS AND SPACE ADMINISTRATION
under Grant NsG-242-62

UNIVERSITY OF ILLINOIS
URBANA, ILLINOIS
AUGUST, 1963

ME TECHNICAL REPORT 242-1 August, 1963

THERMAL CONTACT RESISTANCE IN A VACUUM ENVIRONMENT

by

A. M. Clausing and B. T. Chao

RESEARCH GRANT NO.

NASA NsG-242-62

Department of Mechanical and Industrial Engineering
Engineering Experiment Station
University of Illinois
Urbana, Illinois

ACKNOWLEDGEMENT

The authors wish to express their sincere appreciation of the financial support of the National Aeronautics and Space Administration under Research Grant NsG-242-62.

The authors also thank Mr. D. R. Jeng who built and operated the conductive-liquid analog, Mr. M. P. Moriarty who helped in preparing the test specimens, and the shop personnel of the Department of Mechanical and Industrial Engineering for the construction of the experimental apparatus. During the course of the investigation, the authors had, on several occasions, the privilege of discussing the problem with Dr. J. M. F. Vickers of the Jet Propulsion Laboratory of Pasadena, California.

The material in this report is a dissertation submitted in partial fulfillment of the requirements for the Ph. D. degree at the University of Illinois by Dr. A. M. Clausing. This thesis was written under the direction of Dr. B. T. Chao.

ABSTRACT

A survey of the literature on thermal contact resistance reveals that there is a dearth of adequate information and that considerable discrepancy exists between known theories and experimental data. An attempt is thus made to inquire into the physical nature of such resistance and to seek explanations for the many apparent contradictions. A new model is proposed and a restrictive analysis is given which leads to a satisfactory prediction of the thermal contact resistance for engineering surfaces in a vacuum environment. Limitations of the proposed model are discussed.

For the title problem, radiative transfer and interstitial conduction are shown not to be of importance; metal-to-metal conduction is the dominating mechanism. The resistance to heat flow due to imperfect interfacial contact is conceived to consist of three resistances in series, namely, the film resistance, the microscopic constriction resistance and the macroscopic constriction resistance. It is demonstrated that, for many surfaces commonly encountered in engineering practice, the macroscopic constriction has a commanding influence. It is under the latter condition that the present analysis is carried out, and, in this sense, the theory is restrictive. Nevertheless, the results obtained have thrown considerable light on the physics of the overall problem.

The experimental technique used in the investigation and some of the common pitfalls are described and discussed in detail. Extensive results are given for brass, magnesium, stainless steel and aluminum surfaces showing the effects of material properties and the degree of conformity of mating surfaces. Limited results are presented to show the influence of surface films,

10144

surface roughness, annealing, creep, environmental gas pressure, additional interstitial material, etc. Good agreement between the measured and predicted values has been found over wide ranges of the applied load and other system variables.

AUTHOR

TABLE OF CONTENTS

1. INTRODUCTION

It has long been an acknowledged fact that the interface formed by two members in contact represents an additional resistance to the flow of heat from one member to the other. Until recent years little attention was given to this problem. The recent publications on the subject are concerned mainly with the experimental determinations of such resistance in the presence of a conducting fluid. Many of these are prompted by the technological application in nuclear power reactors where an extremely large heat flux passes from the fuel element to its sheath; thus, even a moderate contact resistance could cause a large, undesirable temperature drop.

Literature on thermal contact resistance in a vacuum is extremely scarce. This is somewhat surprising considering: a) the greater importance of such resistance in the absence of a conducting fluid, b) the vast research effort being conducted on problems connected with thermal design of space vehicles, and c) the advantage this approach offers in developing an understanding of the physics of thermal contact resistance.

The technical importance of thermal contact resistance can be readily realized by examining Figure 1. This figure illustrates two aluminum plates of 1/2" thickness in contact under a pressure of 30 psi. The two outer surfaces of the plates are held at temperatures of 100 and 0° F as shown. The heat flow is one-dimensional. Using representative values of interface conductance from data reported in literature [7, 22],* the heat flux (q) and the temperature drop across the interface (ΔT) have been calculated and are listed in the table of Figure 1. Three cases are being considered:

* Numbers in brackets, [ ], indicate references listed in the Bibliography

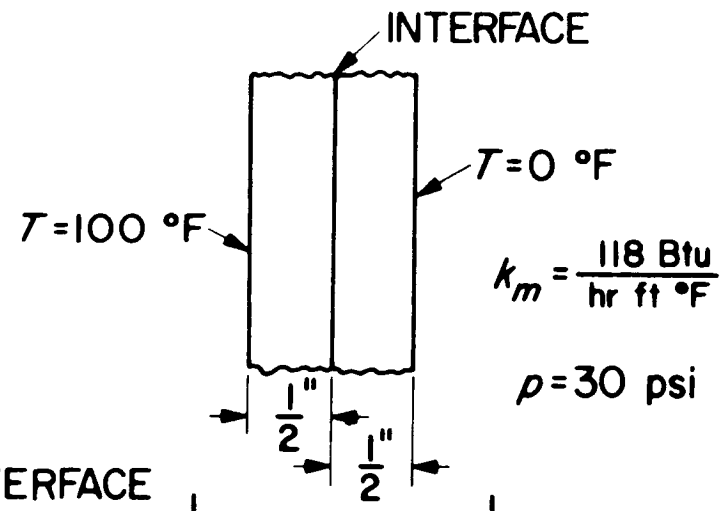

	INTERFACE CONDUCTANCE $\frac{\text{Btu}}{\text{hr ft}^2 \text{ °F}}$	HEAT FLUX $\left(\frac{\text{Btu}}{\text{hr ft}^2}\right)$	TEMPERATURE DROP ACROSS INTERFACE (°F)
NEGLECTING CONTACT RESISTANCE	———	142,000	———
INTERFACE IN AIR	900	55,000	61
INTERFACE IN VACUUM	90	8,500	94

FIGURE 1 THE SIGNIFICANCE OF THERMAL CONTACT RESISTANCE

a) neglecting the contact resistance due to the interface;

b) assuming the interface is in air, i.e., the voids due to the surface roughness and waviness are filled with air; and

c) assuming the interface is in vacuum.

The heat flux through the plates in vacuum is only six per cent of the amount which would flow through them if the interface resistance were neglected. Of the 100° F temperature drop across the members, 94° F occurs at the interface. Although the accuracy and suitability of the data used is questionable, it does demonstrate the magnitude of the problem, especially in a vacuum environment. This is particularly true considering the large number of joints which often exist in the heat flow path between the source and sink in a space vehicle or in other types of apparatus. Welded or brazed joints would alleviate the problem; however, since many of the joints frequently have to be broken during normal handling of the components, they cannot always be fabricated in this manner. Thus, this problem is of paramount importance if efficient heat transfer is to be obtained and accurate predictions of temperature levels are to be made. Reliability of a space vehicle greatly depends on accurate thermal design. Elaborate analyses of radiating fin profiles would have little practical value if the resistance of internal heat paths is not accurately known. Likewise, realistic design of thermal switches is impossible without a better understanding of thermal contact resistance.

With the meager amount of data and analysis available in literature, the mechanisms involved and the important variables of the problem were very dubious. The objective of this investigation is, as has been stated in the thesis proposal, to perform a predominantly experimental study of the nature of thermal contact resistance with the aim of clarifying the mechanism involved and obtaining a model by which such resistance can be predicted. Emphasis has thus

been placed on obtaining accurate data from planned experiments in accordance with the said objective.

A brief review of the published studies is given in Chapter 2. The literature is divided into two parts: the studies concerned predominantly with thermal contact resistance in the presence of a conducting fluid, and those pertaining to a vacuum environment. Chapter 3 presents a general discussion of the mechanism of heat transfer at an interface. Included is an analysis of the relative importance of radiation and interstitial conduction in comparison with metal-to-metal conduction.

Chapter 4 presents the proposed model for the prediction of thermal contact resistance. The approach is quite foreign to the prevailing studies reported in the literature. Emphasis is placed on the analysis of the macroscopic constriction resistance and evidence is given to support the view. This resistance has previously been grossly overlooked; however, it appears to be dominating in many cases.

Chapter 5 gives a description of the experimental apparatus and procedure along with a discussion of the measurement accuracy. Chapter 6 gives the experimental results and compares them with theoretical predictions. Chapter 7 presents a critical comparison between published studies and the present analysis. The theoretical models and experimental results are compared and discussed.

The conclusions drawn from this study are summarized in Chapter 8. Chapter 9 gives some recommendations for future extensions of this investigation.

2. REVIEW OF LITERATURE

A search of the literature shows that the study of thermal contact resistance is a relatively recent undertaking. Almost all literature available on this problem has been published during the last fifteen years. The majority of these studies were for joints in a conducting fluid; therefore, the fluid in the interstices also provided a path for the conduction of heat across the interface. The conduction of heat through this interstitial fluid is often large or dominating; thus, the problem is vastly different from the one being studied. However, if close attention is given to this difference, it is believed that much can be learned from the trends reported and methods employed in these studies. Hence literature of this category will be reviewed.

2.1 LITERATURE ON THE STUDY OF THERMAL CONTACTS IN THE PRESENCE OF A CONDUCTING FLUID.

One of the early experimental analyses of contacts in air was presented by Brunot and Buckland [14]. Tests were made with two types of two inch square steel test specimens. One consisted of solid blocks and the other, laminated blocks. The laminations were perpendicular to the contact surface. The effect of placing cement and shims of steel and aluminum between the specimens was also studied. The contact resistance was reported as a function of the contact pressure which was varied between 0 and 300 psi. Data were reported for a wide range of surface finishes.

Weills and Ryder [61] made an experimental study of the thermal contact resistance with the objective of improving the prediction of metal temperatures in aircraft engines. The joints were formed from steel, aluminum and bronze.

The contact pressure ranged from 2 to 8000 psi. The temperature at the interface ranged from 300 to 500°F and the temperature drop across the interface from 1 to 100°F. Both rough surfaces (70 to 90 microinches rms) and smooth surfaces (3 to 16 microinches rms) were investigated. Some hysteresis-like variations of thermal contact resistance with apparent contact pressure were indicated.

Kouwenhoven and Potter [39] conducted a group of experiments investigating the thermal resistance between steel surfaces in air. The thermal resistance results are reported at two temperature levels for pressures ranging from 195 to 2055 psi. The high temperature tests were conducted in an argon atmosphere in order to eliminate oxidation of the surfaces. In all tests one specimen had a 3 microinch rms surface roughness. The other specimen's roughness ranged from 3 to 4150 microinches rms. The authors concluded that the thermal resistance decreased with pressure in a manner which was essentially exponential, but for very smooth surfaces, it was almost independent of pressure. At constant pressure and in the absence of corrosion, the contact resistance was essentially constant as the temperature was increased; however, reported data showed an increase in contact resistance with increasing temperature. This is an apparent contradiction of the data reported elsewhere [6, 7] and the models presented in the literature.

Centinkale and Fishenden [16] made a theoretical and experimental investigation of thermal contacts in air. In their analysis, the microscopic contact areas were assumed to be evenly distributed and formed by cylinders of radius a. The heat channel associated with each contact point was taken as a coaxial cylinder of radius b. A fluid of conductivity k_f was assumed to be present in the voids of uniform thickness, δ. The steady-state temperature distribution was obtained by the relaxation method. Using these results, an equation was developed for the interface conductance. Several parameters in

this equation were then determined from experimental data. These parameters contained the constriction ratio a/b and the gap thickness δ. Their experimental data were not reported; however, they stated that the parameters were found to be independent of the nature of the metal or fluid and were constant for a given type of surface roughness. The actual contact area employed in their analysis was determined from the Meyer hardness and the relationship $p_a/H = A_s/A_a$. The materials they investigated were steel, brass and aluminum which were ground to various degrees of roughness. Air, spindle oil and glycerol were utilized as the interstitial material.

Barzelay, et al., reported a considerable amount of experimental data on thermal contact resistance. Their specific area of interest was aircraft structural joints. In Ref. [6] the effects of heat flow, temperature drop, temperature level, and surface conditions were studied. In all tests the contact pressure was kept at a constant value of approximately 7 psi. The materials employed were either stainless steel (AISI 416) or aluminum (75ST6). In several tests the contact surfaces were separated by foil or insulating sheets. Several were joined by strength-giving bonds. The surface roughness ranged from 12 to 120 microinches rms, and the mean temperature of the interface ranged from approximately 200 to 500°F.

In a later report by Barzelay, et al. [7], the work was extended to include the effect of pressure on thermal conductance. The pressure was varied from 5 to 425 psi. The specimen materials, range of surface finish, and range of mean interface temperature were all similar or identical to the previous report. In some instances it was found that warping influenced the conductance far more pronouncedly than either roughness or initial flatness. For smooth and flat surfaces the interface conductance values varied widely with minute changes in the matching configuration. Many data were given showing the effects of the

various parameters.

Barzelay and Holloway [8, 9] performed several experimental studies of thermal contact resistance in riveted aircraft joints. The results are highly specific and of less value for the analysis and understanding of the problem. Considerable scatter was experienced in interface conductance measurements. The scatter was found to be largest in the thin-skin configurations. It occurred not only from specimen to specimen, but also from one test run to the other, even during a given test of short duration. Warping of the skin and stringer was observed visually and was probably the source of much of the reported scatter. An extension of these investigations was also given at a much later date by Barzelay [10]. The specimens tested were aluminum alloy and high temperature alloy structural joints consisting of a stringer joined to a skin surface. Detailed data were given for the characteristics of the thermal contact resistance of more than 100 specimens.

Boeschoten and Van der Held [12] made an analysis in which an endeavor was made to separate the interface conductance into two parts: that due to the interstitial gas, and that due to the points of metallic contact. Interface conductance values were reported for aluminum-aluminum, aluminum-steel, and aluminum-uranium interfaces. The gap between the surfaces was filled with air, helium or hydrogen at gas pressures varying between 1 and 750 mm Hg. Varying gas pressures were reported only for one contact pressure of 35 kg/cm^2. In addition, data were given for contact pressures of 1, 6, and 70 kg/cm^2 at atmospheric pressure. The surface roughness was about 10 microns and the interface temperature was approximately 150°C. Some oils also were introduced in the joints to obtain more data for the analysis of the interstitial heat conduction. In their model, the contact areas were assumed to be uniformly

distributed, circular contacts of radius a_s formed by the plastic deformation of the asperities. The number of contact areas for a given load was expressed in terms of the hardness, H. Their resulting equation for the interface conductance, h_c, due to the metal-to-metal conduction mode was: $h_c = \frac{p_a k_c}{H a_s}$ where p_a is the apparent contact pressure and k_c the conductivity of the metal. With the experimentally determined values of the interface conductance, the size of the contact areas could be calculated. Their results showed that a_s was about 30 microns, independent of the material and, to some extent, independent of the contact pressure. The interstitial conductance, h_f, was estimated from roughness measurements and the relation $h_f = k_f/\delta$ where k_f is the thermal conductivity of the fluid and δ the thickness of the gap. In their analysis they assumed that h_c and h_f were independent. This assumption will be reviewed later. They asserted that the interface conductance must always be determined experimentally if a reliable value is required; however, they stated that their procedure provided a means of estimating the interface conductance.

Skipper and Wotton [55] reported data on a series of tests with particular reference to nuclear reactor fuel elements. The joints investigated were those formed from uranium and Magnox (a magnesium alloy) or aluminum. They showed the effect of surface temperature, gas pressure in the interstices, and oxide films on the interface conductance. Most of the data were for joints in an atmosphere of argon or helium at relatively high pressures (16.1 to 25 psia); however, others were also given showing the variation of contact resistance with gas pressure in which the pressure was varied from 10^{-4} to 10^{+3} mm Hg. Included were curves showing the effect of relatively thick, artificially produced oxide films on interface conductance for joints in an argon or helium atmosphere. The conditions of these tests were not specified in detail. The effects of the variables were discussed only in general terms.

Graff [26] attempted to correlate the data on thermal contact resistance of other investigators by two dimensionless groups: i) $hp_a/k_c\rho$, where p_a is the apparent contact pressure, ρ the material density, and k_c the thermal conductivity of the material, and ii) p_a/H, the ratio of the apparent contact pressure to the Brinell hardness number. Most of the data used in the correlations were from tests with an interstitial gas. Only one set of data was obtained in a vacuum environment. It was found that the data could not be correlated in these dimensionless coordinates. The author attributed this to the omission of a roughness parameter.

An experimental procedure was described by Mizushina, et al. [45], for the determination of the thermal contact resistance between stagnant mercury and a solid metal surface. The thermal conductivity of the mercury was simultaneously determined. Their interest in this problem was stimulated by the discrepancies found in investigations employing liquid metal as a heat transfer medium. Their results showed the existence of a small thermal contact resistance between a chromium or nickel-plated surface and pure liquid mercury. The interface conductance for these surfaces ranged from 9,500 to 42,000 Btu/hr $ft^{2o}F$. Their results also indicated that there was no thermal resistance between the copper base and the plated chromium film.

Schmidt and Jung [54] measured the contact resistance between liquid sodium and stainless steel. In their experiments, up to 24 interfaces were placed in series. In this way they multiplied the surface resistance by a factor of about 20, thus making possible an accurate determination of the small resistance at each interface. The contact resistance was found to be less than that of a stainless steel sheet 0.015 mm thick.

Barzelay, et al. [7], reported that when steel and aluminum specimens were in contact, the interface conductance depended upon the direction of heat flow.

Motivated by these results, Rogers [5] made an investigation for interfaces of dissimilar metals. He devised an apparatus in which the direction of heat flow could be reversed without disturbing the interface. The contact pressure was 122 psi for all tests. The mean interface temperature ranged from 40 to 140°C; the surface roughness varied between 2 and 10 microinches; and the specimens were parallel to within 0.0003 inches. The results for air at atmospheric pressure showed that the interface conductance was approximately 20 percent higher with heat flow from steel to aluminum than for the opposite direction. In a vacuum the numerical difference was about the same, but due to the smaller conductance values in a vacuum, the percentage difference rose to about 100 percent. Other dissimilar metallic joints which were investigated (chromel-alumel and copper-steel joints) did not clearly show any directional effect.

The cause of this directional phenomenon in the resistance to heat flow at the interface of dissimilar metals is not understood. Rogers suggested that it could be associated with the mechanism of conduction at the points of metallic contact. In a discussion of Rogers' paper, Williams [64] suggested that the phenomenon was a direct result of surface contamination. Moon and Keeler [46] applied the theory of heat conduction in the solid state to explain this asymmetric behavior at the interface of two dissimilar metals. They stated that this effect cannot be predicted quantitatively due to the lack of accurate work functions of various metals and their oxide films, although solid state theory qualitatively explains the directional behavior.

A considerable amount of work on thermal conductance was done at the Massachusetts Institute of Technology under the sponsorship of the U.S. Atomic Energy Commission. The results were first reported by Fenech and Rohsenow [20, 21], and were submitted by Fenech as a Sc.D. thesis. The latter consisted of a predominantly theoretical analysis. The geometry of contact was

imagined to be cylinders of radius a evenly distributed over the surface. The heat flow channel associated with each contact was taken as a coaxial cylinder of larger radius b. The voids were assumed to be of uniform thickness filled with a fluid of conductivity k_f. Radial conduction and natural convection were neglected. The boundary value problem was solved by dividing a representative heat channel into three subregions and satisfying the average boundary conditions between each subregion. An appropriately weighted average for the thickness of the fluid film was obtained in order to have a more realistic model for a contact. The following quantities are required for evaluating the interface conductance: i) the ratio of the real area of contact to the apparent area of contact, ii) the number of contact points per unit area, iii) the volume-averaged thickness of the interstices, and iv) the thermal conductivities of the metals and of the interstitial fluid.

The geometrical properties of the contact listed above were determined by a very time-consuming graphical analysis applied to recorded surface profiles. The Knoop hardness was introduced as a means of relating the apparent contact pressure to the actual area of contact. Good agreement with experimental results was reported; however, a comparison with experimental data was given for only an iron-aluminum contact with maximum surface roughness of 150 microinches rms. Other experiments were performed with the following types of artificial contact models: i) solid cylinders with a neck machined into them, hence, providing one contact spot of a specified radius; and ii) specimens whose surface consisted of several machined pyramids.

Several progress reports giving extensions of the above analysis have since been published [41, 42]. The apparent objective was to find a more convenient method of determining the geometrical properties of contacting surfaces for use in the equation developed by Fenech and Rohsenow. One procedure employed an analog computer and the other was by a statistical analysis. The latter was only

applicable for a rough surface in contact with a smooth, flat surface.

Adamantiades [1] conducted an experimental study to provide adequate data for comparison with the theory of Fenech and Rohsenow; however, a comparison was not given in this report. Three series of tests were conducted with three sets of stainless steel specimens. Data were obtained for a range in pressure from a few hundred psi to 20,000 psi. Those given for the higher pressures are of limited value due to considerable reported error. In some cases a negative temperature drop was obtained across the interface. A very recent report by Henry [30] which summarized the past research at the Massachusetts Institute of Technology gave a comparison of these data with theory. These results will be considered further in Chapter 7.

Wheeler, who was concerned with reactor fuel element design, wrote a short appraisal of thermal conductance data reported in the literature [62]. Later he performed an experimental analysis of the interface conductance between many different fuel element materials [63]. Part of this experimental study was performed in a vacuum of 10^{-4} mm Hg, the remainder in a gas of specified pressure up to one atmosphere. In general, the results showed considerable scatter. The deduced apparent thickness of the gas film was several times that of the total roughness. It appeared to be independent of the surface roughness. Attempts to evaluate the geometrical parameters associated with the interfaces studied produced results which were reported to have no statistical significance.

Recently, Sanderson [53] investigated the thermal contact resistance between uranium and Magnox. The object was to obtain a better understanding of the heat transfer process from the uranium fuel to the Magnox sheath in a gas-cooled reactor. The effects of the interface temperature, the interstitial gas and gas pressure, the contact pressure, and the surface films were investigated. The test surfaces were ground to a flatness of 100 to 200 microinches and a surface

roughness of 5 to 10 microinches. Data were given showing the effect of pressure on the contact resistance in vacuum as well as in argon and helium atmospheres of 17.7 psia. The contact pressure ranged from 47 to 295 psi, and the temperature ranged from 150 to 450°C. Some results showed the effect of relatively thick oxide and nitride films.

Laming [40] recently presented an analysis of the thermal contact resistance between machined matal contacts. Experimental values of conductance versus load were obtained for contacts of steel and brass, steel and aluminum, brass and aluminum, and brass and brass. Air, glycerol, and water were utilized as interfacial fluids. Very rough surfaces were employed. The roughness varied from 2440 to 170 microinches ('peak-to-mean' surface distance). In the analysis the total interface conductance, h_t, was set equal to the sum of the metal-to-metal conductance, h_c, and the interstitial conductance, h_f. The former was determined from the expression: $h_c = 2nak_c/A_a(1 - f)$, where f is a constriction alleviation factor based on an equation given by Roess [50], a is the mean radius of a contact point, A_a is the apparent contact area, n is the number of contact points, and k_c is the conductivity of the material. a was expressed in terms of the load and Meyer hardness value. n was obtained from the equation: $n = A_a(\sin \alpha)/\lambda_1 \lambda_2$. It was assumed that: i) all machined surfaces have a regularly pitched ridging due to the periodical nature of the machining process where λ_1 and λ_2 are the wavelengths of these ridges on surfaces one and two, respectively; ii) all ridge crests lie in the same plane; and iii) the angle between the ridges on surfaces one and two is α, which is a function of the orientation of these surfaces. The factor, $\sin \alpha$, was later dropped because the orientation indicated no clearly separable trend. The wavelengths varied from 0.0280 to 0.0029 inches. They were generated by a single point cutting tool. The interstitial conductance, h_f, was calculated from: $h_f = k_f/\delta$ where δ is the effective film thickness and

k_f is the fluid conductivity. Various possible reasons were given and discussed for the discrepancies between the model and the results.

2.2. LITERATURE ON THERMAL CONTACTS IN A VACUUM ENVIRONMENT.

One of the first published studies of thermal contacts in vacuum was performed by Jacobs and Starr [33]. They investigated the problem of thermal contact resistance in connection with the use of mechanical thermal switches in cryogenic apparatus. The effect of pressure on interface conductance was studied. They investigated only good conductors - gold, silver, and copper - with "optically flat" surfaces for apparent contact pressures ranging from approximately zero to 2.5 kg/cm^2. Unfortunately, the hardness of the specimens, the pressure in the vacuum chamber and the quantitative flatness deviation of the specimens were not reported. Data were presented at two temperatures: room temperature and the temperature of boiling nitrogen (- 195°C). They found that the conductance was several times greater at room temperature than at liquid nitrogen temperature.

Berman [11] was also interested in the problem of thermal switches for low temperature work and the potential of mechanical heat switches. He performed an experimental study of thermal contact resistance in a vacuum at very low temperatures, i.e., from 1.8 to 77°K. The chamber pressure in all cases was about 10^{-4} mm Hg. The main points investigated were: i) the dependence of conductance on load, ii) the variation of conductance with temperature, and iii) the applicability of the Wiedemann-Franz-Lorenz relation. The contact pressure was varied between about 300 and 1600 psi. At helium temperature (4.2°K), the conductance between all types of surfaces that were examined was reported to be proportional to T^2, but the temperature dependence was reported to be small at nitrogen temperature. It was found that the electrical conductance according to

the Wiedemann-Franz-Lorenz law was always much less than the thermal conductance. The two conductances behaved quite differently during cycles of the load. This suggests that most of the heat transport took place through electrically insulating regions of the surfaces at these low temperatures. The specimens in these tests were made of either steel or copper. Aluminum oxide powder or a thin disc of Teflon was placed between the metallic surfaces in several tests.

Mikesell and Scott [44] performed an experimental study of the heat conduction through insulating supports of storage vessels for cryogenic liquids. Two types of supports were tested: multiple-contact supports in the form of stacks of thin metallic plates, and nonmetallic spheres. The tests were conducted at a pressure of 10^{-5} mm Hg or less, with the boundary temperatures of the stack of plates at either 76 and 296°K or 20 and 76°K. The apparent contact pressure was varied from a few psi to 2500 psi. Plates varying in thickness from 0.008 to 0.0195 inches were employed in stacks consisting of 52 to 315 plates. Curves were given showing the effects of temperature, pressure, number of plates, and plate thickness on the thermal contact resistance. The results showed that the heat conducted through a stack of stainless steel plates, each 0.008 inches thick at a load of 1000 psi, was only two percent of the conduction by a solid sample of the same metal having the same dimensions. These results showed the large resistance present in multiple thermal contacts even at relatively large apparent contact pressures. Multiple thermal contacts offer the designer of cryogenic equipment a means of obtaining strong, efficient insulation.

The only study directly connected with thermal contact resistance in a space environment was that made by Fried and Costello [22]. The experimental data they presented were obtained at an ambient pressure of between 10^{-4} and 10^{-6} mm Hg. The specimens, in contrast to most other tests, were plates

5" x 5" with a 1/8" thickness. The specimen materials employed were aluminum and magnesium. The surface finish ranged from 6 to 65 microinches rms, and the contact pressure varied between a few psi and 35 psi. The authors indicated that this covered the range of interest for bare space vehicle joints. However, according to torque specifications on spacecraft structural fasteners [32], such a pressure range appears to be too low. Fried and Costello presented data graphically showing the variation of interface conductance with the contact pressure. The surface finish, flatness deviation, type of material, and type (if any) of shim material between the surfaces,. were parameters in these plots. Later reports [23, 24] also included the effects of silicone grease on the interface conductance. Their results indicated: i) flatness and surface roughness had large effects on contact resistance; ii) the introduction of a soft shim material or silicone grease can appreciably improve interface conductance; and iii) the thermal contact conductance at low contact pressures is very strongly pressure dependent. At higher pressures their conductance versus pressure curves became less steep, showing a lesser dependence of conductance on contact pressure. In general, the various parameters changed between tests and the limited amount of data presented make it difficult to differentiate between the individual influences of the many variables.

While a large amount of literature exists on the general topic of thermal contact resistance, little information is available to clarify the mechanics involved. Most of the data reported have been obtained in the presence of a conducting fluid. Our present understanding of the problem does not enable us to separate the interstitial fluid contribution from the total conductance. The meager data reported on interfaces in a vacuum environment also are of limited value. Often the test conditions were not completely stated or controlled to a sufficient degree. It is believed that the failure of investigators of this

problem to adequately recognize the controlling mechanism and the importance of several parameters makes their analytical and experimental studies of limited value. The basis for this statement is given in the remaining sections of this thesis.

A few references on thermal contact resistance have not been included in the survey of literature presented in this chapter. They are of minor importance, especially in relationship to the analysis and results presented in this investigation. In most cases a review of these additional references has been given in one or several of the articles listed in the Bibliography.

3. THE MECHANISM OF HEAT TRANSFER AT AN INTERFACE

When heat is flowing through two members in contact, an additional temperature drop, ΔT, will occur due to the presence of the interface. This interface represents an additional resistance to the heat flow which is commonly known as the contact resistance. By definition the contact resistance, R, is given by:

$$R = \frac{\Delta T}{A_a q} = \frac{1}{A_a h} \tag{3.1}$$

where q is the heat flux per unit area. The reciprocal of the product of the apparent contact area, A_a, and this resistance is called the interface conductance, h.* This quantity is commonly referred to in the literature. Experimentally, ΔT can be determined by projecting the temperature gradient in both members to the interface. The projected gradient must be determined in a region where the disturbance due to the interface is negligible (see Figure 2).

Contact resistance is a result of the constriction of heat flow to the actual areas of metallic contact. Large scale constrictions, resulting from flatness deviation or possible warping, extend the thermal disturbance to a considerable distance from the interface into both contact members. If the average temperature versus distance plot could be obtained, it would probably appear similar to that shown in Figure 2. Fried [23] obtained ΔT by averaging four values acquired from distributed temperature readings taken at a distance of about 0.070" from the 5" x 5" test interface. Such procedure could result in

---

* The conductance, h, which is employed in the field of thermal contact resistance is a misnomer. The common definition of conductance is the reciprocal of resistance, i.e., $C = 1/R$.

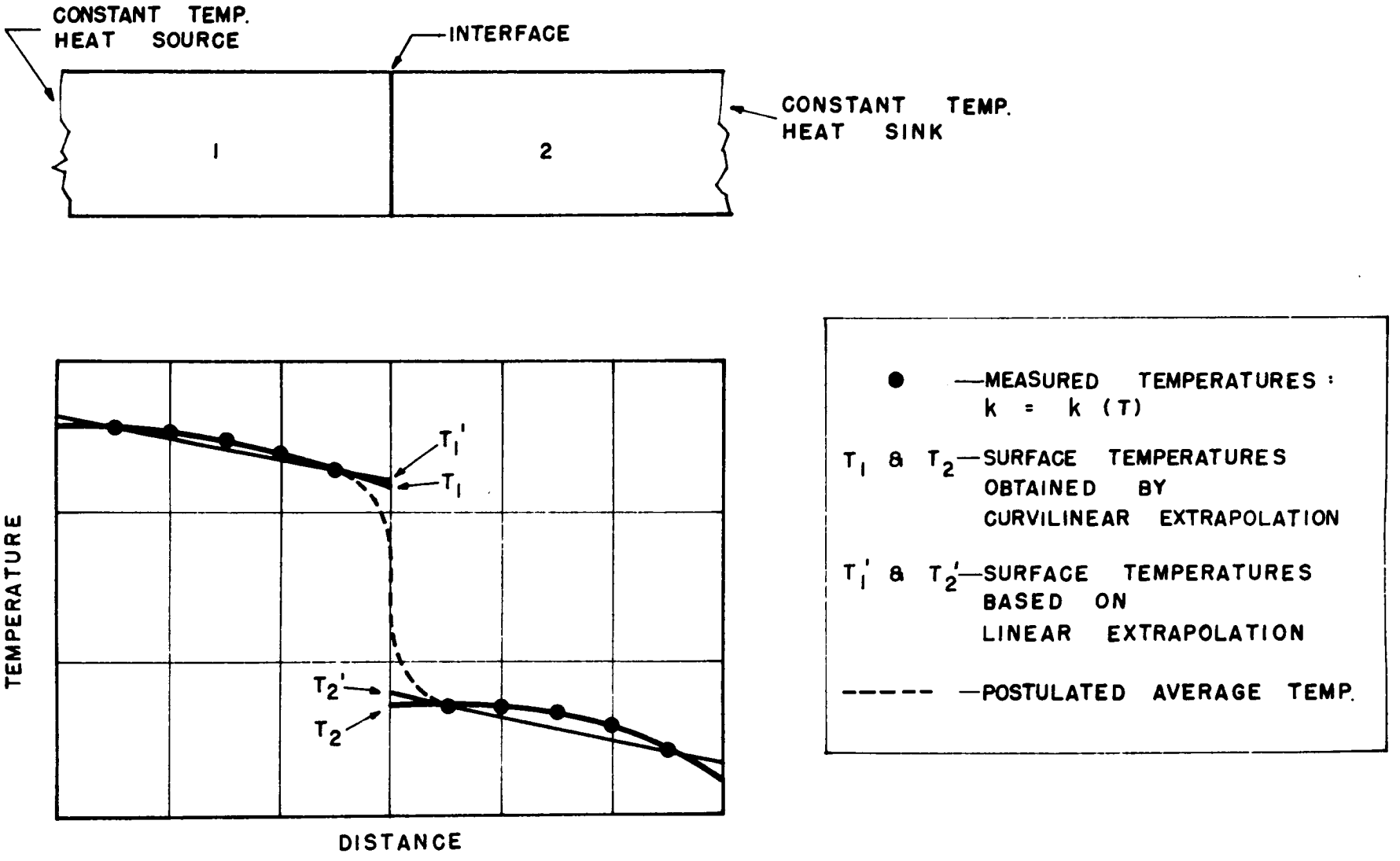

FIG. 2 EXTRAPOLATION OF MEASURED TEMPERATURES TO DETERMINE ΔT — POSTULATED AVERAGE TEMPERATURE VS. DISTANCE PLOT

serious error. The values of ΔT which Fried reported in his example ranged from 7.6 to $3.9^{o}F$; hence, his readings were most likely taken in the disturbed region.

The thermal conductivity, k, of a material is usually a function of its temperature. In steady one-dimensional heat flow, in the absence of internal sources, the slope of the temperature versus distance plot, dT/dz, is proportional to the reciprocal of the thermal conductivity. Hence, for variable conductivity, an appropriate curvilinear extrapolation is required to determine the specimen temperature at the contact plane, unless the following conditions are true. If $k_1 = k_{o,1}\ (1 + a_1 T)$ and $k_2 = k_{o,2}\ (1 + a_2 T)$ where $k_{o,1} \cong k_{o,2}$ and $a_1 \cong a_2$, then a linear extrapolation based on the mean thermal conductivity of the specimens, as is shown in Figure 2, may be employed. If the above conditions are true, the error introduced by this extrapolation is $(T_1 - T_1')$; however, the error introduced in the other specimen, $(T_2 - T_2')$, is of the same sign and is approximately equal (see Figure 2). Thus, the two errors tend to cancel each other in the calculation of the temperature drop ΔT, across the interface.

Heat is transferred across an interface by three different modes. They are: 1) thermal radiation, 2) interstitial conduction, and 3) metal-to-metal conduction. The subscripts r, f, and c, respectively, will be used to designate the three modes. These three modes of heat transfer are interrelated. In order to simplify the discussion and analysis of the problem, they will be considered as three separate, parallel paths of heat transfer as shown in Figure 3. Thus, the total interface conductance is:

$$A_a h_t = \frac{1}{R_r} + \frac{1}{R_f} + \frac{1}{R_c} . \qquad (3.2)$$

The inaccuracies introduced by neglecting the interdependence among the heat transfer modes will become clear as the development proceeds. Obviously, if

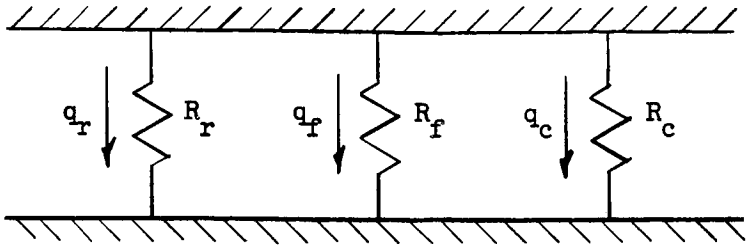

FIGURE 3
HYPOTHETICAL MODEL REPRESENTING THE THREE MODES OF HEAT TRANSFER ACROSS AN INTERFACE

one mode is predominant, this simplification will not affect the accuracy of the results.

3.1 THERMAL RADIATION MODE

The surfaces for the analysis of the heat transferred by thermal radiation will be approximated by two parallel, gray, plane surfaces (see Figure 4). The radiant heat exchange between these surfaces is:

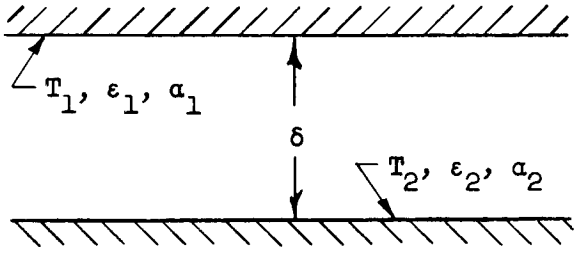

FIGURE 4
IDEALIZED MODEL FOR THE ANALYSIS OF INTERSTITIAL CONDUCTION AND RADIATION

$$q_r = \varepsilon_{1-2}\, \sigma\, (T_1^4 - T_2^4) \qquad (3.3)$$

where σ is Stefan-Boltzmann's constant; T_1 and T_2 are the temperatures of the surfaces; and ε_{1-2} is the interchange factor due to multiple reflections which according to [19] is:

$$\varepsilon_{1-2} = \frac{1}{\frac{1}{\varepsilon_1} + \frac{1}{\varepsilon_2} - 1} \qquad (3.4)$$

From Eqs. 3.1 and 3.3 it follows that the interface conductance due to radiative

heat transfer is:

$$h_r = \frac{q_r}{\Delta T} = \varepsilon_{1-2}\,\sigma\,\frac{T_1^4 - T_2^4}{T_1 - T_2} \qquad (3.5)$$

If $T_1T_2 - T_m^2$ is small, then

$$h_r \cong 4\,\varepsilon_{1-2}\,\sigma\,T_m^3 \qquad (3.6)$$

where T_m is the arithmetic mean interface temperature, $\frac{T_1 + T_2}{2}$. Thus, the interface conductance due to radiation is a function of the emissivities of the surfaces and cube of the mean interface temperature. If this mode were important, the interface conductance would vary considerably with the mean interface temperature.

The importance of the thermal radiation mode can be ascertained by examination of Table 1. In this table a comparison is made between h_r and the experimentally determined value for the interface conductance, h_t, for the stainless steel specimens of Series 1_s.* Comparisons were made for the lowest and highest values of contact pressure employed where the value of h_r/h_t was respectively a maximum and minimum. The emissivities of both surfaces were assumed to be 0.2. Since T_m was approximately the same in both cases, h_r was also nearly the same. Its value in all cases was approximately 0.25 BTU/hr.ft^{2}°F. The comparison given in Table 1 between Eqs. 3.5 and 3.6 shows that $T_1T_2 \cong T_m^2$ is a valid approximation. The calculated value of h_r was never greater than 2% of the total conductance, h_t, for Series 1_s. Since the stainless steel specimens of this series had the lowest conductance experienced, the contribution of the radiation mode was less in other cases. Thus, unless extremely poor

* The experimental tests have been divided into categories. A list of these categories is given in Appendix B along with a description of the specimens employed.

conductors or very high resistances are investigated, the heat transferred across the interface by radiation can be neglected. The use of an idealized geometry in the foregoing analysis, as indicated in Figure 4, will not alter the validity of this conclusion.

Contact Pressure (PSI)	T_1 (^oR)	T_2 (^oR)	T_m (^oR)	h_t ($\frac{BTU}{hr ft^2 {}^oR}$)	h_r/h_t Eq. 3.5	h_r/h_t Eq. 3.6
11.1	776	596.5	686.2	17.2	0.0145	0.0144
987	696	693	694.5	2300	1.11×10^{-4}	1.11×10^{-4}

Table 1

Comparison Between h_r

and the Experimentally Determined Value of h_t

3.2 INTERSTITIAL CONDUCTION MODE

Since the thickness of interstices is in most cases small compared with their other dimensions, both natural convection and conduction parallel to the interface can be neglected in the calculation of the heat transferred through the interstitial substance. Using the same model as was utilized for the radiation mode (see Figure 4), the interstitial conductance is:

$$h_f = \frac{k_f}{\delta} \quad , \tag{3.7}$$

where δ is the distance between the assumed plane surfaces and k_f is the thermal conductivity of the interstitial substance which is usually air. Other gases, greases, oils, glues, etc., may also be employed as the interstitial material. If δ is small, the thermal conductivity of the interstitial

substance can be quite low, yet the resulting interstitial conductance can be high, provided the substance adequately flows into the voids. This is the case with air at atmospheric pressure.

It is the object of this investigation to study thermal contact resistance in a vacuum or space environment. Thus, it is of interest to determine the effect of the rarefied gas present in the vacuum chamber on the interface conductance. Consider again two parallel plane surfaces, as shown in Figure 4, at temperatures T_1 and T_2 with accommodation coefficients α_1 and α_2. For free-molecule heat conduction between these plates the heat flux as given by Kennard [35] is:

$$q_f = \frac{\alpha_1 \alpha_2}{\alpha_1 + \alpha_2 - \alpha_1\alpha_2} \frac{\gamma + 1}{2} \frac{C_v p'}{(2\pi RT')^{1/2}} (T_1 - T_2) , \tag{3.8}$$

or, since $C_v = \frac{R}{\gamma - 1}$ and $h_f = \frac{q_f}{\Delta T}$,

$$h_f = \frac{\alpha_1 \alpha_2}{\alpha_1 + \alpha_2 - \alpha_1\alpha_2} \left(\frac{\gamma + 1}{\gamma - 1}\right) \left(\frac{R}{8\pi T'}\right)^{\frac{1}{2}} p' \tag{3.9}$$

where R is the gas constant, γ the ratio of specific heats, p' the pressure of a Maxwellian gas having the same density as the gas between the plates but a temperature T', and T' the temperature of a Maxwellian gas corresponding to the mean speed of the molecules. If $\alpha_1 = \alpha_2$, T' is equal to T_m. Equation 3.9 shows that at a given temperature the heat flux due to free-molecule conduction is directly proportional to the gas pressure and independent of the distance, δ, between the surfaces. Free-molecule flow is generally considered to exist for a Knudsen number, $\frac{\lambda}{\delta}$, greater than 10 where λ is the mean free path. Assuming the maximum value of δ encountered in thermal contact resistance studies is 0.002",

Equation 3.9 is applicable for λ greater than 0.02". This corresponds to a pressure less than 100 microns of Hg. In our calculations it was assumed that $\alpha_1 = \alpha_2 = 0.9$ (Hartnett [29], in his survey of thermal accommodation coefficients, stated that little data are available on accommodation coefficients for air on engineering surfaces. He further stated that one should not place too much faith on the values near unity reported by Wiedmann and Trumpler).

The importance of free-molecule conduction can be ascertained by an examination of Table 2. Comparisons of h_t with the calculated values of h_f are given for chamber pressures of 1, 100, and 2000 microns of Hg. The value of h_t employed in the calculation of the ratio, h_f/h_t, is the lowest experimental value of the interface conductance obtained (17.2 BTU/hr ft^2 $^\circ$F); thus, this ratio in most cases is much smaller. The experimental value of h_t was obtained at a pressure of 3×10^{-4} mm of Hg. A series of experimental tests also were performed to determine the effects of the chamber pressure on interface conductance. These data, Series 7_B, are given in tabulated form in Appendix C. The experimental values of h_f reported in Table 2 were determined from: $h_f = h_t(p') - h_t$ $(p' = 1\mu)$, p' being the chamber pressure. This relationship, in the strict sense, is not correct since the presence of the gas causes a change in h_c. However, it does give an indication of the magnitude of h_f. With the present understanding and the improved accuracy of the apparatus, the effect of free-molecule conduction could be evaluated more accurately. However, since the present study indicates that the free-molecule conduction is negligible even at pressures of several microns of Hg, a more sophisticated analysis of this effect cannot be justified presently. These results clearly show that the heat conducted across the interface by the rarefied gas in the chamber was negligible for all the tests conducted in this investigation.

Consider now actual surfaces in contact at zero contact pressure. These

p' (μ Hg)	λ/δ (δ = 800 μin.)	h_f (Eq. 3.9) (BTU/hr ft^{2}F)	h_f (exp.) (BTU/hr ft^{2}F)	$\frac{h_f}{h_t}$ (Eq. 3.9) / (exp. at p' = 0.3μ)
1	3000	0.02	0	0.0011
100	30	2.0	not discernable	0.11
2000	1.5	40.	24 $\pm$ 50%	2.3

Table 2

Comparison of h_f Calculated from Equation 3.9 with Experimentally Determined Values of h_f and h_t for Various Chamber Pressures

actual surfaces are a series of peaks and valleys; hence, δ varies from zero to some unknown maximum value. However, the heat flux due to free-molecule conduction is independent of δ; thus, Equation 3.9 is still applicable. The continuum region, on the other hand, becomes considerably more complicated when rough surfaces are introduced. An effective distance δ must be determined which will satisfy (3.7). At first glance the arithmetic-mean distance δ_m may appear to be appropriate; however, this results in a value of h_f which is too small. Keller [34] calculated δ for several assumed surface geometries. For example, for paraboloids of revolution making point contact at their apices with a smooth surface, he found δ equal to $\delta_m/1.86$. Thus, for rough surfaces, it is seen that the geometry of the surface must be considered. If this conductance is large or if one simultaneously considers the presence of metal-to-metal conduction, the surfaces can no longer be considered as isothermal surfaces. In addition, as was discussed in the previous section, the extrapolated temperatures, T_1 and T_2, would not be the average temperatures of the surfaces 1 and 2 respectively. Since interstitial conduction is negligible and the presence of an interstitial material is not being studied in the present investigation, these points will

not be considered in any more detail at this time.

3.3 METAL-TO-METAL CONDUCTION MODE

It has been shown that the heat transferred by thermal radiation and interstitial conductance is small for the conditions of this investigation. Thus, the total interface conductance is, for all practical purposes, the same as the metal-to-metal conductance. From now on these classifications will be disregarded and the term interface conductance with its symbol, h, will be employed. The model employed for the analysis of the metal-to-metal conduction mode is presented in the next chapter.

4. A THEORETICAL MODEL AND ITS ANALYSIS

It has been shown that the contribution to the heat transferred across a joint due to interstitial conduction and radiation is negligible for most cases pertinent to this study. Metal-to-metal conduction plays the dominant role. The study of the physics and chemistry of surfaces, electrical contact resistance, friction and wear, and thermal contact resistance has revealed the complexity of this mode because of our lack of understanding of the physical nature of surfaces and, more specifically, surfaces in contact.

Geometrically flat surfaces are nonexistent. Real surfaces are characterized by a series of peaks and valleys. An enlarged section of the interface formed by two members in contact may appear similar to that shown in Figure 5. The actual areas of contact are relatively small and widely separated. The constriction of the flow of heat to these small areas of contact manifests itself as a thermal contact resistance at the macroscopic level.

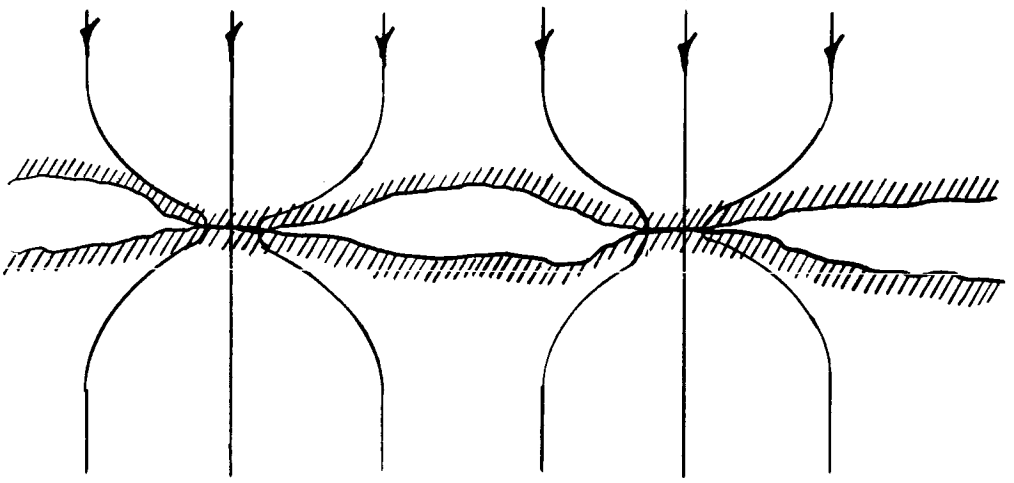

FIGURE 5
SCHEMATIC REPRESENTATION OF THE CONSTRICTED FLOW
OF HEAT ACROSS AN INTERFACE

4.1 THE PROPOSED MODEL

For the analysis of the problem, the apparent contact surface will be divided into two regions: the contact region and the non-contact region. The non-contact region, by definition, is the portion of the contact surface which contains few or no microscopic contact areas. Occasional microscopic contacts are permitted in this region, provided that the heat transferred through these contact points is a negligible portion of the total. The contact region, which will also be referred to as the macroscopic contact area, is by definition the portion of the contact surface where the density of the micro-contact areas is high. The dimensions of both of these regions will be of the same order of magnitude as those of the apparent contact area for normal contact pressures. The division of the apparent contact area into these two regions is suggested by the following observations: i) large scale waviness or flatness deviation of the contact surfaces is always present, and ii) surface warpage occurs as a result of differential thermal expansion and nonuniform mechanical properties. The size of these regions is governed by the elastic deformation of the contact members in most cases. This is a consequence of the relatively low pressures exerted between surfaces in practical joints.

The foregoing observations of the nature of contact have led to the belief that the constriction to heat flow due to imperfect metal-to-metal contact may be represented by two resistances in series: the large scale or macroscopic constriction resistance, R_L, and the small scale or microscopic constriction resistance, R_S. First the flow of heat is constricted to the large scale contact regions, and then it is further constricted to the microscopic contacts within this macroscopic area. Hence, the contact resistance is given by:

$$R = R_L + R_S \quad . \tag{4.1}$$

If a film, usually a metallic oxide, is present, its effect should be included. Thus:

$$R = R_L + R_S + R_O \qquad (4.2)$$

where R_O represents the resistance due to the film existing between the microscopic contacts.

In previously published studies of thermal contact resistance, the emphasis was always placed, without exception, on the analysis of microscopic effects. In order to ascertain the importance of the component resistances in Equation 4.2, an analysis of each will be given. A discussion of their relative importance will also be given. Clean surfaces will be considered first. An investigation of the effect of surface films will follow.

4.1.1 Microscopic Constriction Resistance

In the analysis of the microscopic constriction resistance, the following initial assumptions will be made:

i. the surfaces are free from films

ii. the microscopic contact areas are all circular and of identical radius, a_s

iii. the contact areas are uniformly distributed over the contact region in a triangular array. The distance between the centers of any two areas is $2b_s$.

The mathematical problem is to find the solution to the equation $\nabla \cdot (k \nabla T) = 0$ with the required boundary conditions for the constriction region. For constant thermal conductivity this equation is:

$$\nabla^2 T = 0 \qquad (4.3)$$

If the solution of this equation with the appropriate boundary conditions is obtained, the resistance between any two isothermal surfaces, A_c and A_e bounding an imaginary tube of heat flow, can be determined by:

$$R = \frac{|T_c - T_e|}{k \int_{A_c} \left|\frac{\partial T}{\partial n}\right| d A_c} \qquad (4.4)$$

where n is the normal to the surface. The solution for the constriction resistance of an isothermal circular area of radius a on the flat surface of a semi-infinite body was given by Holm (Ref. 31, p. 17). It is:

$$R = \frac{1}{4 a k} , \qquad (4.5)$$

where k is the thermal conductivity of the material. For two semi-infinite bodies of the same material in contact over a circular area of radius a the total constriction resistance would be:

$$R = \frac{1}{2 a k} . \qquad (4.6)$$

Holm stated that if both members consisted of the same material and had equal constrictions, the contact area would be isothermal due to symmetry. However, the requirement of identical material is not necessary. For dissimilar materials the total constriction resistance would be:

$$R = \frac{1}{4 a k_1} + \frac{1}{4 a k_2}$$

or

$$R = \frac{1}{2 a k_m} \qquad (4.7)$$

where $$k_m = \frac{2 k_1 k_2}{k_1 + k_2} .$$

For the idealized contact geometry assumed, the total parallel resistance of the

n_s contact points in a particular region can be approximated by:

$$R_s = \frac{1}{2\, a_s\, k_m\, n_s} \tag{4.8}$$

if a_s is much less than b_s. When a_s is the same order of magnitude as b_s, it becomes necessary to determine the effect of the constriction alleviation caused by the neighboring contact points. Each contact area in its triangular array has a hexagonal heat flow channel feeding it. This hexagonal channel will be approximated by a cylinder of radius b_s. Roess [50] determined the constriction resistance due to a constant potential circular spot of radius a which feeds into a coaxial right circular cylinder of radius b. Initially, a cylinder of finite length L was considered; however, a later assumption resulted in the same solution that would have been obtained for a semi-infinite cylindrical region. In addition, although the problem was formulated as the constriction resistance of a constant potential circular area, the boundary condition he employed was that the flux distribution across this area was proportional to $(1 - \frac{r^2}{a^2})^{-1/2}$ where r is the radial coordinate. This heat flux distribution resulted in an isothermal contact area, unless a/b was near unity. For large values of this parameter the average temperature of the contact was employed. The results of the analog study and the next section indicate that this is a good approximation. Roess' solution is:

$$R(x) = \frac{g(x)}{4\, a\, k} \tag{4.9}$$

where

$$g(x) = 1 - 1.40925\, x + 0.29591\, x^3 + 0.05254\, x^5 + 0.02105\, x^7 + 0.01107\, x^9 + \ldots \tag{4.10}$$

and x, the constriction ratio, is equal to a/b. Figure 6 shows the variation of

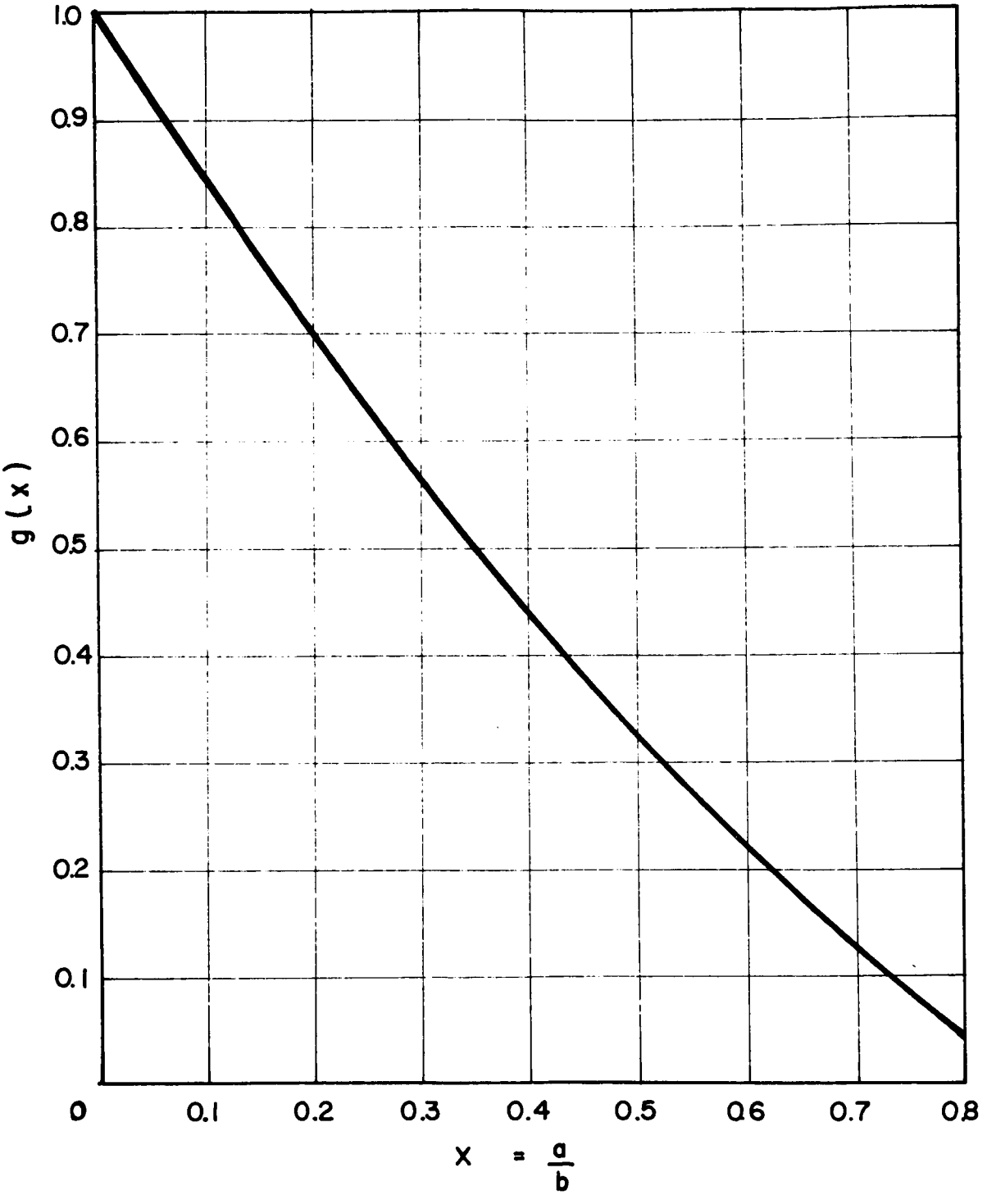

FIG. 6 THE INFLUENCE OF THE CONSTRICTION RATIO

g (x) with x. Clearly, as x approaches zero, Equation 4.9 simply reduces to Equation 4.5. By incorporating g (x) into Equation 4.8, the following expression is obtained for the microscopic constriction resistance:

$$R_s = \frac{g(x_s)}{2 a_s k_m n_s} \quad . \tag{4.11}$$

Equation 4.11 may be written in terms of the interface conductance h.

$$h = \frac{2 a_s k_m n_s}{g(x_s) A_a} \tag{4.12}$$

In the present investigation, the apparent contact area A_a is πb_L^2, b_L being the specimen radius. The two unknowns involved are a_s and n_s. If they are known, x_s can be calculated.

Many of the models presented in the literature (see references 12, 13, 16, 20, and 40) assumed that the asperities carried the load P and deformed plastically such that the average pressure on them, p_s, equaled the contact hardness, H. Thus, the load-bearing area or microscopic contact area, A_s, was:

$$A_s = \frac{P}{H} = n_s \pi a_s^2 \tag{4.13}$$

Accurate experimental determinations of the microscopic contact area and the number and shape of these areas are difficult to obtain. No reliable data on the actual microscopic contact area is believed to exist. Many of the available data have been determined from contact resistance measurements. These data are no better than the assumptions involved in obtaining the equation from which this area is calculated. Therefore, the validity of this equation for rough, flat surfaces in contact and its applicability to microscopic thermal contacts is questionable.

In a vacuum environment there is still the question: how perfect is the microscopic contact area between asperities? There could conceivably be a spectrum of constrictions and not just the macroscopic and microscopic constrictions defined in this analysis. However this does not mean that they are all of importance. The hypothesized imperfection of the contact area between asperities is suggested by Moore's results [47]. He showed that even with considerable bulk deformation on a macroscopic level, the asperities often deform very little. Tabor [56] states that hardness values do not appreciably depend on the surface roughness. This, combined with the results of Moore, indicates that employment of a macro-hardness number in Equation 4.13 would not give the true microscopic contact area.

For contacts between clean surfaces, the quantum mechanical tunnel effect will improve the conduction between microscopic contact areas and will also provide an effective enlargement of this area. The quantum mechanical tunnel effect provides a significant contribution to the flow of heat across gaps of less than about 20 $\mathring{A}$ (see Ref. 31, p. 429); however, if films are present on the metal surfaces, this effect will be eliminated or at least greatly reduced.

The next question that arises is whether or not the microscopic contact areas are formed by purely plastic deformation. Holm (Ref. 31, p. 35) suggested that the contact pressure between asperities be represented by ξH in order to include the effects of elastic deformation. He proposed a value of ξ between 1/3 and 1; however, he also stated that values as small as 0.02 have been obtained by polishing the contact members. The dominance of elastic deformation for polished surfaces has been substantiated by other investigators. Haines and Hirst [27] reported asperities from 50 to 100 $\mathring{A}$ in height and 1 to 2 μ in width on polished surfaces. Such asperities could easily be in complete contact at microscopic contact pressures which are considerably below

the hardness, H. Halliday [28] stated that for polished aluminum surfaces intimate contact could occur over the complete surface before any plastic flow occurred, except for very limited regions around minute ridges and valleys which cross the surfaces. Dyson and Hirst [18] found, in their contact area measurements with polished specimens, that true contact existed over almost the entire general region of contact, i.e., the macroscopic contact area. Wear experiments suggest, as was stated by Archard [4], that multiple contacts are formed by elastic rather than plastic deformation.

In thermal contact problems the microscopic elastic deformation could also be of importance because surfaces are often made very flat to reduce macroscopic effects. This results in a large contact area; consequently, the load on individual asperities is reduced. Furthermore, contact pressures between thermal contacts are considerably below those which occur in friction problems or in structural elements. A thermal contact is not stationary, although it appears so on a macroscopic scale. Differential thermal expansion between the two surfaces, which occurs as a result of changes in the temperature of the members, is often considerably larger than the height of the asperities. A protuberance may be plastically deformed at the first encounter with its mating surface; however, a slight amount of differential motion would cause an increase in the contact area. The same load may be eventually borne by elastic deformation.

Since the slope of the asperities is larger for rough surfaces, elastic deformation should not be very important. However, small asperity slopes also exist for rough surfaces. Halliday [28] reported that although angles of 30 degrees and more occur across the abrasion direction, angles of asperity slope of 2 degrees and less occur along the direction of the abrasion. The microscopic contact areas for such surfaces could still be partially formed by elastic deformation, and they are of elliptical shape. Elliptical contacts

have a lower constriction resistance than circular ones of the same area (see Ref. 31, p. 19). The contact areas measured by Dyson and Hirst [18] for ground surfaces were often found to be highly elliptical.

By replacing the hardness H by ξH in Equation 4.13 and substituting it into Equation 4.12, one obtains the following expression for the microscopic interface conductance:

$$h = \frac{2}{\pi} \frac{p_a}{\xi H} \frac{k_m}{a_s g(x_s)}$$

which in dimensionless form reads:

$$\frac{h a_s}{k_m} = \frac{2}{\pi} \frac{p_a}{\xi H} \frac{1}{g(x_s)} \quad . \qquad (4.14)$$

An equation similar to (4.14) was previously employed by Boeschoten and van der Held [12] in their prediction of thermal contact resistance. The effect of $g(x_s)$ was not included in their analysis, ξ was assumed to be equal to 0.5, and a_s was taken to be independent of the load. It was determined from the measured conductance values. The independence of a_s with load has been partially substantiated by the results of Dyson and Hirst. They reported that the number of contact points increases with load due to an increase in the area of the contact regions; therefore, the size of the contact was not appreciably affected. A given microscopic contact may grow with load; however, the addition of new but smaller microscopic contact areas may result in an average size which remains relatively constant.

In the light of the foregoing discussion, the following assumptions are made in order to enable an estimation of the microscopic constriction resistance:

i) An average value of $\xi = 0.3$ is assumed to take into account both the

decrease in resistance due to the non-circular contact areas and the greater contact area due to microscopic elastic deformation. This value may be low for rough surfaces and is undoubtedly too high for well polished surfaces.

ii) A value for $g\,(x_s)$ of unity is assumed. Calculations show that this is a reasonable approximation except for very smooth surfaces and for extremely high contact pressures.

iii) The microscopic contact areas are assumed to be independent of the load, and their average size is assumed to be of the same order of magnitude as the surface roughness. The latter assumption is not valid at high loads or for asperities whose base is considerably larger than their height. In such cases a_s will be larger; however, these effects are partially offset by: a) the greater importance of elastic deformation for very small slopes, (thus, ξ would be less than 0.3) and b) at large loads $g\,(x_s)$ becomes steadily smaller than unity. It is clear from Equation 4.14 that h depends on the product of $(a_s)(\xi)[g\,(x_s)]$. a_s is still present in the equation below. When this equation is used, a value of a_s consistent with the above assumptions must be employed.

With these assumptions Equation 4.14 becomes:

$$\frac{h\,a_s}{k_m} \cong \frac{2\,p_a}{H} \qquad (4.15)$$

Since the asperity hardness is appropriate, a microhardness number is recommended for use in Equation 4.15. Diamond pyramid hardness numbers were employed in

this investigation.

4.1.2 Macroscopic Constriction Resistance

Macroscopic constriction resistance results from the constriction of heat flow to the macroscopic regions of contact. This resistance, in spite of its importance, has escaped the attention of many investigators. Since our knowledge of this resistance is still rudimentary, we must be satisfied with an approximate analysis based on a simple model. The limitations imposed by the simplicity of the model are believed to be outweighed by the extent of the analysis.

Consider the contact region between two cylinders, of length L and identical radius b_L, placed end to end. A single circular contact area of radius a_L whose center coincides with that of the apparent contact area is assumed. Thus, the non-contact region is an annulus whose inside and outside radii are a_L and b_L, respectively. Since the geometry, as defined, is symmetrical with respect to the contact plane, the cylindrical region represented by one of the specimens can be considered. It is shown in Figure 7. Assuming that a perfect contact exists over the region of radius a_L, the following partial differential equation and boundary conditions describe the temperature field:

$$\frac{\partial^2 T}{\partial r^2} + \frac{1}{r}\frac{\partial T}{\partial r} + \frac{\partial^2 T}{\partial z^2} = 0 \qquad (4.16a)$$

$$T(r,o) = T_1 , \quad 0 \leq r \leq a_L \qquad (4.16b)$$

$$\frac{\partial T}{\partial z}(r,o) = 0 , \quad a_L \leq r \leq b_L \qquad (4.16c)$$

$$\frac{\partial T}{\partial r}(b_L,z) = 0, \quad 0 < z < L \qquad (4.16d)$$

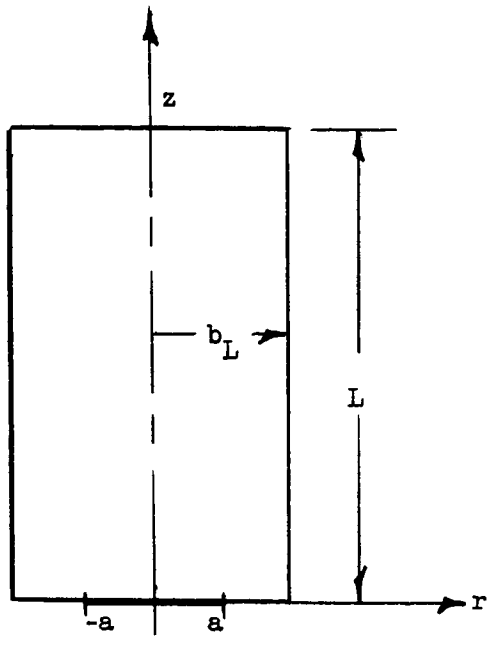

FIGURE 7

FINITE CYLINDRICAL REGION

$$T(r,L) = T_3 ,$$

$$0 \leq r \leq b_L \qquad (4.16e)$$

If L/b_L is greater than approximately 0.6 (see the results of the analog study, Section 6.2), the solution given by Roess, as discussed in Section 4.1.1, applies. The constriction resistance is given by:

$$R_L = \frac{g(x_L)}{4 a_L k} \qquad (4.17)$$

It is seen that even if the nature of contact is fully specified, the macroscopic constriction resistance depends on the specimen length as well as the boundary conditions. In other words, if the macroscopic constriction resistance is of importance, thermal contact resistance is <u>not</u> a property.

In reality, the macroscopic contact is not a perfect contact due to the existence of the small scale constriction resistance, R_s, even if the surfaces considered are ideally "clean." The presence of R_s alters the heat flux distribution over the macroscopic contact area. To determine the effect of R_s on R_L, let us consider the limiting situations. If R_s is very small compared with R_L, the boundary condition of an isothermal contact plane applies (see Equation 4.16b). The constriction resistance is then given by Equation 4.17. If, on the other hand, R_s is very large compared with R_L and is uniform over

the macroscopic contact area, it follows that the heat flux through the contact region is approximately uniform. The equation and boundary conditions given previously still apply, with the exception of Equation 4.16b which should now read:

$$- k \frac{\partial T}{\partial z} (r,o) = q_1 , \qquad 0 \leq r \leq a_L \tag{4.18}$$

where q_1 is a constant. In this case, the definition of the thermal resistance given by Equation 4.4 is no longer applicable. Based on the temperature at the center of the contact area, Holm (Ref. 31, p. 21) obtained the following expressions for the constriction resistance. His solutions are only valid for small values of x_L. For the uniform flux contact:

$$R_L = \frac{1}{\pi a_L k} , \qquad x_L < 0.01 , \qquad R_s >> R_L \tag{4.19}$$

and for the uniform temperature contact:

$$R_L = \frac{1}{4 a_L k} , \qquad x_L < 0.01 , \qquad R_s << R_L \tag{4.20}$$

These indicate a 25% difference in the constriction resistance for the two cases; however in evaluating ΔT the employment of the temperature at the center of the contact area results in a value of the constriction resistance of the uniform flux contact which is too large.

Let us consider the resistance between two surfaces which may not be isothermal planes. Consider a differential stream tube (heat flow tube) under the condition of steady heat flow in the absence of internal sources (see Figure 8). An energy balance gives:

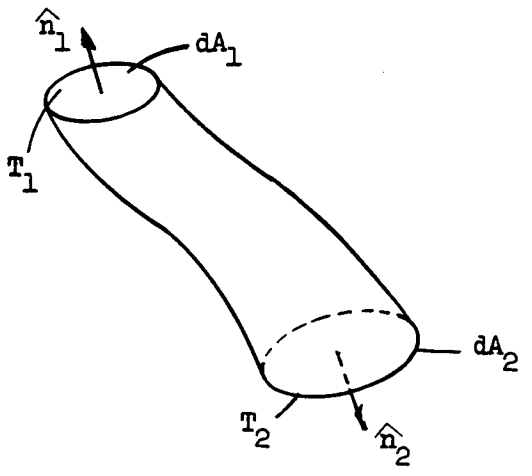

FIGURE 8

DIFFERENTIAL STREAM TUBE

$$\bar{q}_1 \cdot \hat{n}_1 \, d A_1 + \bar{q}_2 \cdot \hat{n}_2 \, d A_2 = 0$$

where $\hat{n}_1$ and $\hat{n}_2$ are the outward drawn normals and $\bar{q}_1$ and $\bar{q}_2$ the heat flux vectors. By definition, the thermal conductance of the differential stream tube is:

$$dC = \frac{-\bar{q}_1 \cdot \hat{n}_1 \, dA_1}{T_1 - T_2} = \frac{\bar{q}_2 \cdot \hat{n}_2 \, dA_2}{T_1 - T_2} \tag{4.21}$$

the total conductance is:

$$C_t = \int_{A_1} \frac{- \bar{q}_1 \cdot \hat{n}_1 \, d A_1}{T_1 - T_2} = \int_{A_2} \frac{\bar{q}_2 \cdot \hat{n}_2 \, d A_2}{T_1 - T_2} \tag{4.22}$$

Thus, for the region given in Figure 8 and the boundary conditions given by Equations 4.16c, 4.16d, 4.16e, and 4.18, the total conductance is:

$$C_t = \int_0^{a_L} \frac{2 \pi r \, q_1 \, d r}{T(r,o) - T_3} \, . \tag{4.23}$$

The constriction resistance R_L is:

$$R_L = R_t - \frac{L}{\pi b_L^2 k}$$

or

$$R_L = \frac{1}{\int_0^{a_L} \frac{2\pi r q_1 dr}{T(r,o) - T_3}} - \frac{L}{\pi b_L^2 k} \, . \tag{4.24}$$

Let $a_L/r = y$ and $T(r,o) - T_3 = \Delta T(y) + \Delta T_1$ where ΔT_1 is the temperature drop which would occur if $(\pi a_L^2)\, q_1$ passed through the cylinder of length L without being constricted, i.e., $\Delta T_1 = \dfrac{L}{\pi b_L^2 k}\, q_1 \pi a_L^2$. With these relationships, Equation 4.24 becomes:

$$R_L = \frac{1}{\pi a_L^2 q_1} \left[\frac{1}{\int_o^1 \frac{2y\, dy}{\Delta T(y) + \Delta T_1}} - \Delta T_1 \right] \quad . \quad (4.25)$$

If L is large such that $\Delta T_1 >> \Delta T(y)$, then the denominator of the integral can be approximated by the first two terms of its binomial expansion.

$$R_L \cong \frac{1}{\pi a_L^2 q} \left[\frac{\Delta T_1}{1 - \int_o^1 2y \frac{\Delta T(y)}{\Delta T_1}\, dy} - \Delta T_1 \right]$$

which may be simplified further to:

$$R_L \cong \frac{\int_o^1 2y\, \Delta T(y)\, dy}{\pi a_L^2 q_1} \quad . \quad (4.26)$$

Roess [50], in examining the influence of the heat flux distribution on the local temperature over the circular contact area, found and reported the temperature distribution over this area for six values of x (0 to 0.5) and four different distributions of the heat flux. These results were obtained from numerical calculations. Using his tabulated results for the case of uniform heat flux, R_L was determined from a numerical integration of Equation 4.26. The results are given in Table 3. The values for the constant temperature boundary condition are included for comparison. It is interesting to see that the constriction resistance of the two different problems is practically identical.

	T = const. (Eq. 4.16)	$\partial T/\partial z$ = const. (Eq. 4.26)
x = 0	$R_L = \frac{0.250}{a_L k}$	$R_L = \frac{0.252}{a_L k}$
x = 0.4	$R_L = \frac{0.114}{a_L k}$	$R_L = \frac{0.116}{a_L k}$

Table 3

Influence of the Contact Boundary Condition on the Constriction Resistance

This result, which apparently was not previously realized, has a significant bearing on the calculation of the macroscopic constriction resistance. It indicates that the macroscopic constriction resistance is, within limits, independent of the magnitude and radial distribution of the microscopic constriction resistance for the model considered. On the basis of this finding, Equation 4.16 will hereafter be employed regardless of the value of R_s.

For two cylindrical regions in contact over a circular, concentric region of radius a_L, the total constriction resistance becomes (see Equation 4.16):

$$R_L = \frac{g(x_{L,1})}{4 a_L k_1} + \frac{g(x_{L,2})}{4 a_L k_2} \quad . \tag{4.27}$$

If $b_{L,1} = b_{L,2} = b_L$

$$R_L = \frac{g(x_L)}{2 a_L k_m} \tag{4.28}$$

where k_m is again the harmonic mean of k_1 and k_2. The interface conductance, h, in dimensionless form is:

$$\frac{h b_L}{k_m} = \frac{2 x_L}{\pi g(x_L)} \quad . \tag{4.29}$$

Figure 9 shows the variation of hb_L/k_m, with the constriction ratio x_L. This figure clearly shows the low conductance obtained for small values of x_L. Since

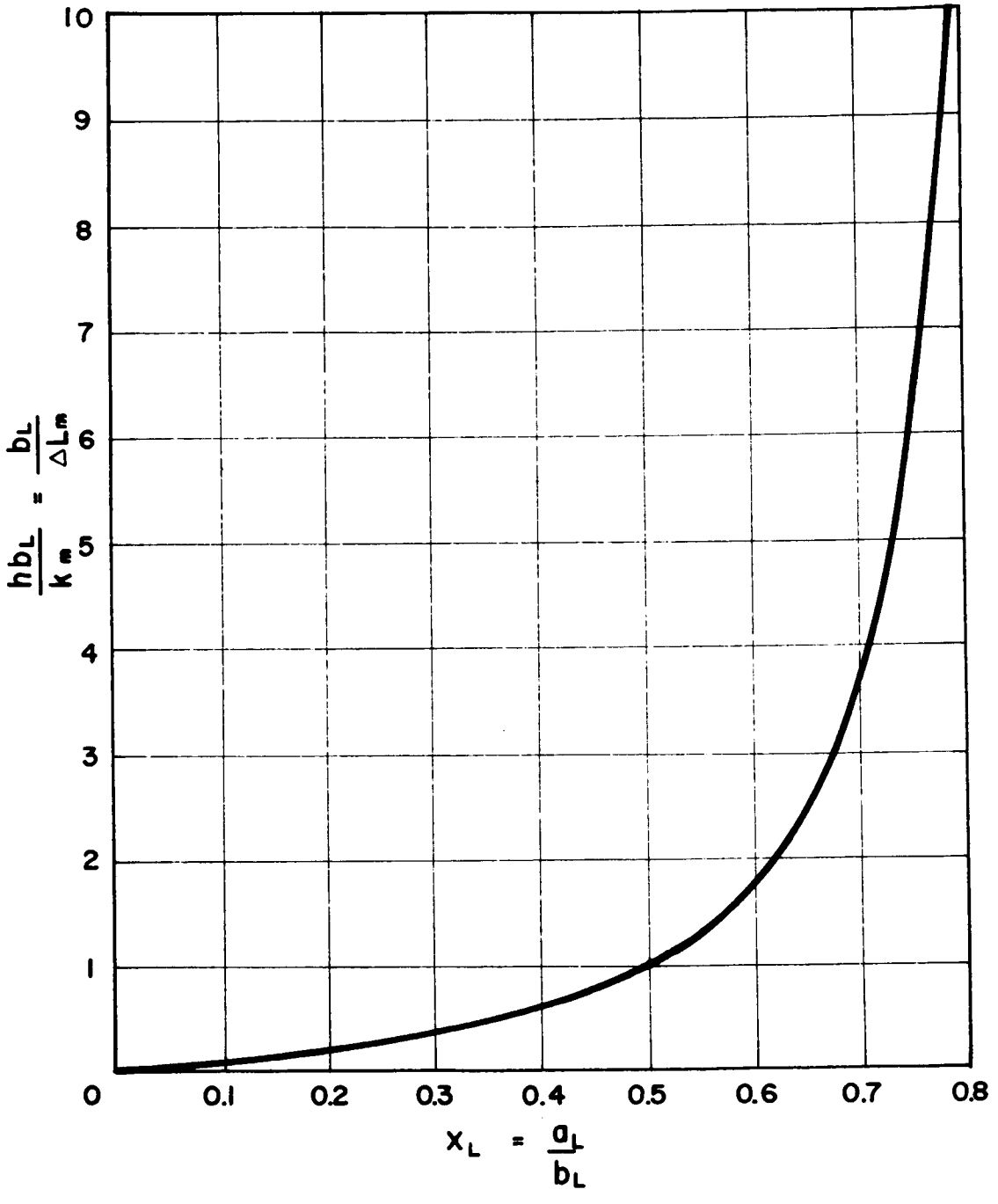

FIG. 9 THE BIOT MODULUS VS THE CONSTRICTION RATIO

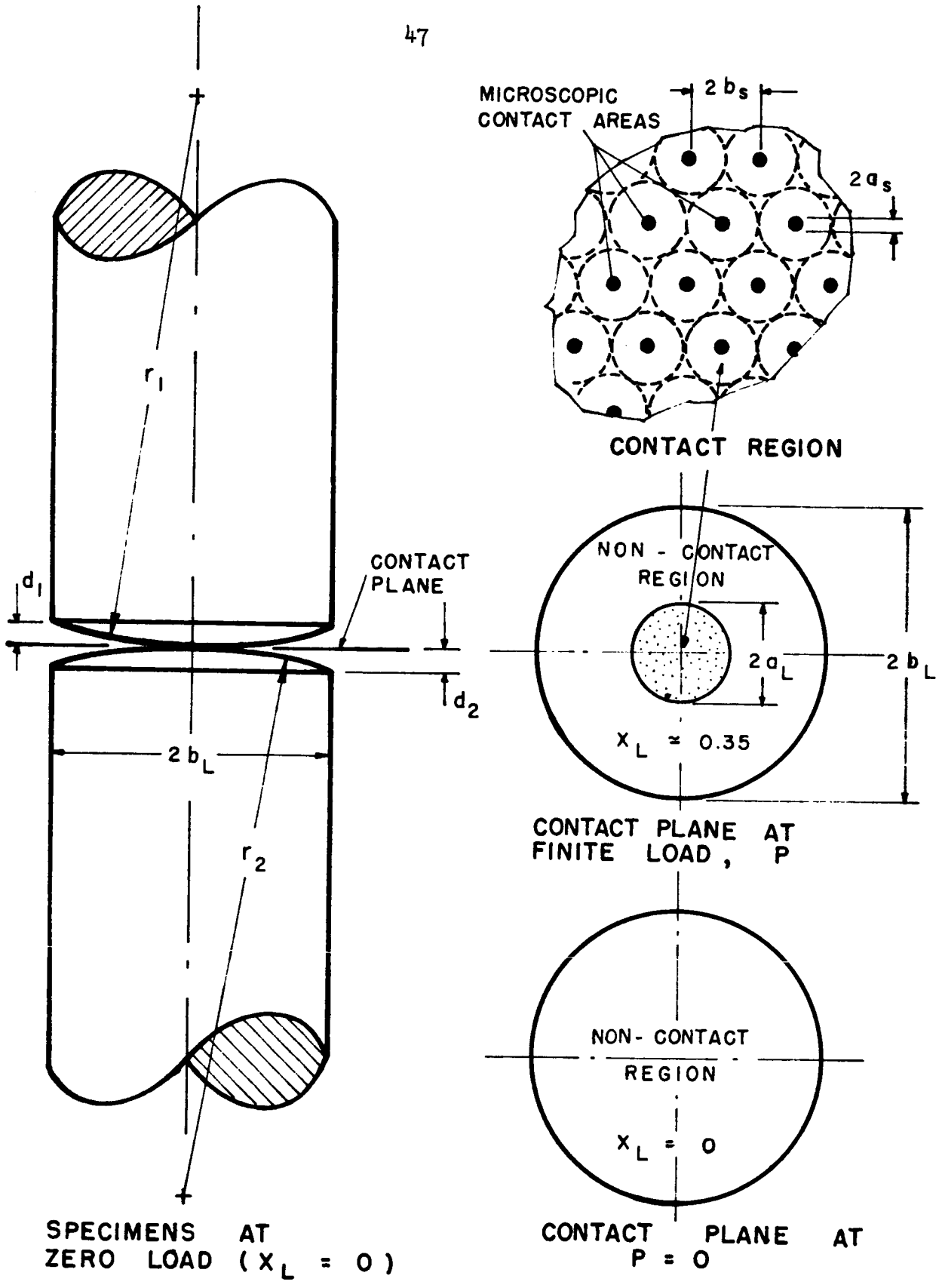

FIG. 10 MODEL OF CONTACT SURFACE

h is proportional to k_m, this is especially true of poor conductors such as stainless steel.

The contact area associated with the large scale constriction region is governed by elastic deformation of the contact members. In order to ascertain the change of area with load, the flatness deviation of the specimens will be simulated by spherical caps of radii r_1 and r_2, situated on the end surfaces of the cylindrical specimens (see Figure 10). Their centers lie on the centerline of the specimen which is also the axis of the applied load. The distance, d, from the base of the spherical cap to the apex, as shown in Figure 10, will be called the equivalent flatness deviation. Since the flatness deviation of a surface is usually very small compared to its other dimensions, the radii of the spherical surfaces of interest are extremely large. Thus:

$$\frac{d}{b_L} \cong \frac{b_L}{2r} \qquad (4.30)$$

The ratio of the equivalent flatness deviation to the radius of the specimen is the significant quantity in the analysis which follows. As a consequence of the spherical geometry, the flatness deviation, d, or the ratio, d/b_L, can be misleading in describing the flatness of the contacting portions of the apparent contact area. For example, in many instances x_L is less than 0.5. In this region of the apparent contact area, the flatness deviation is less than d/4 as is shown in Figure 11.

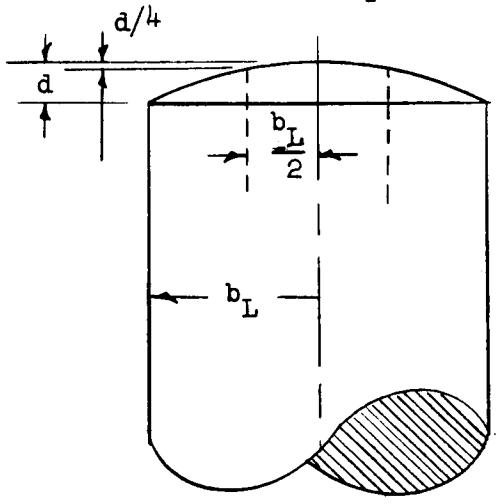

FIGURE 11
SPECIMEN FLATNESS DEVIATION

The geometry of the contacting surfaces has been defined. It remains to be determined how the macroscopic contact area varies with the load exerted between the contacting members. The classical problem of the determination of the contact area between two spherical bodies in elastic contact was solved by Hertz [59]. The radius of the circular contact is:

$$a = \left[\frac{3P}{4} \left(\frac{1 - \nu_1^2}{E_1} + \frac{1 - \nu_2^2}{E_2} \right) \left(\frac{1}{r_1} + \frac{1}{r_2} \right)^{-1} \right]^{1/3} \tag{4.31}$$

where ν is Poisson's ratio, E the modulus of elasticity, P the load, and r the radius of the sphere. In deriving this equation it was assumed that the dimensions of the bodies in contact were large in comparison with the radius of the boundary of the surface of contact. For this reason Equation 4.31 can be applied to our model only for small values of x_L. For larger values of x_L, the value of a_L predicted from this equation is too high. The results reported in Chapter 6 seem to indicate that Equation 4.31 is applicable for x_L less than approximately 0.65. Further work remains to be done to enable the prediction of a_L for x_L greater than this value.

Employing Equation 4.30, r can be eliminated from Equation 4.31. For most metals one may assume $\nu_1^2 = \nu_2^2 = 0.1$. Inaccuracies in the value of ν will have only a minor effect on a. With these, Equation 4.31 becomes:

$$a_L = \left[\frac{2.7}{4} P b_L^2 \left(\frac{E_2 + E_1}{2E_1 E_2} \right) \left(\frac{1}{d_1 + d_2} \right) \right]^{1/3}, \quad x_L < 0.65$$

or, since $x_L = a_L/b_L$ and $p_a = \dfrac{P}{\pi b_L^2}$,

$$x_L = 1.285 \left[\left(\frac{p_a}{E_m} \right) \left(\frac{b_L}{d_t} \right) \right]^{1/3}, \quad x_L < 0.65 \tag{4.32}$$

where E_m is the harmonic mean of the moduli of the two contacting materials and $d_t = d_1 + d_2$, i.e., the total equivalent flatness deviation. The dimensionless group $(p_a/E_m)(b_L/d_t)$ will be called the elastic conformity modulus and is designated for convenience by the Greek letter ζ. Its significance in thermal contact problems is discussed in Section 4.3.

By substituting Equation 4.32 into Equation 4.29, the following equation is obtained for the Biot number $h\, b_L/k_m$:

$$\frac{h\, b_L}{k_m} = \frac{2\, x_L}{\pi\, g\,(x_L)} = \frac{(2)(1.285)\,[\zeta]^{1/3}}{\pi\, g(1.285\,\zeta^{1/3})}$$

or

$$\frac{h\, b_L}{k_m} = \phi(\zeta)\,, \qquad x_L < 0.65 \qquad (4.33)$$

The macroscopic constriction resistance in dimensionless form becomes:

$$\frac{k_m}{h\, b_L} = \frac{\Delta L_m}{b_L} = \frac{1}{\phi(\zeta)}\,, \qquad x_L < 0.65 \qquad (4.34)$$

where ΔL_m may be interpreted as the additional length of the contact members required to produce the same resistance as the interface.

Figure 12 was plotted from Equation 4.33 to show the variation of the dimensionless conductance, hb_L/k_m, with the elastic conformity modulus, ζ. Alternatively a resistance plot is given in Figure 13. Resistance plots are often employed in this investigation instead of the more common conductance plot for the following reasons:

i) It does not mask scatter at low values of conductance. Low conductance regions are more important and should be emphasized. This is the area where the adverse effects of thermal contact resistance must

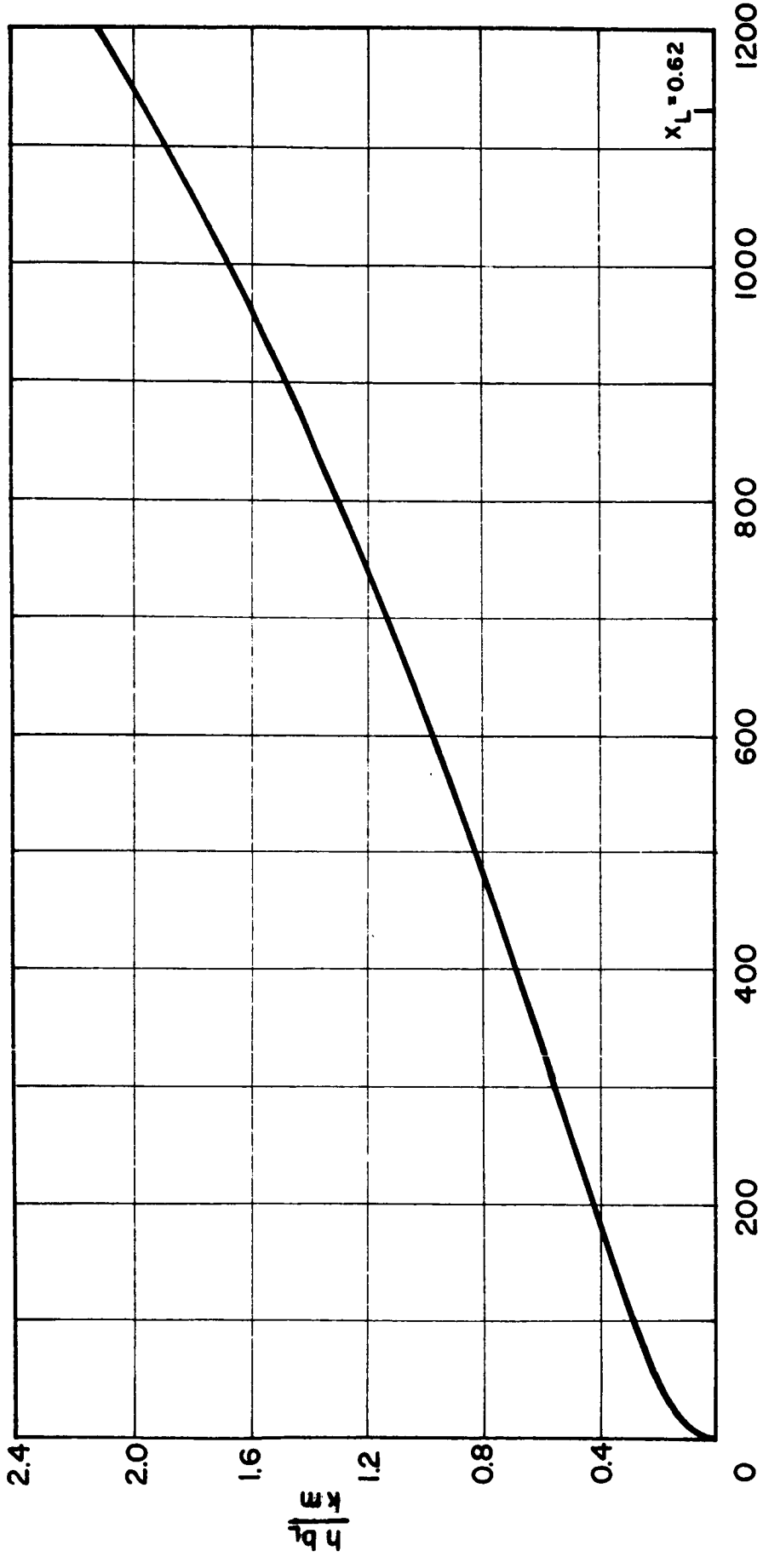

FIG. 12 THE BIOT MODULUS VS THE ELASTIC CONTACT NUMBER

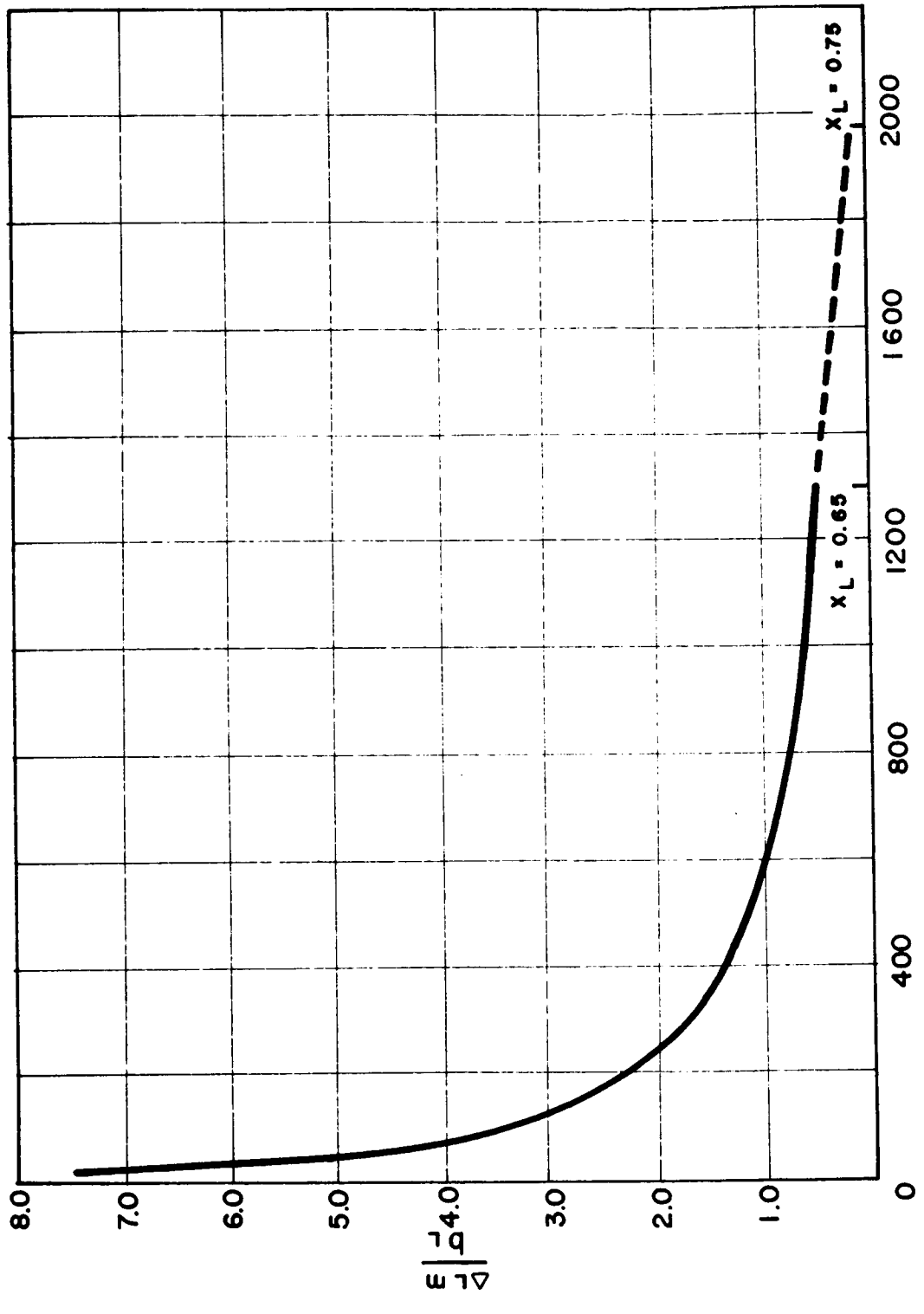

FIG. 13 THE DIMENSIONLESS EQUIVALENT RESISTANCE VS THE ELASTIC CONTACT NUMBER

be considered.

ii) When the resistance is expressed in terms of the equivalent length, it presents a more vivid demonstration of the importance of the thermal joint. Conductance values have been reported which amount to an equivalent resistance of only a few thousandths of an inch of material. Such low resistance interfaces are clearly of no importance to the designer.

The slope of these curves is particularly illuminating. For very small values of x_L, $g(x_L) \cong 1$, and Equation 4.33 reduces to:

$$\frac{h\, b_L}{k_m} = 0.819 \left[\left(\frac{p_a}{E_m}\right) \left(\frac{b_L}{d_t}\right) \right]^{1/3} \qquad (4.35)$$

which shows that under this condition the interface conductance varies as $p_a^{1/3}$. In actuality, such small values of x_L are rare; however, this does explain the highly nonlinear variation of h at small values of p_a that is exhibited in the experimental results. If Equation 4.33 is expanded, an expression of the following form is obtained for hb_L/k_m which is valid for x_L less than approximately 0.65 (limitation due to Equation 4.32):

$$\frac{h\, b_L}{k_m} = A_1\, p_a^{1/3} + A_2\, p_a^{2/3} + A_3\, p_a + A_4\, p_a^{4/3} + \ldots. \qquad (4.36)$$

where A_1, A_2, ... are independent of p_a. The first term of this equation is identical to Equation 4.35. The coefficients of the higher order terms are relatively small; however, as p_a becomes large, these terms gain importance. This explains why the variation of h with contact pressure becomes linear for certain ranges of contact pressure as is exhibited in Figure 12. If Equation 4.33 is employed in the evaluation of h for x_L greater than 0.65, the variation

of h with p_a again becomes nonlinear. As x_L increases, this nonlinearity becomes quite pronounced. If the correct variation of a_L with p_a were known so that it could be employed in the evaluation of h, this nonlinearity would not be as pronounced.

The effect of the presence of a conducting fluid on the macroscopic constriction resistance and on the total interface conductance will now be considered qualitatively. The addition of a conducting fluid would provide a path for the conduction of heat through the otherwise non-contact regions. This path could cause a considerable increase in the total heat flow through the interface. It not only contributes its conductance, $1/R_f$, but it also decreases R_L. Thus, by substituting 4.29 into 3.2, the total conductance becomes:

$$A_a h_t = \frac{1}{R_f} + \frac{2 a_L k_m}{g(a_L/b_L')}$$

where b_L' is the diameter of the adiabatic surface which divides the heat that flows through the macroscopic contact area from that which flows through the non-contact region. Perhaps a more tractable approach is to simply consider that the presence of the conducting fluid causes an increase in a_L to an effective value, a_L'. The total conductance in this case becomes:

$$A_a h_t = \frac{2 a_L' k_m}{g(a_L'/b_L)} \quad .$$

4.1.3 The Effect of Surface Films

Films are always present on metallic surfaces. They vary widely in properties and thickness; hence, their resistance to the flow of heat and electrical current also varies considerably. The insulating effect of surface films in electrical contacts is known to cause severe disturbances. Holm [31] in his book on electrical contacts gives an excellent treatment of surface films and

their effect on electrical contacts. Knowledge of the effect of surface films on thermal contacts, on the other hand, is meager. Several investigators have shown that a considerable increase in thermal contact resistance occurs when relatively thick films are present on the surfaces (see, e.g., references 53 and 55) However, the effect of relatively thin films on freshly machined surfaces is not known. Fenech and Rohsenow [20] stated:

> "Films of oxides, always present on metallic surfaces, do not appreciably affect the thermal resistance of a contact, but has a major importance on the electrical resistance. This comes from the fact that although the thermal conductivity of oxides is not greatly different from the conductivity of the base metal, the electrical conductivity of oxides are considerably smaller than the one of the base metal (theory of semiconductors)."

These arguments may be valid for an interface in the presence of a conducting fluid. However, heat flow for interfaces in a vacuum environment is confined to the relatively small areas of actual contact which results in a large heat flux through these areas. The film effects in this situation may no longer be negligible.

Assuming that the contact model employed for the analysis of the microscopic constriction resistance applies, the resistance due to the presence of a film over the microscopic contact areas becomes:

$$R_o = \frac{\rho}{n_s \pi a_s^2} \quad . \tag{4.37}$$

In this equation, ρ is the resistance across a unit area of the film; n_s is the number of these microscopic contact areas; and a_s is their average radius. If the film is of thickness s, which is large enough to prevent conduction by the

quantum mechanical tunnel effect, ρ can be replaced by:

$$\rho = \frac{s}{k_o} \tag{4.38}$$

where k_o is the intrinsic conductivity of the film. On the other hand, if s is very small, then the tunnel effect furnishes a heat flow independent of k_o, even if k_o vanishes. Holm [31] discusses conduction by the tunnel effect and the calculation of ρ for this case. The reader is referred to this excellent book for more detailed information.

In the analysis of microscopic constriction resistance, Equation 4.13 was employed to determine the microscopic contact area. When it is substituted into Equation 4.37, the following equation results:

$$R_o = \frac{\rho \xi H}{P} \quad . \tag{4.39}$$

This equation for the estimation of film resistance should be used with great caution because:

i) According to Holm (Ref. 31, p. 159) films are partially ruptured when the microscopic contacts are formed. The extent of rupture does not lend itself to analysis or even specification.

ii) Determinations of the thickness and uniformity of thin films, which are of interest in this study, are not reliable. It is also difficult to control the thickness of these films.

iii) The ability to determine the "actual" contact area by the employment of an equation such as Equation 4.13 is subject to question. This was partially discussed in Section 4.1.1. When applied to the analysis of microscopic constriction resistance, the contact area, $n_s \pi a_s^2$, could consist of 99% "holes" and still not affect R_s.

In the case of film resistance, however, this is no longer true. When one deals with distances of a few angstroms or a few atomic diameters, what is a "contact" area?

4.2 THE RELATIVE IMPORTANCE OF MICROSCOPIC AND MACROSCOPIC CONSTRICTION RESISTANCES

As previously stated, the overall resistance to the flow of heat due to the presence of an interface can be represented by a sum of three resistances in series:

$$R = R_L + R_s + R_o$$

All three of these resistances are not always important. Ideally, contact problems could be divided into regions where one of the above three resistances dominates and where two or perhaps all three of them are of importance. In the literature almost all studies have concentrated solely on the analysis of R_s. R_L and R_o have been grossly overlooked.

Since at the present time the magnitude of the film resistance cannot be estimated with any certainty, the relative importance of only the macroscopic and microscopic constriction resistances will be examined. The magnitude of the film resistance can only be determined experimentally. To facilitate discussion, the ratio R_L/R_s will be considered. From equations 4.15 and 4.33, one readily finds:

$$\frac{R_L}{R_s} = \frac{2\left(\frac{p_a}{H}\right)\left(\frac{b_L}{a_s}\right)}{\phi(\zeta)} \qquad (4.40)$$

To evaluate this ratio, H, E_m, b_L, d_t, and a_s must be known. These quantities depend on the materials employed, the specimen geometry and the surface finish.

Since the material and specimen design are usually known, all of these quantities can be easily ascertained except a_s. It was assumed that a_s is independent of the load and that the average size of the microscopic contact areas is of the same order of magnitude as the surface roughness. These assumptions were discussed in Section 4.1.1. Since R_s is a function of $(a_s)(\xi)[g(x_s)]$, it was concluded that the error introduced through an incorrect value of a_s is often partially canceled by the resulting value of $(\xi)[g(x_s)]$.

Table 4 gives calculated values of R_L/R_s for the materials and specimen geometry employed in this study. Representative values of d_t/b_L and a_s were used. The materials which were used cover a wide range of E and H; thus these

Parameters*	R_L/R_s Brass	Stainless Steel	Magnesium	Aluminum
$2a_s = 40$, $p_a = 100$, $d_t/b_L = 400 \times 10^{-6}$	64	49	80	49
$2a_s = 40$, $p_a = 200$, $d_t/b_L = 400 \times 10^{-6}$	78	65	88	58
$2a_s = 40$, $p_a = 100$, $d_t/b_L = 200 \times 10^{-6}$	39	38	44	29
$2a_s = 40$, $p_a = 400$, $d_t/b_L = 800 \times 10^{-6}$	156	130	176	116
$2a_s = 80$, $p_a = 400$, $d_t/b_L = 800 \times 10^{-6}$	78	65	88	58

*$2a_s$ is given in microinches and p_a is given in psi.

Table 4

Comparison Between Macroscopic and Microscopic Constriction Resistances.

comparisons should be representative of most metallic interfaces. In addition, this ratio was found not to vary greatly for the materials that were utilized.

The values of R_L/R_s given in Table 4 show that the macroscopic constriction resistance is approximately two orders of magnitude larger than the small scale constriction resistance. Although there are many assumptions involved in the calculation of R_s, it is difficult to see how these results could be in error by even as much as an order of magnitude. Hence, it is concluded that in many cases the resistance due to the small scale constrictions is negligible, and the macroscopic constriction resistance is the dominating resistance. All previous investigators of thermal contact resistance have placed the emphasis on the analysis of microscopic effects in the development of their models. In the light of the foregoing analysis, it is doubtful that their models can be valid.

The experimental investigation which follows was designed specifically for the analysis of the macroscopic constriction resistance. The theoretical curves, with which the experimental data were compared, include only the effects of this resistance.

4.3 PERTINENT DIMENSIONLESS PARAMETERS AND THEIR SIGNIFICANCE

The application of dimensional analysis to heat transfer problems has enabled many experimentors to correlate their data and to rationally plan new experiments. Dimensional analysis has been especially popular in the field of convection. Recently, an attempt was made by Graff [26] to correlate extensive thermal conductance data using the dimensionless groups, $hp_a/k\rho$ and p_a/H where ρ is the material density. It was found that the data could not be correlated in these coordinates. This was attributed to the omission of a surface roughness parameter.

From the analysis presented in this chapter, one naturally arrives at the dimensionless parameters pertinent to the problem. If macroscopic constriction resistance is dominating, the relevant dimensionless groups are (see Equation 4.33):

i) $\dfrac{h\, b_L}{k_m}$ -- Biot modulus

ii) $\zeta = \left(\dfrac{p_a}{E_m}\right)\left(\dfrac{b_L}{d_t}\right)$ -- elastic conformity modulus .

The Biot modulus is a measure of the relative importance of the thermal contact conductance to the internal conductance. Since k_m/h has the dimension of a length, the reciprocal of the Biot modulus is expressible as:

$$\frac{k_m}{h\, b_L} = \frac{\Delta L_m}{b_L} \quad .$$

As pointed out earlier, ΔL_m may be interpreted as the equivalent length of the contacting members required to give the same resistance to heat flow as the interface. The elastic conformity modulus, ζ, is the ratio of <u>elastic deformation</u> to the <u>flatness deviation</u>. It is a measure of the degree of conformity of the mating surfaces at the macroscopic level.

If the microscopic constriction resistance was dominant, the relevant dimensionless groups would be (see Equation 4.15):

i) $\dfrac{h\, a_s}{k_m}$ -- Biot modulus

ii) $\dfrac{p_a}{H} = \dfrac{p_a}{p_s}$.

The dimensionless group, p_a/H, can be thought of either as a ratio of the

macroscopic stress, p_a, to the microscopic stress, p_s, or as a ratio of the microscopic contact area, A_s, to the apparent contact area, A_a.

5. THE EXPERIMENTAL APPARATUS AND PROCEDURE

Experimentally, the thermal contact resistance was determined by passing an initially uniform heat flux, q, through an interface and determining the additional temperature drop, ΔT, due to the presence of this interface. It is shown in Section 6.2 that the constriction resistance becomes independent of L/b_L if this ratio is greater than approximately 0.6. A ratio of L/b_L of 5.5 was employed in this investigation. Since the study of thermal contact resistance in a vacuum environment was of concern, the specimens were placed in a small vacuum chamber. The load was applied to the test column by means of a loading pin. A vacuum seal between this pin and the chamber wall was effected by employment of a brass bellows. A general view of the apparatus is given in Figure 14 (the diffusion pump had not been installed at the time this picture was taken). Figure 15 is a schematic diagram of this installation. A representative sketch of the test column is given in Figure 16. The test specimens consist of two cylinders which are 1 inch in diameter and 2-3/4 inches long. Five thermocouples were mounted in each specimen to determine the axial temperature gradients. A typical set of specimens is shown in Figure 17. A combination heat source-heat sink (see Figure 19) is located at both ends of the specimen set. This design was employed principally to enable the reversal of the direction of the heat flow without disturbing the test interface. The various parts of the experimental system will now be considered.

5.1 THE VACUUM SYSTEM

The test chamber was constructed of materials with desirable vacuum properties. Thermocouples with Teflon insulation were employed. They entered the

FIG. 14 GENERAL VIEW OF EXPERIMENTAL SYSTEM

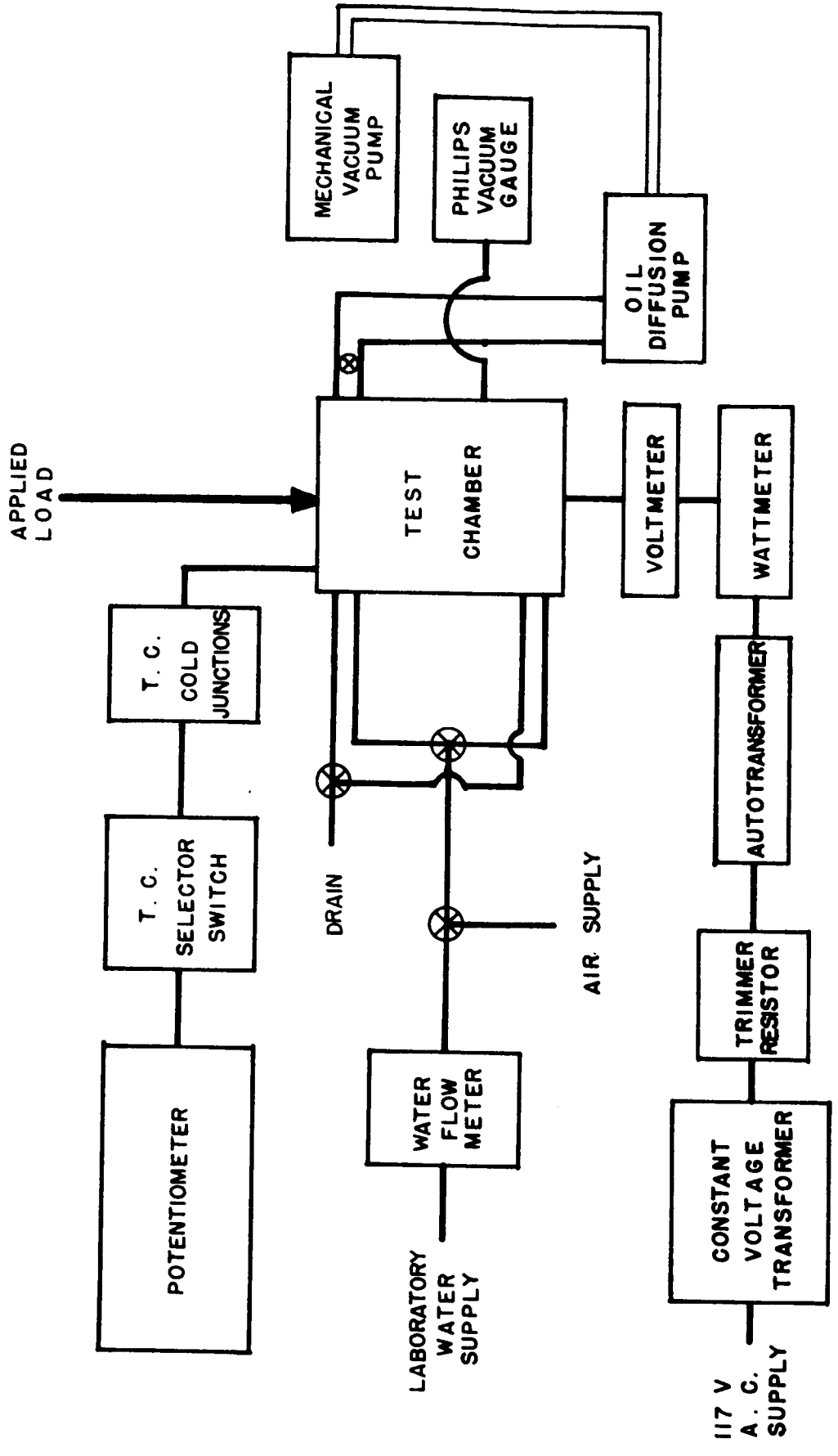

FIG. 15 SCHEMATIC DIAGRAM OF EXPERIMENTAL SYSTEM

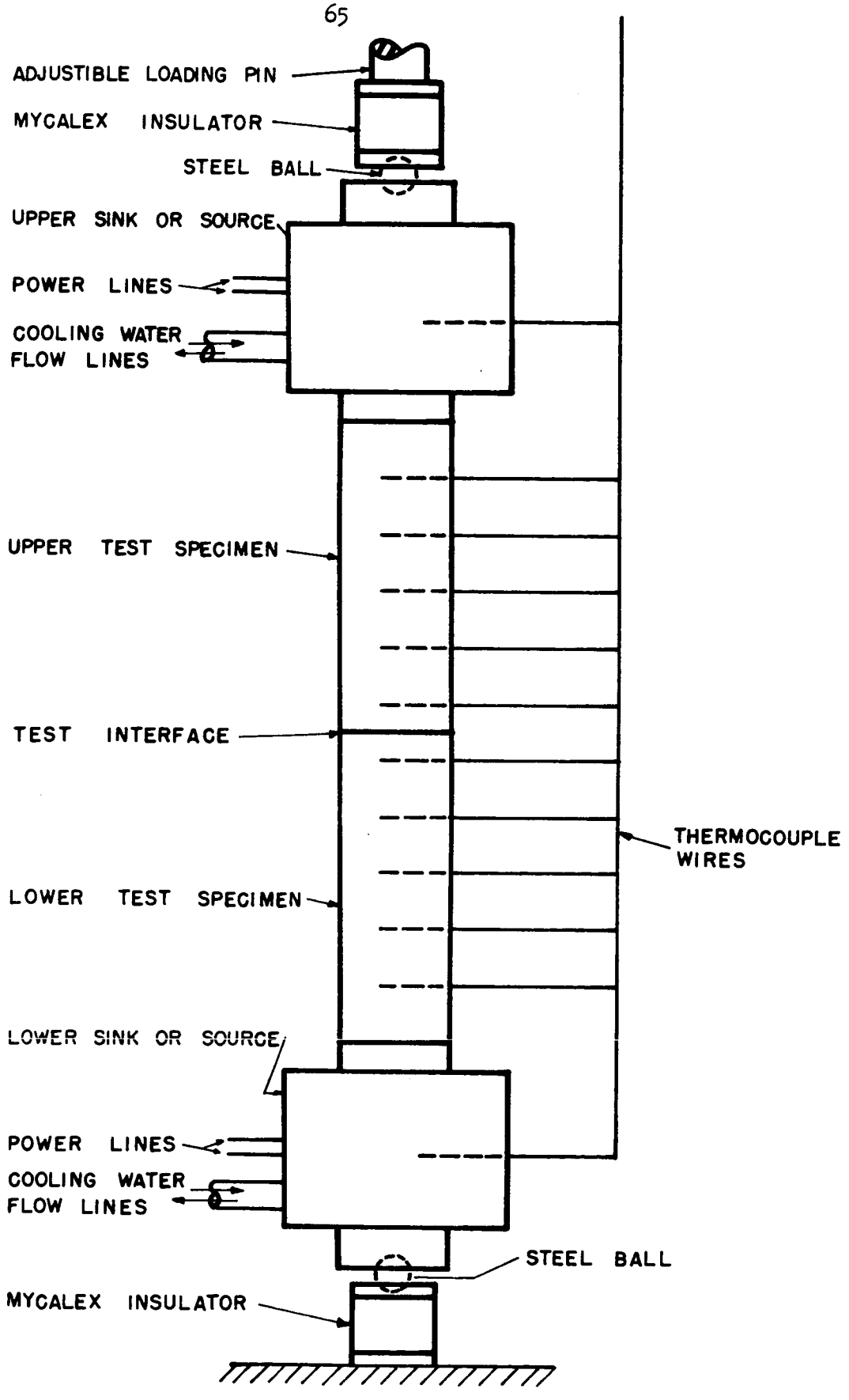

FIG. 16 REPRESENTATIVE SKETCH OF TEST COLUMN

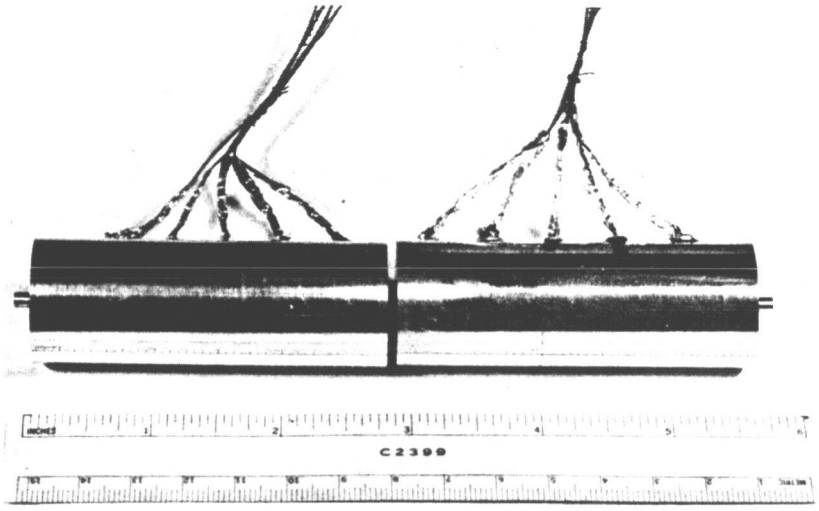

FIG. 17 TYPICAL SET OF TEST SPECIMENS

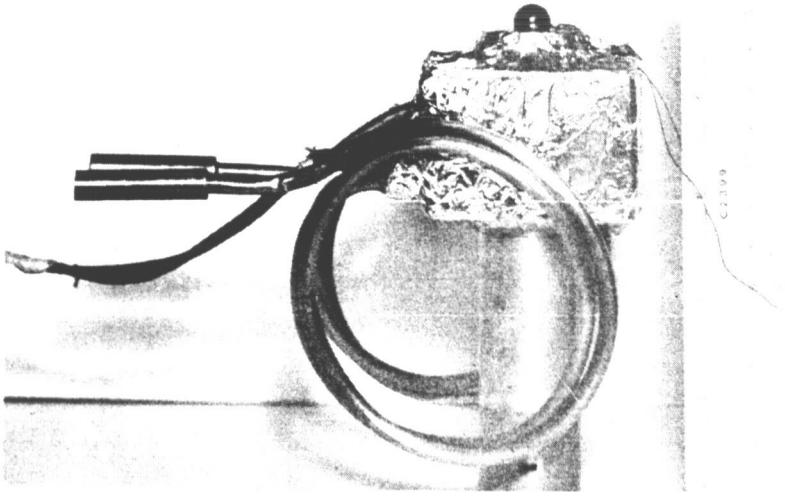

FIG. 18 COMBINATION HEAT SINK & HEAT SOURCE

chamber through Kovar glass-to-metal seals in which they were anchored by means of red sealing wax. It was possible to seal the thermocouple wires without removing the insulation. Initially, the chamber was evacuated solely by means of a 1405 H Welch mechanical pump. Curves showing the evacuation rate are given in Figure 19. Later a Consolidated Vacuum Corporation type VMF-20 oil diffusion pump was added. Using only the mechanical pump, the ultimate vacuum was approximately 8×10^{-4} mm of Hg. With the addition of the diffusion pump, a pressure of about 6×10^{-6} mm of Hg was obtained after only a day of pumping. The ultimate pressure was approximately 3×10^{-6} mm of Hg. A curve showing the evacuation rate after the diffusion pump was installed is also given in Figure 19. All the pressure measurements were made with a Philips PHG-09 vacuum gauge.

Most of the experimental data were taken after the diffusion pump was installed. However, since it has been established that a pressure of one micron of Hg is sufficiently low for our purposes, data taken prior to the installation of the diffusion pump are included. The use of the diffusion pump increased the pumping speed, and the high vacuum it created virtually eliminated the small heat loss due to the residual, rarefied gas. In practice, a day or two was allowed for the complete outgassing of the test interface before its thermal resistance was measured.

5.2 THE LOADING MECHANISM

The apparent contact pressure exerted between the test specimens is one of the most important variables affecting the contact resistance. The contact pressure in these tests was varied from approximately 10 to 1000 psi. This pressure range was established with the aid of the thermal contact resistance measurements reported in the literature and the torque specifications for the

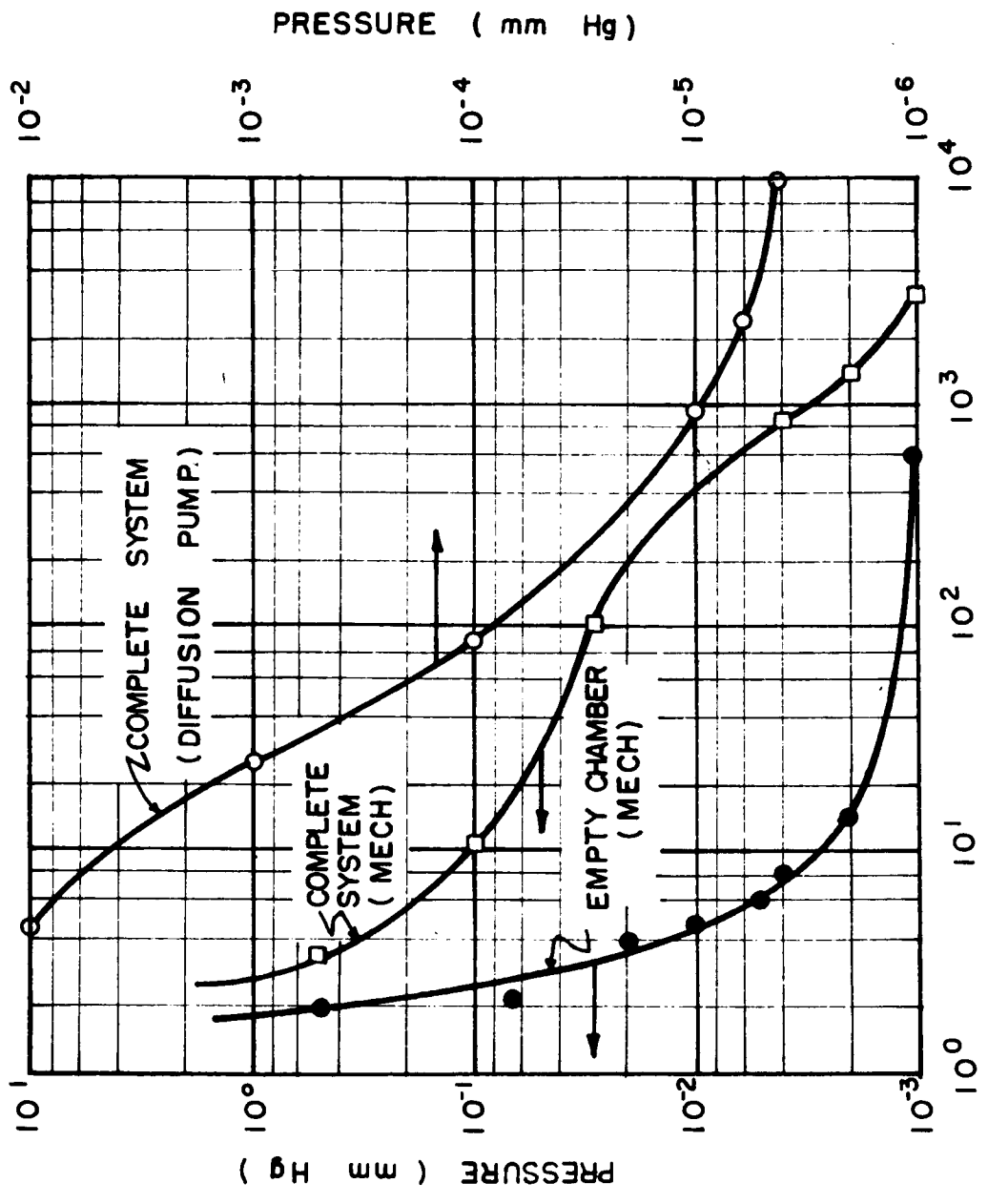

FIG. 19 EVACUATION RATES FOR VACUUM SYSTEM

Ranger series spacecraft [32]. The pressure was applied by means of a dead-weight lever system which eliminated additional loading due to thermal expansion. Small corrections were applied to account for the atmospheric pressure acting on the loading pin and for the weight of the elements in the column above the test interface. The load due to the weight of the lever arm and loading pan was also carefully determined. In order to make the loading effects of the cooling water flow lines small, a flexible coil was constructed from thin-wall, small diameter tubing (see Figure 18). A load cell which consisted of four SR 4 strain gauges mounted on a 1" diameter tube was employed in place of the specimens in order to determine the magnitude of the frictional forces in the loading system. By a comparison of the readings indicated by the load cell when the load was approaching some pre-selected value from either below or above, and when the lever arm system was subjected to slight vibration at that load, the effect of the frictional force was ascertained. These measurements showed that the frictional forces varied from approximately 15% to 3% of the total applied load as the load varied from a few psi to approximately 1000 psi. However, these measurements also revealed that most of this frictional loading could be eliminated by a slight vibration of the lever arm system after the column was loaded and had attained steady conditions. An analysis of the possible error of the loading system indicates that at the lowest value of contact pressure (approximately 10 psi), the error in p_a should be less than 2 psi, i.e., 20%. At the highest value of contact pressure (approximately 1000 psi), the error in p_a should be less than 2%.

5.3 PRODUCTION AND MEASUREMENT OF THE HEAT FLUX - ATTAINMENT OF STEADY CONDITIONS

A combination sink-source was located at each end of the test column (see Figure 16). It consisted of a relatively heavy block of oxygen-free high

conductivity copper. A 100 watt, 3/4" diameter, hermetically sealed cartridge heating element was installed inside this block. A multi-channel passage also was provided for cooling water circulation.

During the early stages of the development of the test apparatus, the heat flux was determined from the temperature gradients in the heat meters which were cylinders 1" in diameter and 1-3/4" long. For reasons to be seen shortly, the specimens were lengthened and the heat meters removed. It was found that the heat loss could be predicted with greater accuracy than anticipated, which, coupled with inaccuracies in determining the temperature gradients in the original arrangement, revealed the superiority of the present design. The heat flux was determined in this design by subtracting the heat losses from the power input that was obtained from the simple relation $P = E^2/R$ (this equation does not assume a power factor of 1). The voltage was determined by a multiple range Weston voltmeter whose accuracy was within 1/4 of 1% of the full scale reading. Thus, E^2 was never in error by more than one percent since all readings were above half scale. R was measured with an ESI Universal Impedance Bridge. The error of this instrument for resistance measurements was less than 0.1%. Although the resistance of the heating elements varied several percent from room temperature to the maximum operating temperature, it presented no difficulties since the resistance measurements were made at the operating temperatures. A small correction was also made for the lead resistance. The calculated power input was in error by less than one percent.

In order to determine the heat flux, Q, the heat losses must be known. The heat losses from the column are a function of the temperature of the various elements in the chamber, the ambient pressure in the chamber, the chamber wall temperature, the load on the column and the emissivity of the specimens' surfaces. An accurate prediction of the heat losses was anticipated to be

difficult; thus, the early design employed heat meters. Later it was determined that the heat losses were relatively small and could be estimated accurately. The latter was possible because:

i) The heat loss due to the rarefied gas in the chamber was negligible at the normal operating pressure.

ii) The heat loss varied almost linearly with temperature; thus it was possible to estimate losses based on a temperature difference instead of the absolute temperature.

iii) The heat lost by the specimens was a small portion of the total loss because of their low emissivity and relatively small surface area.

The heat loss data given in Figure 20 were obtained by determining the temperature at which the heat loss was balanced by the power input. Some of the low load data were obtained by replacing the specimens with a small diameter steel rod. This means was employed to differentiate between the heat lost by the specimens and the total heat loss. These data also showed that the heat loss from two identical combination source-sinks was approximately the same. Figure 20 includes data for both high and low column loads. Hence, the load effect on the heat loss was known. The data presented in Figure 20 were obtained before the installation of the diffusion pump; however, later data showed that a further reduction in chamber pressure caused a negligible change in the total heat loss.

By employing the data of Figure 20, it was possible to estimate the heat loss from the test column with an error of less than 15% except for tests run at elevated chamber pressures. If the contact resistance was small, a 15% error in the heat loss resulted in an error in the heat flux which ranged from 1 to 8% for the materials employed in this investigation. When the contact resistance was large, or when a test was made at an elevated chamber pressure,

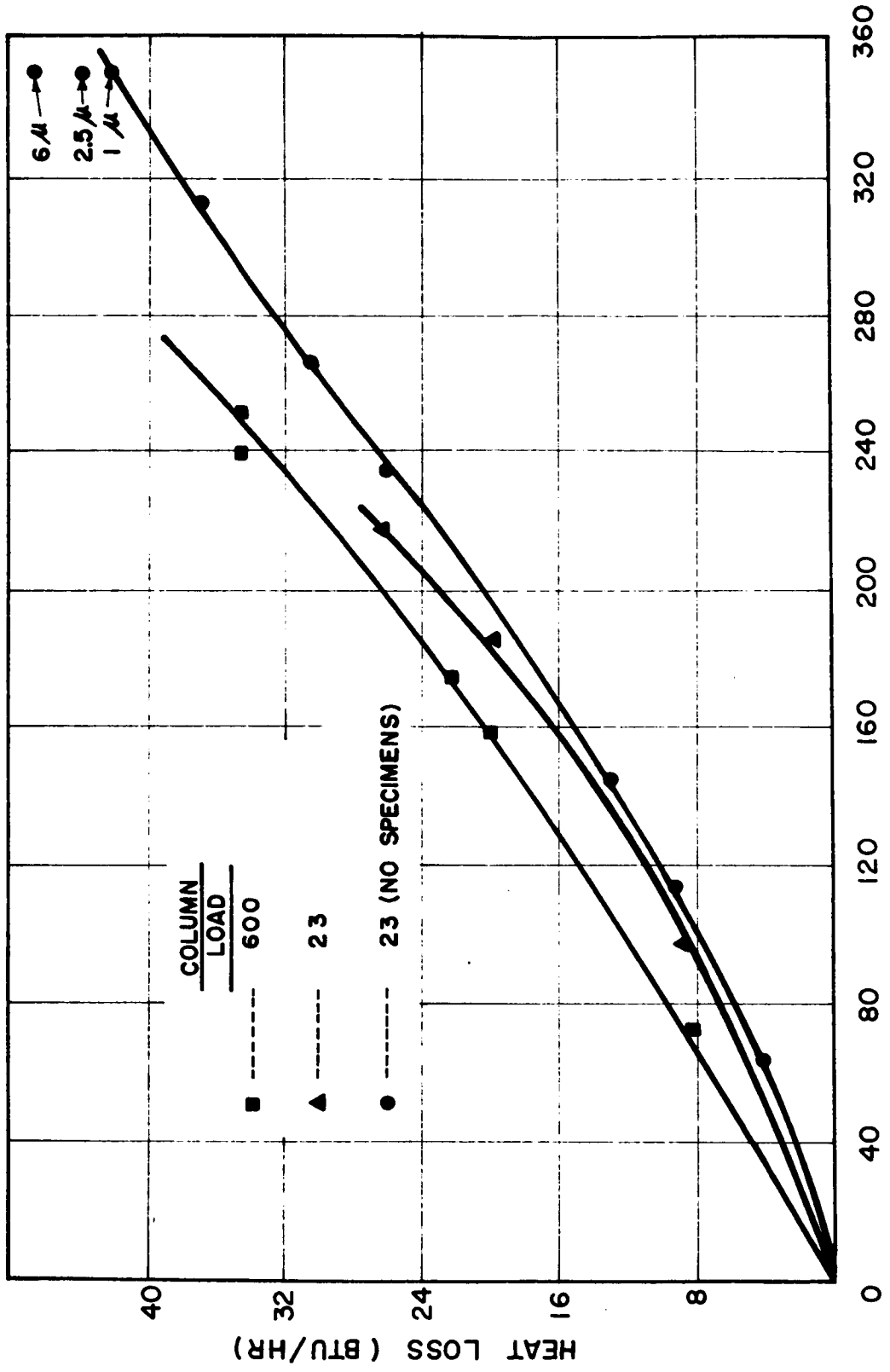

FIG. 20 HEAT LOSS FROM APPROXIMATELY ISOTHERMAL COLUMN VS DIFFERENCE BETWEEN COLUMN TEMP. AND CHAMBER TEMP. (CHAMBER PRESSURE OF APPROX. 1μ OF Hg)

the specimens were employed as heat meters. In this case the heat flux was determined from the temperature drop across the specimens and the previously determined thermal conductivities.

The thermal conductivity of all materials employed, except stainless steel, was determined to an accuracy of a few percent by averaging the values obtained from several tests. These data were believed to be more accurate for the particular specimens employed than the available data in the literature. Stainless steel has a low conductivity; hence, a determination as accurate as those of the other materials was not possible. For this reason, more weight was placed on the thermal conductivity data reported in the literature for this material. It can be seen in Appendix A that the agreement between the data from the literature and the measured conductivities is generally good.

Using the procedures discussed, it was possible to determine the heat flux to an accuracy within 8%; in most cases, the error was less than 3%. Furthermore, it remained relatively constant from test to test; hence it did not mask the influence of the variables under investigation. The accuracy could be further improved if a more meticulous analysis and control of the heat losses were made.

The method employed for evaluating the interface conductance requires that all measurements be made after the system attains steady state. Thus, it was essential to have a constant power input, constant cooling water temperature and constant values of interface conductance. The power input was maintained constant by means of a Westinghouse induction voltage regulator. An autotransformer was employed to select the desired voltage level. To enable very fine voltage adjustments, a small variable resistor was placed in series with the load. By means of these elements a stable power input at any desired level was obtained. There was only a small amount of fluctuation in the cooling water temperature; thus, no regulation was necessary. As an illustration, it was

noted that during the last series of tests the difference between the maximum and minimum sink temperatures encountered over a period of twelve hours was only 1.5°F. The cooling water flow rate was purposely kept quite large to minimize the influence of its fluctuations on the sink temperature.

It was observed that the thermal contact resistance in most cases was, for all practical purposes, independent of time; however, some variation with time was noted for magnesium at all loads and stainless steel at very light loads. This was detected from the monitored potential difference between the thermocouples on the two sides of the test interface. The variation of the thermal contact resistance exhibited by magnesium was caused by the creep of the contact members. Since its effect on the total resistance of the column was practically negligible, no difficulty arose in the determination of the contact resistance at a given time. The fluctuations experienced with stainless steel at light loads was probably a result of the effect of thermal strain. Section 6.1.3 gives a brief discussion of this phenomenon. Due to the difficulty of obtaining steady state conditions for stainless steel, the smallest load was not attempted in several series. The error in the data reported may have been several percent as a consequence of these transient effects.

5.4 TEMPERATURE MEASURING TECHNIQUE

Since the accuracy of the determination of the interface conductance is greatly dependent on accurate temperature measurements, much attention was focused on this aspect of the experimental problem. All temperature measurements were made with #30 gauge copper-constantan thermocouples. Special precision wire was employed and calibrated to within an accuracy of 0.1°F. This was done in a special laboratory furnace using a 25 ohm platinum Thermohm as the standard. A Leeds and Northrup 8686 millivolt potentiometer was employed

for measuring the thermal EMF of the individual thermocouples. Within the temperature range of interest, its maximum error is approximately 3 microvolts, which corresponds to about 0.15°F. A 24 point Leeds and Northrup selector switch made convenient the successive reading of the thermocouples. All thermocouples had individual cold junctions. Copper-constantan quick change connectors were utilized to facilitate changing specimens. They eliminated possible error due to the introduction of additional junctions. Judging from the results of the calibrations and the accuracy of the equipment employed, the relative accuracy of any particular thermocouple should be within approximately 0.15°F. However, an important and difficult problem still remains. Does the test junction assume the temperature of the substance being measured?

In an effort to achieve a satisfactory solution to this problem, the following steps were taken. Number 30 gauge thermocouple wire was employed to minimize conduction of heat through the thermocouple wire. The selection of this particular size was based on correspondence with a Leeds and Northrup Field Engineer [49]. Smaller wires tend to exhibit adverse EMF characteristics caused by the wire drawing operation; they also break easily. The thermocouples were mounted in 0.046" diameter holes drilled 5/8" deep in the 1" diameter specimens.

In the presence of a conducting fluid, a thermocouple mounted in such a hole readily assumed the temperature of the specimen; however, a correct temperature reading was more difficult to obtain in a vacuum environment. Following procedures reported by several investigators (see references 7 and 61), the thermocouple was initially fixed in the small hole with copper dental cement. To check the accuracy of the thermocouple installed in this manner, a small voltage was applied to the two heating elements connected in parallel; hence both ends of the test column became heat sources. It was observed that the entire column eventually reached a nearly isothermal condition when the power

input just balanced the heat loss. However, at a temperature level of 290°F, random variations of the order of 40°F were exhibited by the thermocouples in the same specimen. Silver amalgam, an alloy used for dental fillings, was then tried. The results were considerably better; however, the accuracy of the thermocouple readings deteriorated with time until errors of several degrees became common. This was probably caused by the mercury coming out of solution and evaporating when the alloy was subjected to the temperature levels employed. Reference 36 stated that silver amalgam is unstable at temperature levels greater than approximately 180°F.

Finally, after further searching and testing, the following mounting procedure was adopted and found satisfactory. The thermocouple was inserted into the hole and small pieces of lead foil were tamped around the junction. Tamping was done by hand employing a small metal drill. The hole was filled with lead to a depth of approximately 3/8 of an inch. The remainder was filled with epoxy. It was employed only to reduce the chance of forming a new junction near the specimen surface, which could occur if the Teflon insulation on the thermocouple wires was damaged. With this procedure, the errors in the thermocouple readings were found to be less than approximately 0.2°F.

Another source of error in the temperature measurements was due to uncertainties in the location of the thermocouple junction. The diameter of the twisted junction of number 30 gauge wire was approximately 0.020 inches. It was placed in a 0.046 inch diameter hole (#56 drill). Thus, the thermocouple junction could have been located 0.013 inches from the centerline of the hole. In addition, the location of the hole was possibly a few thousandths of an inch in error. These uncertainties could have resulted in errors as large as 1°F in this investigation.

Macroscopic constrictions at the interface between specimens give rise to appreciable radial temperature gradients in its neighborhood. These result in what appear to be errors in the temperature readings of the thermocouples near these interfaces. Such local disturbances in heat flow cause difficulty in determining the desired undisturbed temperature gradient for the determination of the temperature drop, ΔT. This problem has been greatly reduced by increasing the length of the specimens and using a small amount of silicone high vacuum grease in all joints except the test interface. Figure 21 illustrates the magnitude of this disturbance which was experienced before the above corrective measures were taken.

In projecting the temperature gradient in a specimen to the interface, attention must be given to the curvature in this gradient resulting from the variation of the thermal conductivity with temperature. In some instances appreciable error would result if this curvature were overlooked. All the materials investigated exhibited a variation of the conductivity with temperature; however, by employing the procedure outlined in Chapter 3, this difficulty was removed.

Curvature in the temperature gradient can also result from two other sources: nonhomogenous specimens and heat losses from the specimen's surface. The thermal conductivity of tempered metals, such as 2024T4 aluminum, changes with time due to annealing, even at the temperature levels of this investigation. For example, Reference 15 stated that the conductivity of 2024T4 would increase by approximately 25 percent if it was annealed at 375°F for a few hours. This effect also was revealed by test series 8_A (these results are discussed in Section 6.1.4). Since the temperature of the portion of the specimen nearest the source is the highest, the annealing effect in a test series would be the greatest in this region. Thus, the existence of temperature gradients will result in a thermal

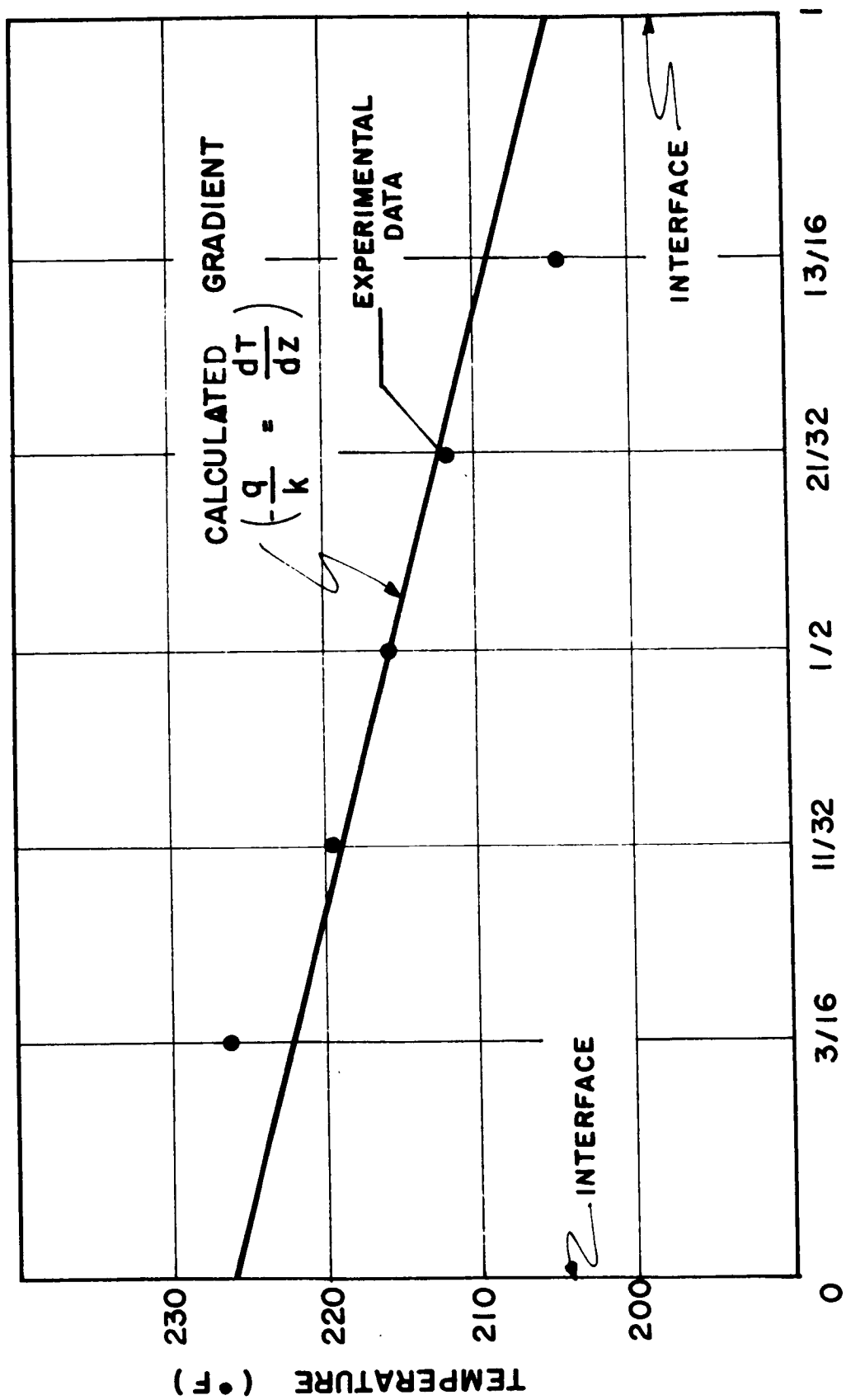

FIG. 21 THE INFLUENCE OF MACROSCOPIC CONSTRICTIONS ON THE TEMPERATURE GRADIENT
(EARLY SPECIMEN DESIGN OF 1" LENGTH)

conductivity gradient. It is difficult to take such effects into account.

In a vacuum, heat loss from the specimen's surface was only by radiation. It was small since the surface was highly polished. In general, it produced a negligible effect on the axial temperature gradient; however, the effect was detectable in the case of stainless steel specimens, particularly when the heat flux was low. It had to be considered in evaluating the temperature gradients for this material.

In conclusion, it can be stated that if the thermal contact resistance is moderate or high, the accuracy with which ΔT can be determined by the procedure established in the present investigation is adequate. On the other hand, if conditions are such that the contact resistance encountered is very low, a more sophisticated apparatus and procedure would be required. Considering the combined effects of all sources of uncertainty, the overall experimental error in the determination of ΔT is not believed to exceed $2^{\circ}F$. The relative error is considerably less. Some of the difficulties discussed above had not been completely resolved when part of the data reported in this study was taken. Thus, for test series 1_B through 7_B and also 1_A and 2_A, an error in ΔT as large as $3^{\circ}F$ may have been present. Fortunately, the contact resistance encountered in these early series was usually large; thus the data were acceptable.

5.5 SPECIMEN DESCRIPTION - MEASUREMENT OF SURFACE PARAMETERS

Figure 22 gives the dimensions of the specimens and the thermocouple locations. Three different procedures were employed in the preparation of the specimens' test surfaces. They were: 1) hand polished on a rotating disk charged with lapping compound, 2) lapped by hand on an optically flat surface, or 3) lapped on a commercial lapping machine. Surfaces of flatness deviation

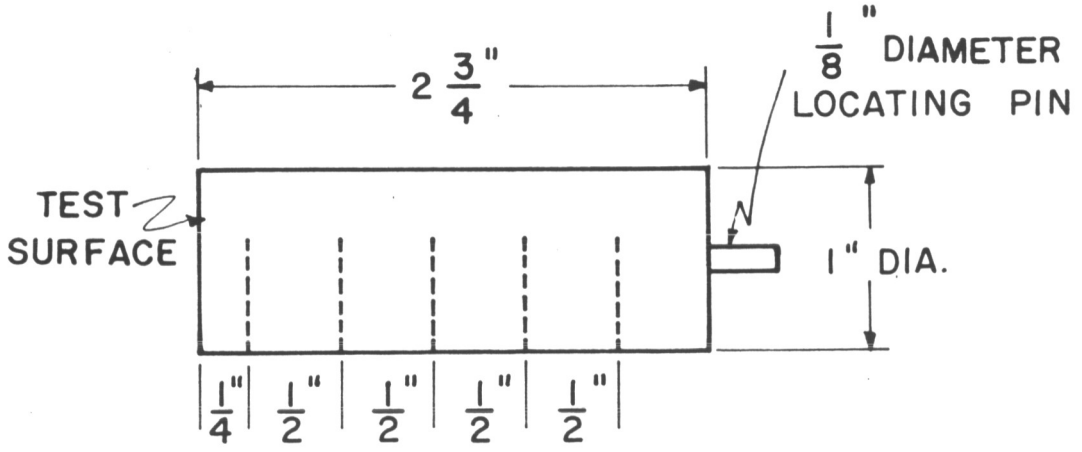

FIG. 22 SPECIMEN DIMENSIONS & THERMOCOUPLE LOCATIONS

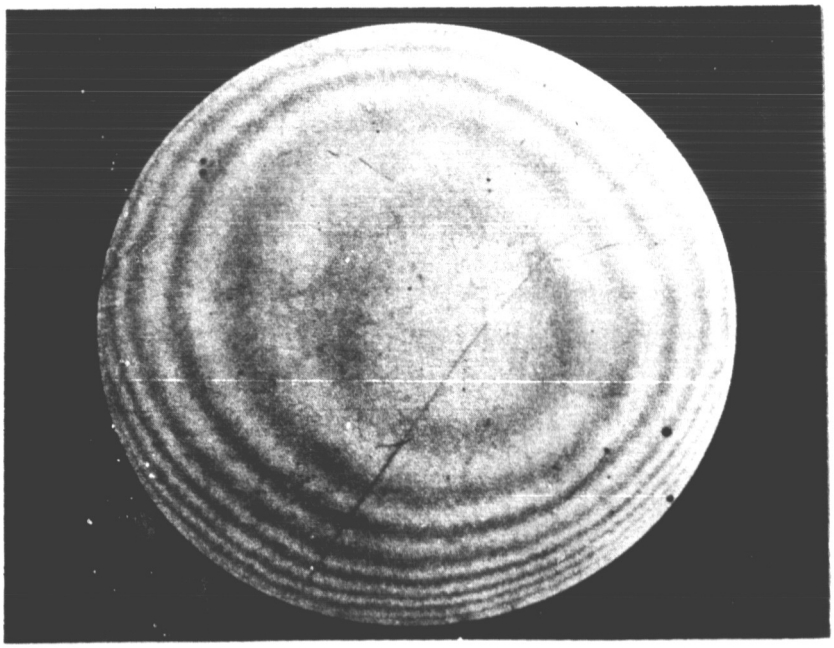

FIG. 23 OBSERVED NEWTON RINGS ON TEST SURFACE

varying from a few microinches to several hundred microinches were obtained. The surface roughness of these surfaces was generally over 12 microinches, rms; thus they had to be polished before optical measurements of flatness were possible. The surfaces were hand polished on an optically flat surface covered with a Buehler nylon polishing cloth, using 0.3μ Al_2O_3 powder along with a copious supply of water. The surface roughness obtained in this manner was about 3 microinches with the exception of a few deeper scratches on some of the surfaces. The degree of irregularity of the interference fringes provides a measure of the roughness (see Reference 58). Optical roughness determinations were slightly lower than the profilometer measurements. This was probably a result of the inclusion of the deeper scratches in the root-mean-square value which the profilometer indicated.

Two procedures were employed to determine the macroscopic contour of the test surfaces. First, a specimen holder with an optically flat base was constructed. It was wrung to the lapped table of a Pratt and Whitney Electrolimit Gage. By moving the test surface under the gage head, the flatness deviation was ascertained. Since the flatness deviation was large for the brass specimens, it could be determined with sufficient accuracy by this procedure. These surfaces were later polished and the contour checked by the optical method. The agreement between the two values was within 10%.

For smoother surfaces, the optical procedure was superior. Both the surface contour and flatness deviation could be determined from the observation of the interference fringes. Between the center of one dark band and the center of the next dark band, the level of the work has risen or fallen 11.6 millionths of an inch relative to the surface of the optical flat (helium monochromatic source). Figure 23 shows an enlargement of the interference pattern on a specimen whose equivalent flatness deviation is approximately six fringes. The sphericity of

the surface was estimated from the relative distance between the fringes. The surfaces were found to be approximately spherical after lapping; however, the magnesium specimens became nonspherical after testing as a result of creep. When the specimens were within one or two fringes of being flat, no accurate way of checking for sphericity was known. It was estimated that when d was between 1 and 3 fringes, the accuracy obtained was within 25%. When d was of the order of 10 fringes, the accuracy was within 10%. A precision, laboratory-quality optical flat must be used in these measurements. Not all commercial flats available are acceptable.

The material hardness was measured using a Tukon microhardness testing machine. These results are given in Appendix A. The effect of the indentor load is also given.

5.6 THE CONDUCTIVE - LIQUID ANALOG SYSTEM

To provide a convenient means of investigating the geometrical aspects of contact on the thermal constriction resistance, a conductive-liquid analog was constructed. Specifically, the influence of the distribution of the macroscopic contact area, the size of this area and the length of the contact members on the macroscopic constriction resistance was studied. The conductive-liquid analog makes use of the well known analogy between electrical and thermal quantities. A photograph of the analog used in this study is given in Figure 24. Distilled water with a resistivity that ranged from 10^4 to 2×10^6 ohm-cm was employed as the electrolyte. To simulate the cylindrical geometry of the actual test specimens, the electrolytic tank was constructed of a cylindrical Lucite tube. Assuming symmetry with respect to a diameter of the contact area, it was sufficient to employ a semi-cylinder. Since the resistivity of Lucite is several orders of magnitude higher than that of the electrolyte, these surfaces

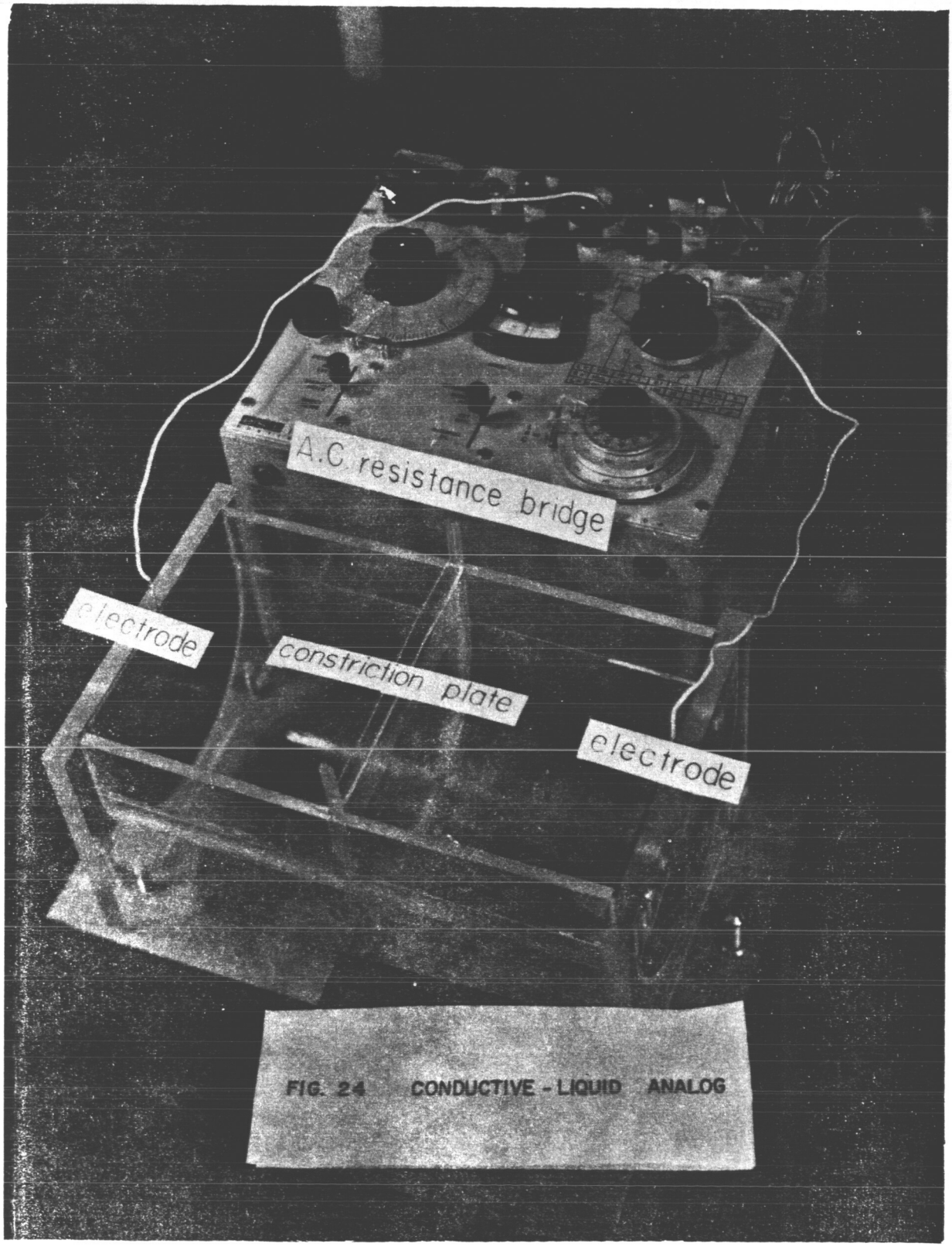

FIG. 24 CONDUCTIVE - LIQUID ANALOG

accurately simulated the adiabatic condition. The electrodes, which were fabricated from etched and graphited brass plates, were placed at both ends of the tank. They gave the desired constant potential boundary conditions. The ratio of the specimen length to its radius could be readily changed by moving the electrodes. A thin sheet of Mylar, 0.002 inches thick, was placed into a central groove of the tank to simulate the contact plane. The macroscopic contact area was represented by a hole or series of holes cut in this Mylar sheet. The resistance between the two electrodes with and without the Mylar sheet was determined with an ESI model 250-DA universal impedance bridge. In this measurement, an AC potential up to 15 volts and of one kilocycle frequency was applied across the electrodes. The reason for an AC voltage source was to avoid polarization at the electrodes. The constriction resistance, R_L, was obtained from the difference of the two resistance measurements. The accuracy of the system is demonstrated and the results are presented in Section 6.2.

6. EXPERIMENTAL RESULTS

The model employed in this analysis involves many assumptions. The complex nature of the problem and our limited understanding of the various mechanisms governing it do not permit a detailed study at the present time. This is especially true since the microscopic properties of the contacting surfaces can be prescribed only in terms of statistical quantities which are not completely established. Considerable weight, therefore, must be placed on the experimental investigation. A prudent analysis of the experimental results is required to test the validity of the assumptions and to assess the relative importance of several factors involved.

Four different materials with widely different properties were employed in the investigation. The results will first be considered individually. Later these materials will be compared and a discussion of their traits will be given.

6.1 CONTACT RESISTANCE MEASUREMENTS - COMPARISON WITH THEORETICAL PREDICTIONS

6.1.1 Brass Specimens

Figure 25 shows the variation of interface conductance with apparent contact pressure for the three different brass specimen sets tested. The total flatness deviations for these specimens were not considerably different. The variation in the interface conductance exhibited is, to a large extent, due to differences in the mean interface temperature which ranged from 160°F to 340°F. This resulted in a considerable difference in E_m and k_m. Figure 26 shows a comparison of these data with theory. The theoretical curve was obtained from Equation 4.34. The resistance in terms of the equivalent length, ΔL_m, varied from

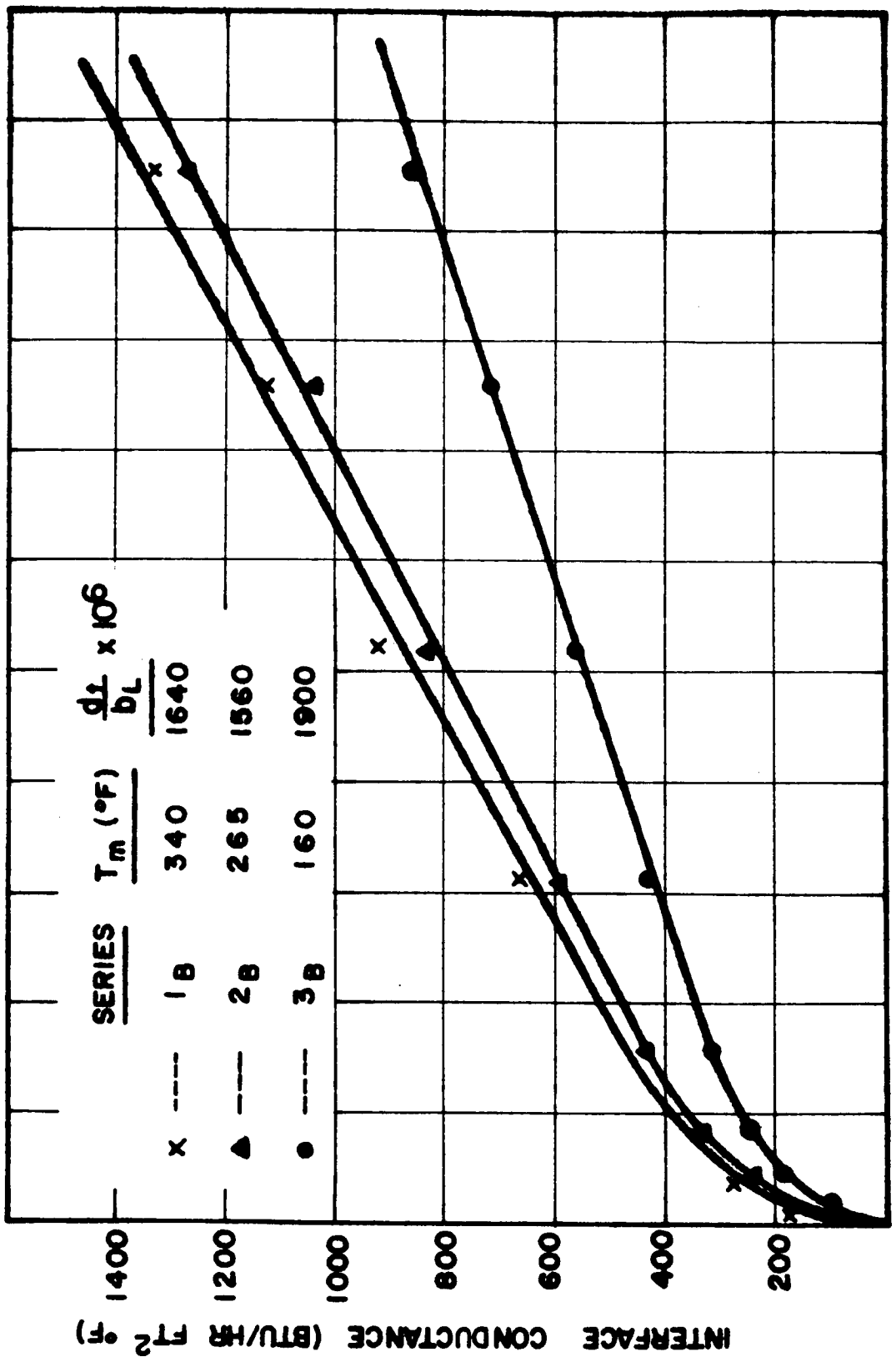

FIG. 25 THE INFLUENCES OF T_m AND $\frac{d_t}{b_L}$ (BRASS SPECIMENS)

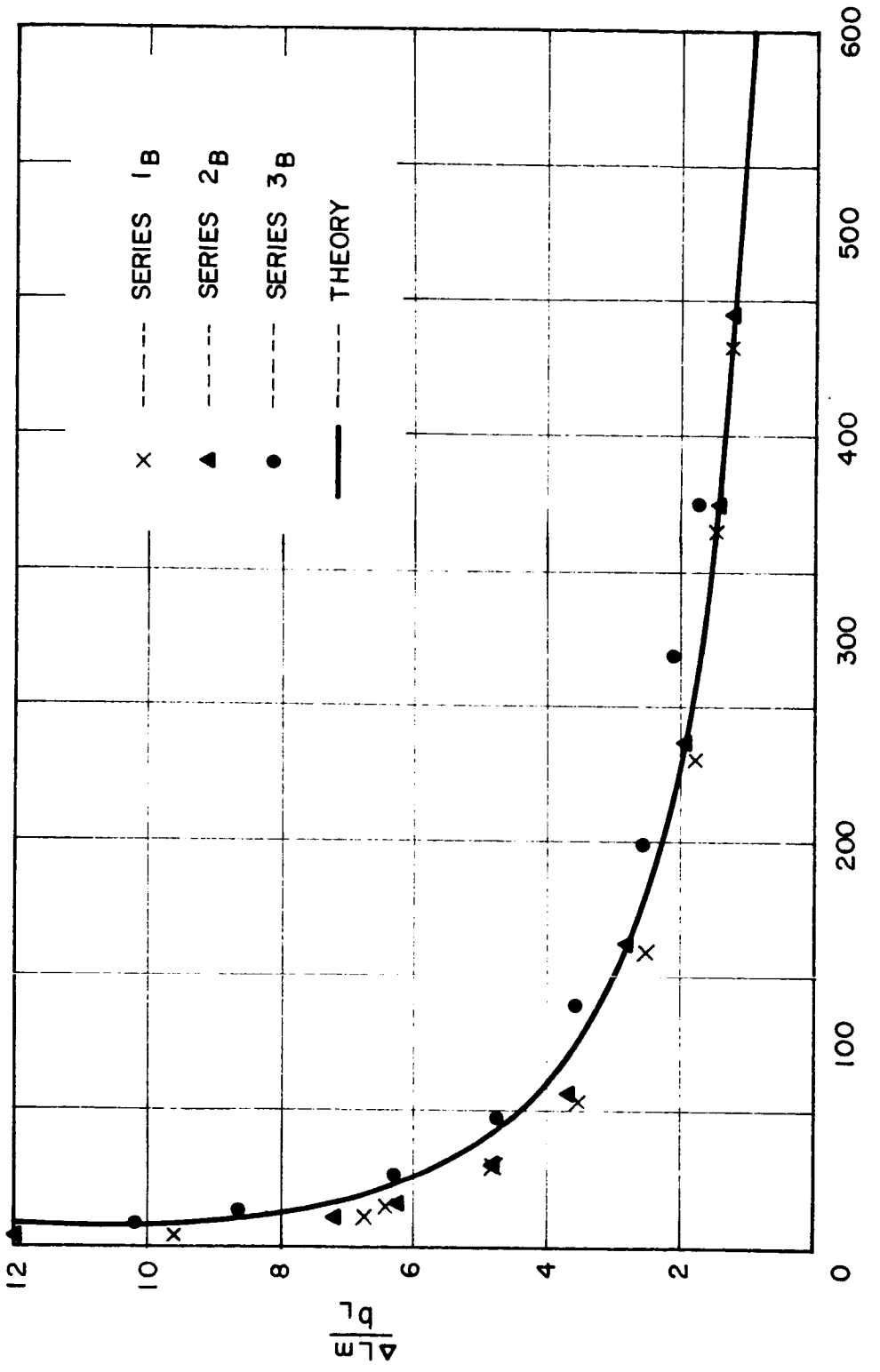

FIG. 26 COMPARISON OF BRASS DATA WITH THEORY

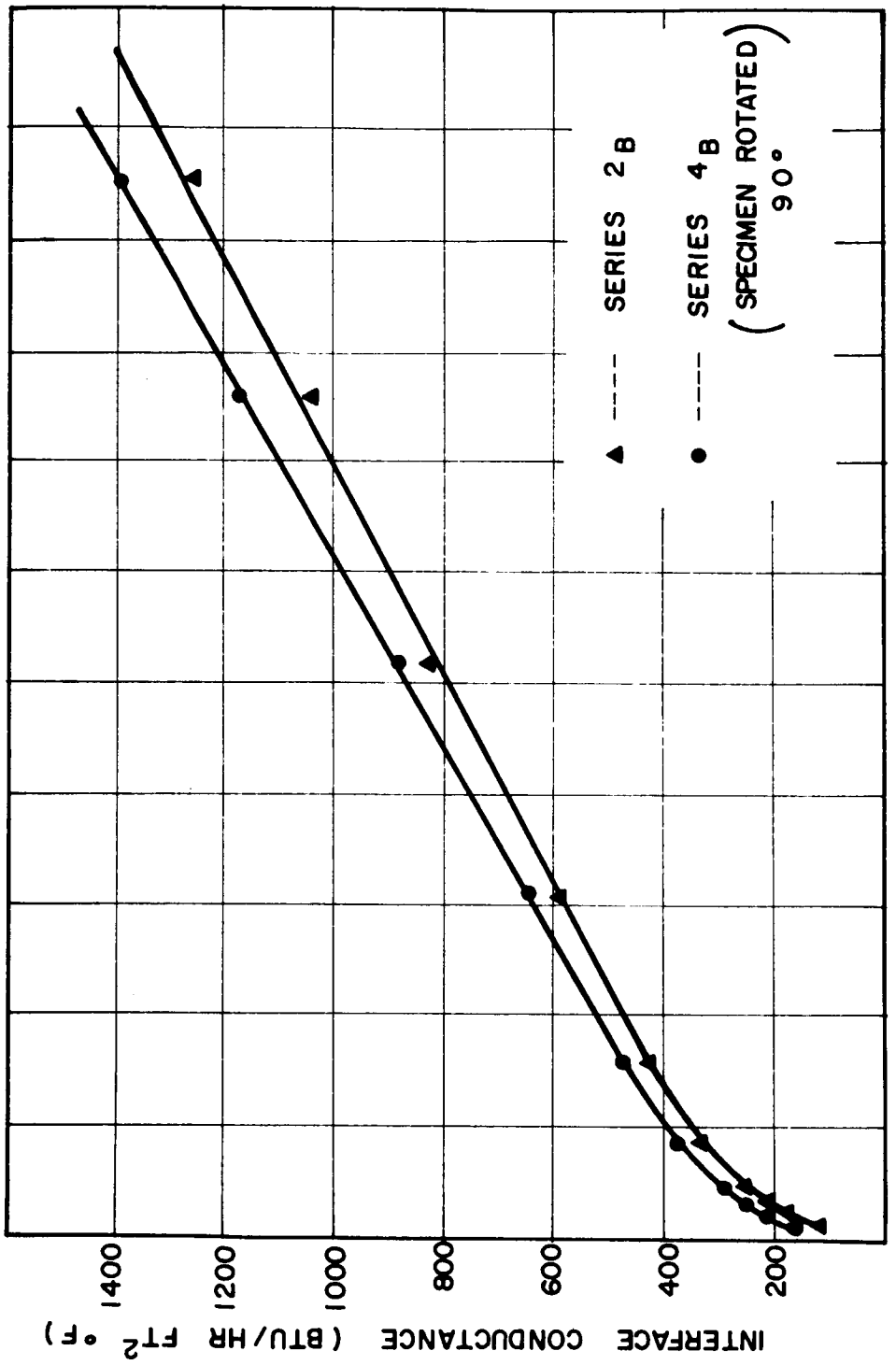

FIG. 27 INFLUENCES OF LOADING HISTORY & SPECIMEN ORIENTATION

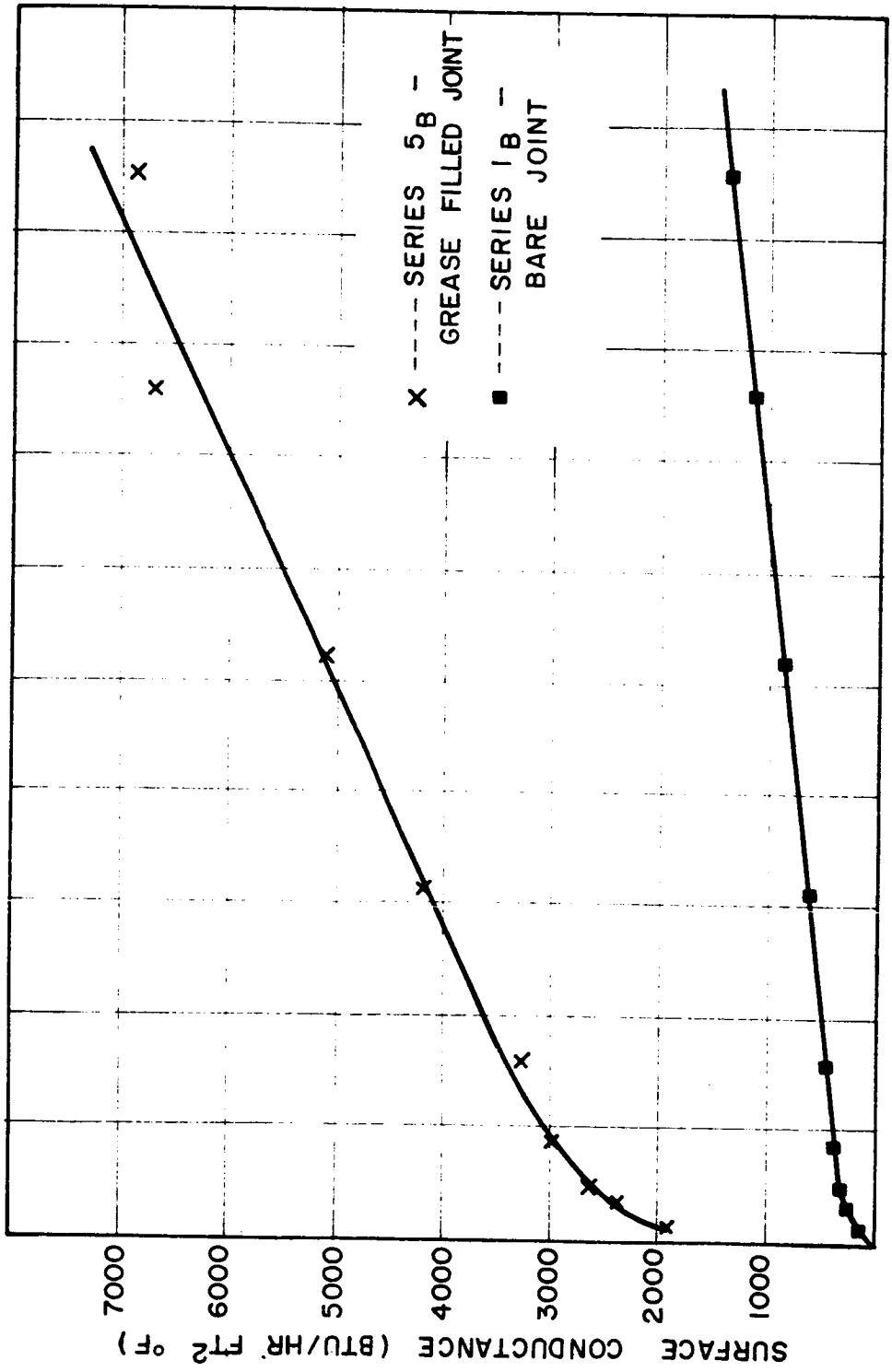

FIG. 28 THE INFLUENCE OF A CONDUCTING FLUID

approximately 6 inches to 0.6 inches for the bare brass interfaces tested. Inasmuch as the total equivalent flatness deviation, d_t, was relatively large, the elastic conformity modulus, ζ, for these tests at any given load was relatively small.

The overall agreement between data and theory was considered very good. The small deviation shown in Figure 26 cannot be attributed to any single cause. It appears to be mainly a result of error in the determination of d_t and uncertainties in the values employed for E_m and k_m.

Several investigators reported large differences in thermal contact resistance with a change in the relative orientation of the surfaces. These differences are easily explained when the properties of macroscopic constrictions are considered. On the other hand, the data presented in Figure 27 show the effect of the orientation to be small in this investigation, which follows from the geometry which was employed. The small increase in conductance for Series 4_B after the upper specimen was rotated 90°, over that of the premier loading, Series 2_B, is attributed to changes in E_m and k_m, due to the gradual annealing of the specimens with time, and also to creep of the contacting members.

Figure 28 shows the influence of silicone high vacuum grease on the interface conductance. Series 1_B was the bare interface; Series 5_B was the same interface after the addition of the silicone grease. The thermal conductivity of the grease was approximately 1.5 times that of air at atmospheric pressure [57]. The significant increase of the interface conductance in the presence of the grease was due to the effective increase in the macroscopic contact area (see Section 4.1.2). In one test at an apparent contact pressure of 29 psi, a further increase of approximately 30% was experienced in the interface conductance when the grease filled interface was exposed to atmospheric pressure.

This indicated that the interfacial voids were not completely filled with grease. The scatter of data at large values of contact pressure, as shown in Figure 28, was due to experimental error. At p_a = 950 psi, the equivalent resistance in terms of specimen length, ΔL_m, was only 0.1". The corresponding temperature drop across the interface was less than $6^{\circ}F$.

6.1.2 Magnesium Specimens

Magnesium alloys are widely used in the construction of space vehicles. For this reason alone it appears desirable to include them for study. In addition, their low modulus of elasticity provides a useful means of testing the validity of the proposed model. At the mean interface temperature level of these tests, the modulus is approximately 6.1×10^6 psi which is about one fifth that of steel. Thus, with the same initial geometry and apparent contact pressure, the macroscopic contact area will be considerably larger for magnesium than for the other materials tested.

Approximately a month elapsed between the polishing of the specimens of Series 1_M and the placement of these specimens into the vacuum chamber. During this time a visible film formed on the test surfaces. Since the possible effects of such a film were of definite interest, these specimens were tested without being repolished. The results are shown in Figure 29. If these data are compared with the theoretical prediction according to Equation 4.33, no agreement will be found. This is to be expected since the film resistance plays a major role, and, due to the relatively small flatness deviation, the macroscopic constriction resistance is small.

The specimens of Series 1_M were removed from the vacuum chamber and repolished. Besides removal of the film, the repolishing operation caused an

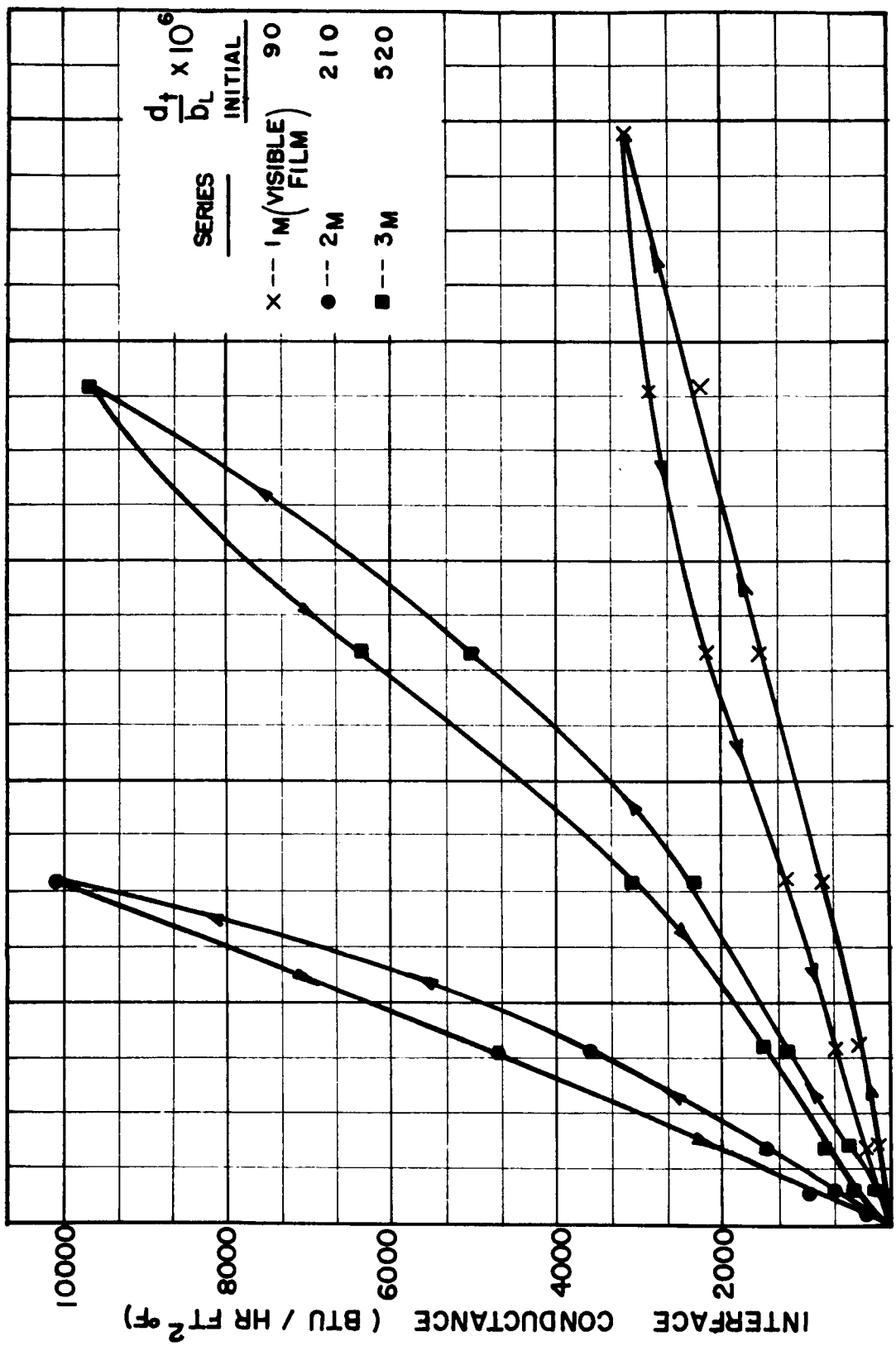

FIG. 29 EXPERIMENTAL RESULTS FOR MAGNESIUM

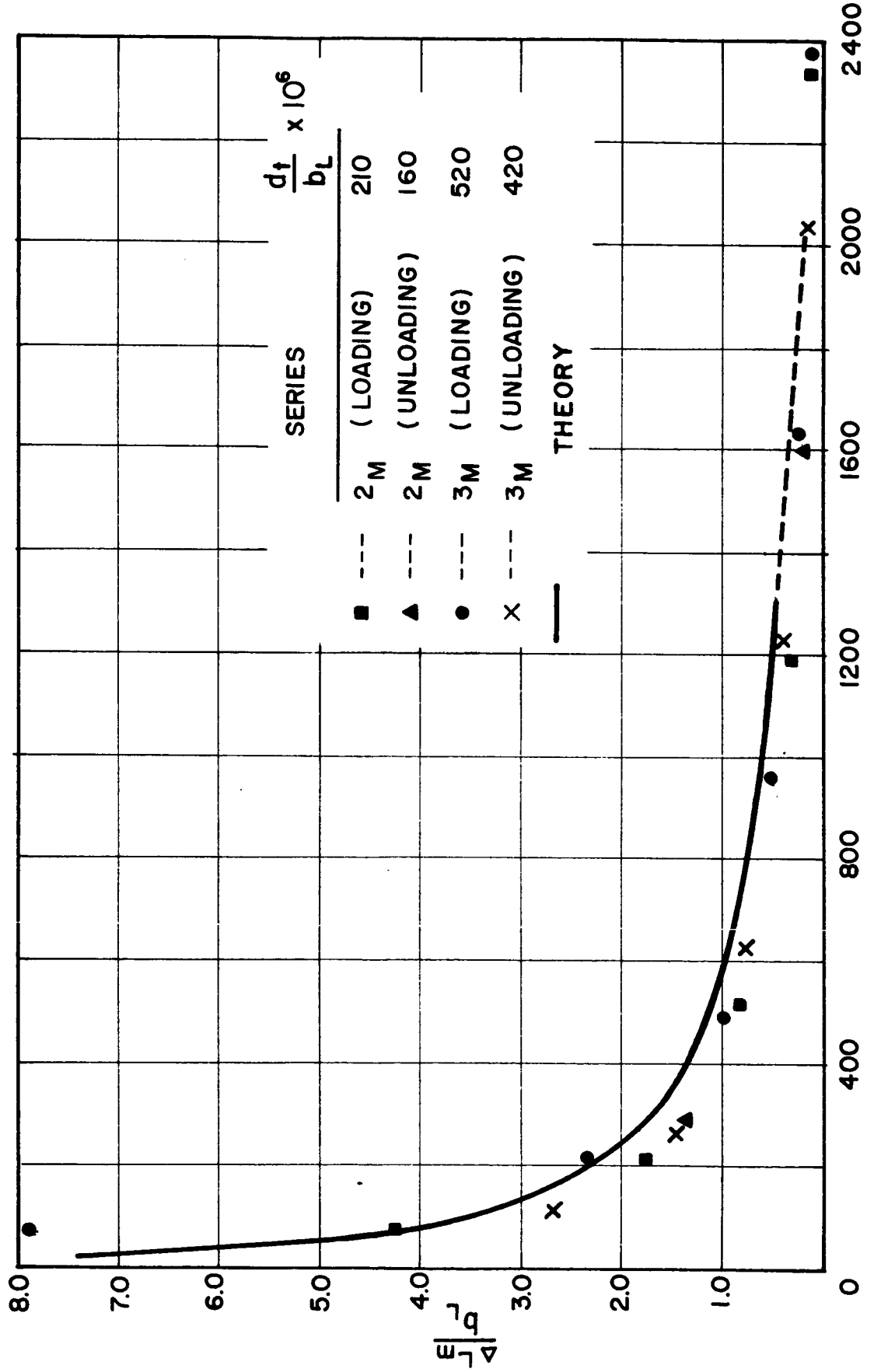

FIG. 30 COMPARISON OF MAGNESIUM DATA WITH THEORY

increase in the total equivalent flatness deviation. A comparison of the interface conductance of the specimens before and after they were repolished (series 1_M and 2_M, respectively) is given in Figure 29. It shows an order of magnitude increase in the interface conductance value in spite of the more than doubled flatness deviation. This lends support to the contention that the high contact resistance exhibited in Series 1_M was mainly due to the film resistance. It is also seen in Figure 30 that good agreement with theory was obtained for the freshly polished specimens. Series 3_M also consisted of freshly polished specimens but with a larger flatness deviation. Again, relatively good agreement with theoretical predictions was obtained.

The magnesium specimens exhibited a change, with time, in interface conductance due to creep. The occurrence of creep was revealed by: i) the continuous decrease, with time, of the contact resistance during a given test run under otherwise fixed conditions, ii) the greater conductance observed during unloading (see Figure 29), and iii) the change in the total flatness deviation observed before and after a test series. In the comparison of the data and theory shown in Figure 30, the total flatness deviation was based on the measurements taken before the test series for the loading curve and after the test series for the unloading curve.

In all tests of magnesium interfaces, the contact resistance in terms of the equivalent length, ΔL_m, varied from 17 inches to 0.06 inches. The latter occurred in Series 2_M at an apparent contact pressure of only 311 psi. The corresponding temperature drop across the interface was only $3^{\circ}F$. Some of the experimental data in Figure 30 are seen to lie below the theoretical prediction. It is most likely that this deviation is due to the combination of error in d_t and the effect of nonspherical contacting members that resulted due to creep.

6.1.3 Stainless Steel Specimens

Stainless steel interfaces were studied because: i) stainless steel is frequently employed in the construction of vacuum apparatus and ii) such contacts, in the absence of a conducting fluid, exhibit low values of interface conductance due to the combined effects of low thermal conductivity and high modulus of elasticity. Again these extreme properties provide a good test of the proposed model.

The data from two sets of stainless steel specimens are given in a dimensional plot in Figure 31 and compared with theory in Figure 32. Series 2_S had a total flatness deviation of 40 microinches, whereas Series 3_S had a total flatness deviation of 150 microinches. The dimensional plot shows that the magnitude of the interface conductance was low compared with that of the other materials tested. This was the expected consequence of the small value of k for this steel ($k_m \cong 9.5$ BTU/hr ft ^oF). In the case of the stainless steel specimens the creep was small. No difference between the flatness before and after a given test series was detected, and the interface conductance was independent of time. Thus, as was expected, Series 3_S showed no variation in the conductance between loading and unloading. However, a variation was experienced for the flatter specimens of Series 2_S. This is shown in Figure 31. It is a consequence of R_L not dominating completely; although, as is shown in Figure 32, the agreement with theory was not bad considering the small value of d_t. The agreement between the theoretical predictions and the experimental data of Series 3_S is good.

The total flatness deviation of the stainless steel specimen sets that were tested was indeed small, i.e., compared with common engineering surfaces and many of the interfaces studied in the literature. Small values of flatness

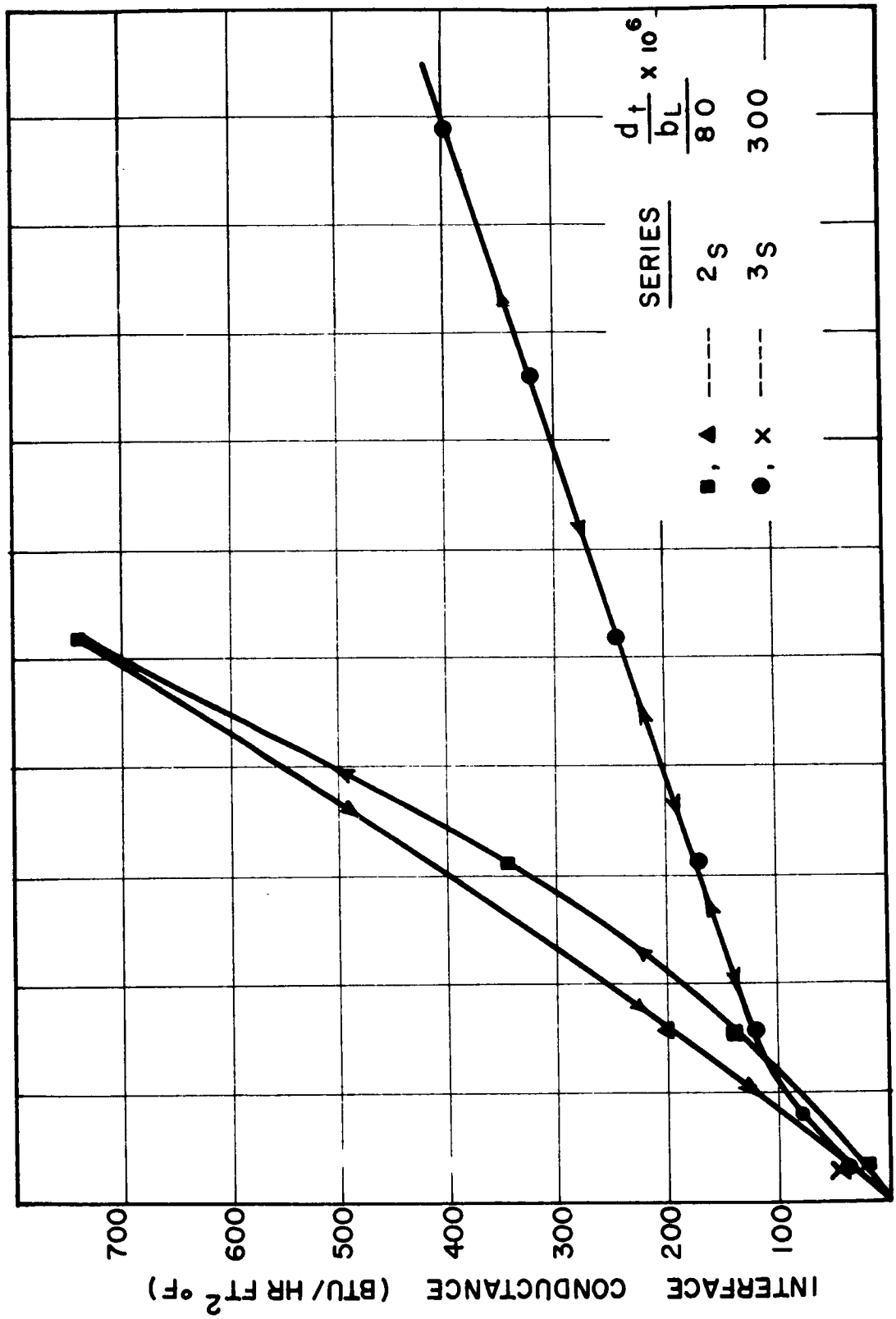

FIG. 31 EXPERIMENTAL RESULTS FOR STAINLESS STEEL

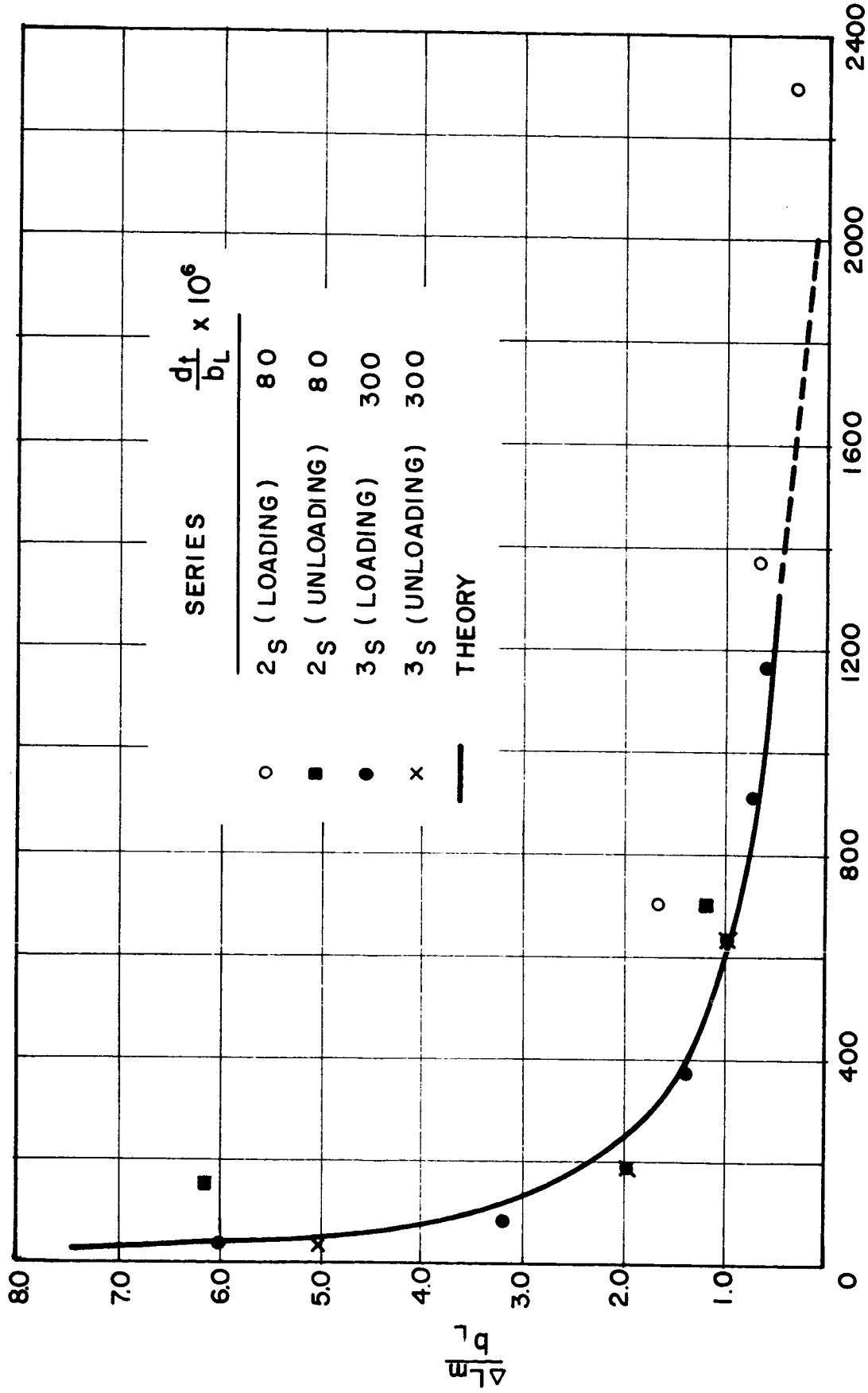

FIG. 32 COMPARISON OF STAINLESS STEEL DATA WITH THEORY

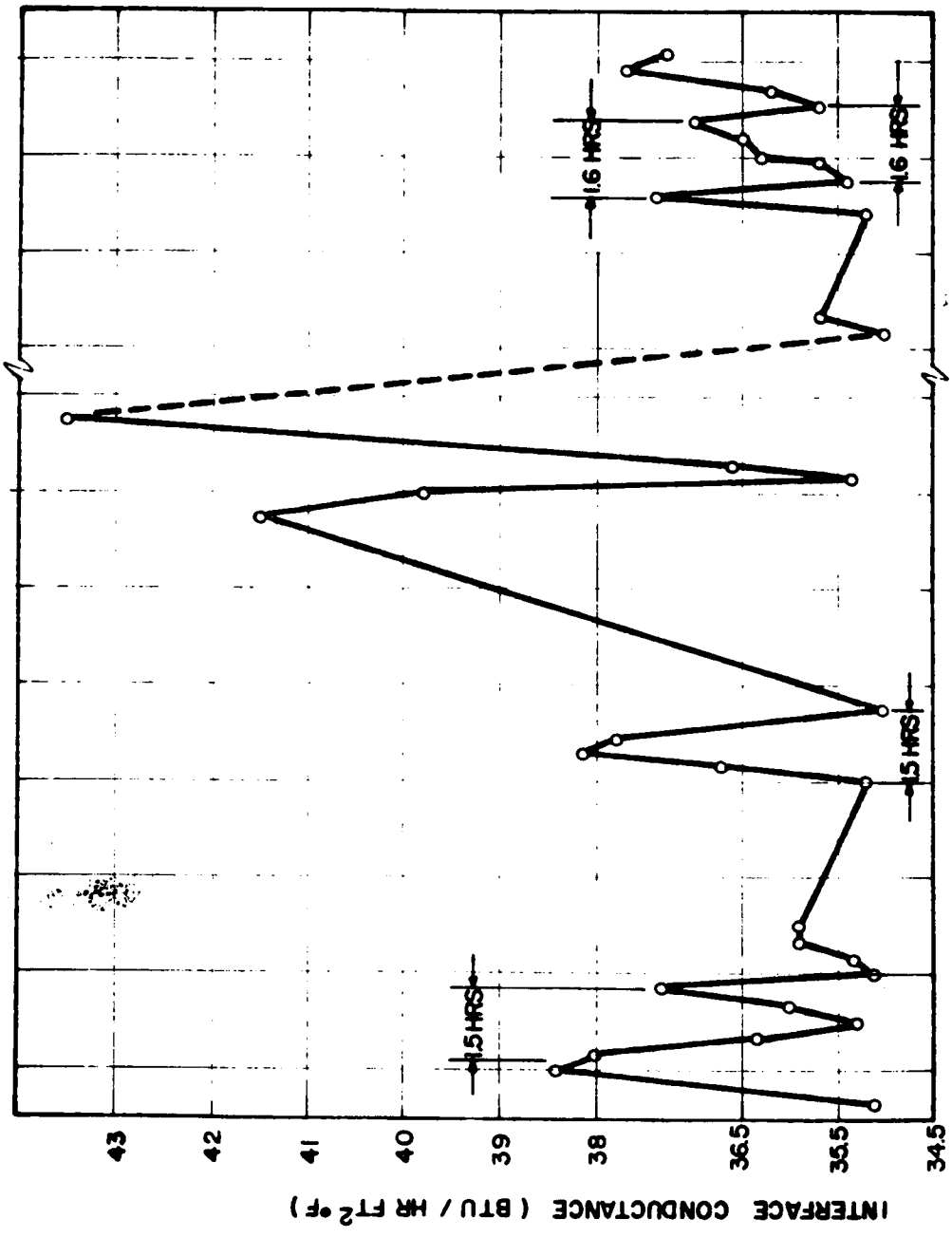

FIG. 33 CONDUCTANCE VS TIME FOR STAINLESS STEEL INTERFACE ($p_a = 29.2$)

deviation were purposely employed in order to obtain a small macroscopic constriction resistance; thus it was anticipated that the effects of the neglected film or microscopic constriction resistance would be seen. These effects were of some importance in Series 2_S, but they could be clearly seen in Series 1_S. The specimens of this series were polished nearly one month before they were tested. In addition, d_t was only 25 microinches. The resulting contact resistances were higher than the predicted values. These data are given in Appendix C.

A considerable amount of fluctuation in the measured data was experienced at low contact pressures in series 2_S and 3_S. For this reason contact resistance measurements were not made below an apparent contact pressure of 29 psi in these tests. After the completion of Series 3_S, a low contact pressure run was carried out in more detail. The results of this test series (4_S) are given in Appendix C and in Figure 33. The phenomenon observed was noteworthy. The interface conductance fluctuated in a cyclic fashion. Before analyzing these results, consider the conditions under which this test was carried out.

The power input was adjusted to obtain the desired temperature level. The variation in heat flux was estimated to be less than 1%. The load was adjusted to give an apparent contact pressure of 29.2 psi. The cooling water temperature was essentially constant throughout the entire test which lasted approximately 40 hours. The temperature drop across the interface fluctuated in an essentially cyclic fashion with varying amplitude. The period appeared to be constant and approximately equal to 1.5 hours. The source temperature fluctuated with approximately the same period and was almost in phase. The amplitude of the temperature fluctuation was greatest in the neighborhood of the interface. This suggests that changes of the interfacial conditions were responsible for the observed fluctuations.

The foregoing observed variations of the contact resistance can be explained in terms of the thermal strain. When the resistance is high, the temperature gradients near the interface are large which results in a greater thermal strain. This is hypothesized to cause an increase in the contact area which is accompanied by a reduction in the constriction resistance. This in turn would cause a decrease of the temperature gradients and hence a reduction in the thermal strain as well as an increase in the constriction resistance. The sequence of events will then be repeated.

Why this phenomenon was observed only for the stainless steel interfaces is not fully understood. It may be a consequence of the difference between the thermal diffusivities of these materials. (The reciprocal of the diffusivity is a measure of the time required to heat a material to some required temperature level.) The thermal diffusivity of the stainless steel employed is approximately 0.17 ft^2/hr, whereas the other materials used had values which were approximately an order of magnitude larger.

6.1.4 Aluminum Specimens

Aluminum surfaces in the presence of oxygen are known to be covered with transparent, tenacious oxide films. The formation of such films is rapid; they grow to a thickness of 20 Å in a few seconds and, even at room temperature, soon reach a thickness too great for conduction by the quantum mechanical tunnel effect (see Ref. 38, p. 114). It would be of interest to examine the effect of such films on the contact resistance for both smooth and rough surfaces. To determine the flatness deviation of rough surfaces, the following two procedures were employed. The test surfaces in Series 1_A and 2_A were lightly polished, after the conductance measurements were made, to enable the use of optical measurements. Judging from the evenness of the polish, it appeared that the

original macroscopic surface contour was not altered during the repolishing operation. The specimens of Series 7_A and 8_A were first highly polished and the flatness deviation determined. The surfaces were then roughened by sequential etching in sodium hydroxide, hydrochloric acid, and hydrofluoric acid solutions. The surfaces were rinsed with water between each treatment. Roughnesses of 45 and 80 microinches rms were produced on the two specimens in this manner. Profilometer measurements indicated that the roughness was relatively uniform.

The experimental results of Series 1_A, 2_A, 7_A, and 8_A are compared with the theoretical predictions in Figure 34. Since the data of the rough aluminum surfaces showed that the differences between the conductance measurements taken during loading and unloading were small, only the loading data are given in this figure. The specimens of Series 1_A were used in Series 2_A; however, before this series was conducted, the upper specimen was rotated 90°. Likewise, the specimens of Series 7_A were used in Series 8_A. Between these series, the specimens were annealed at $400^\circ F$ for seven hours in the vacuum chamber. This caused a change of approximately 13% in the thermal conductivity, which in turn caused an increase in the conductance. Since in a dimensionless plot the effect of the change in k_m is removed, little difference can be detected in Figure 34 between Series 7_A and 8_A. For the rough specimen sets, the total flatness deviation was approximately 230 microinches. In general, the agreement between data and theory for these rough surfaces was good.

The surfaces of the specimens employed in Series 3_A through 6_A were polished to a smooth finish similar to that of the magnesium and stainless steel specimens. In these series, only the total equivalent flatness deviation was varied; it ranged from 20 to 220 microinches. The results are shown in a dimensional plot in Figure 35. The data for the roughened surfaces of Series 7_A are included for comparison. Figure 36 compares the experimental data with theory for

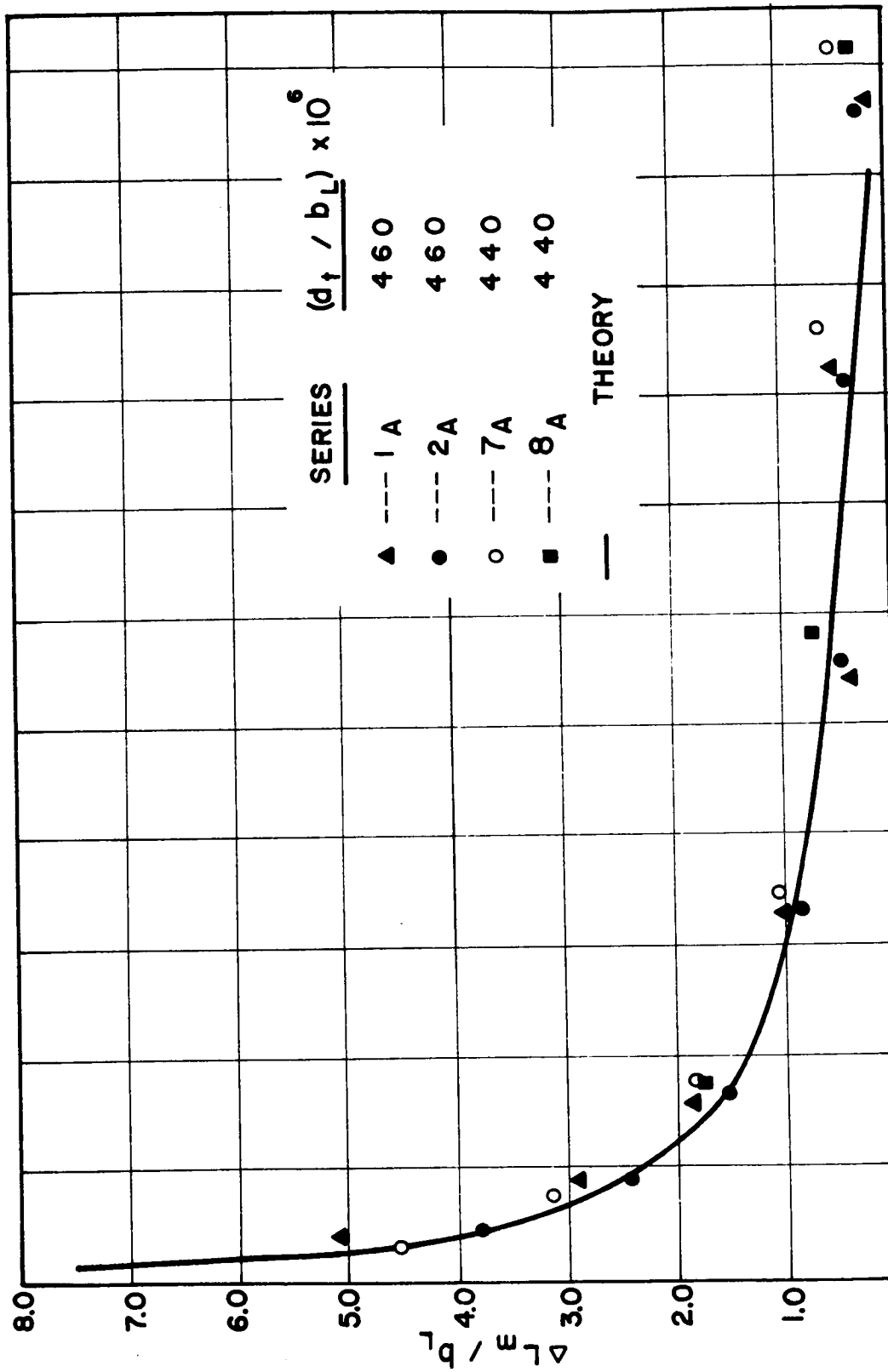

FIG. 34 COMPARISON BETWEEN DATA & THEORY FOR ROUGH ALUMINUM SURFACES

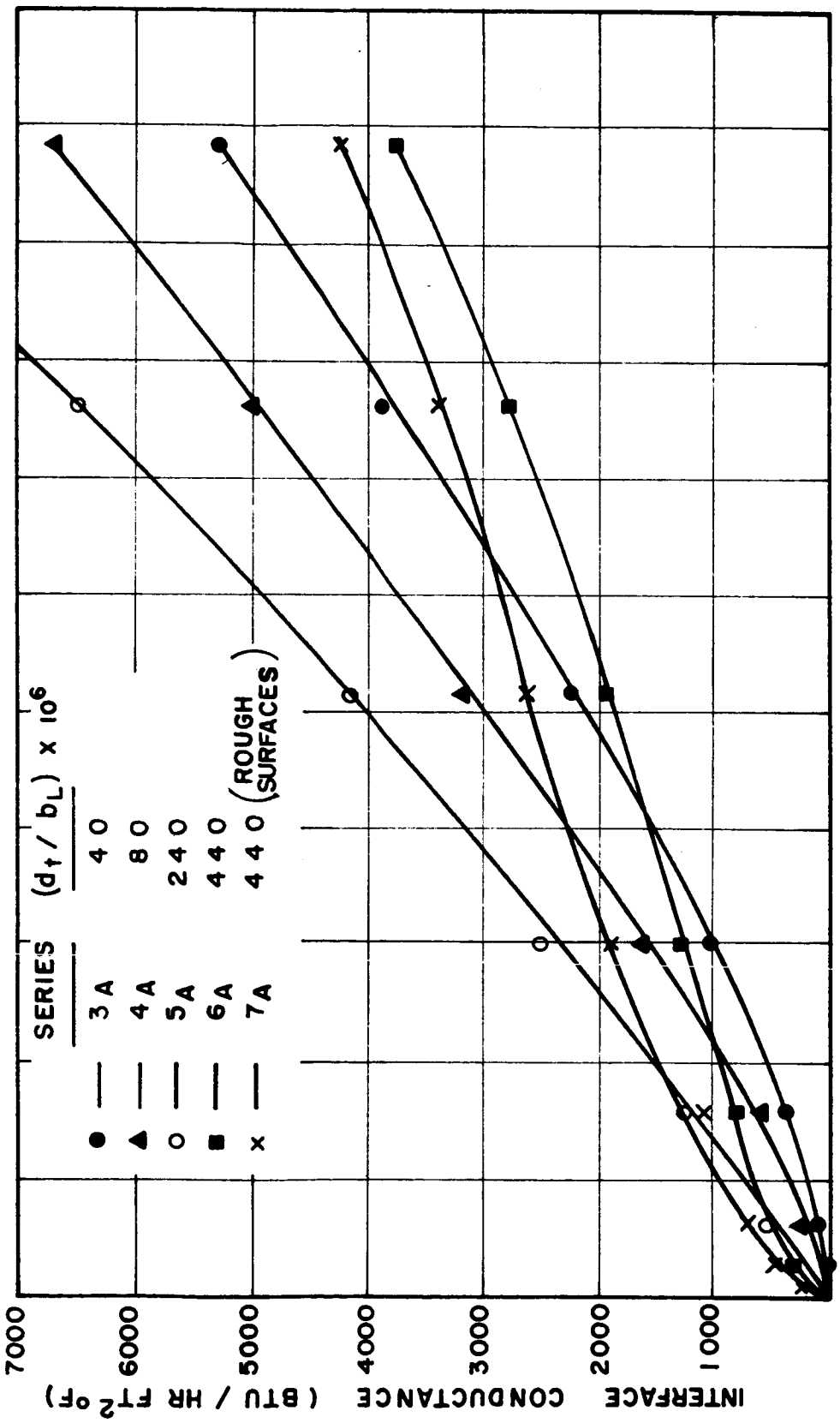

FIG. 35 EXPERIMENTAL RESULTS FOR SMOOTH ALUMINUM SURFACES

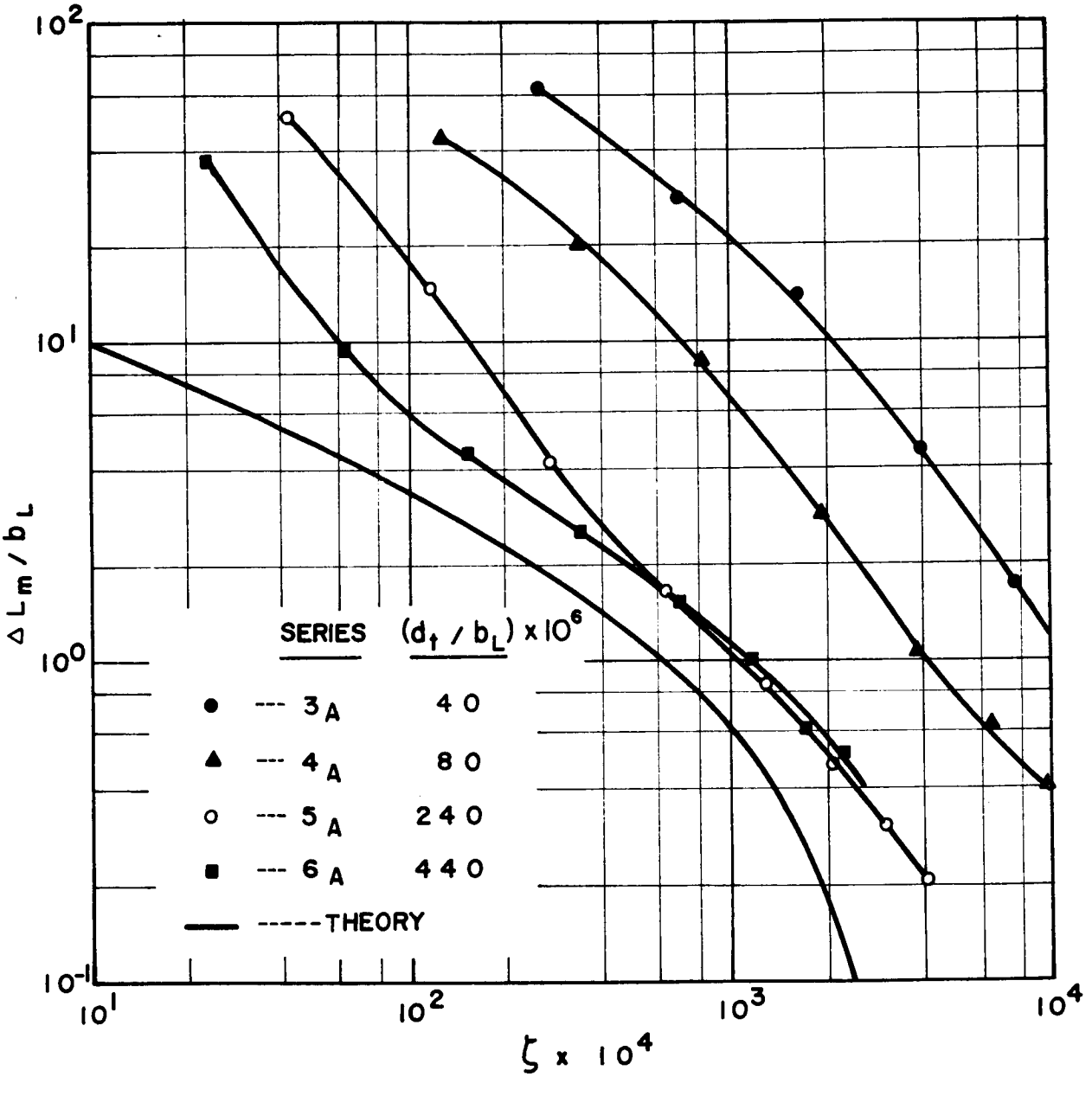

FIG. 36 COMPARISON BETWEEN DATA & THEORY FOR SMOOTH ALUMINUM SURFACES

these smooth aluminum specimens. The disagreement is obvious. At first glance it may be somewhat surprising to see that the data for the rough surfaces agree well with the theoretical predictions, while those for smooth surfaces do not. Upon closer examination of Figure 36, it is seen that the data drew continually closer to the theoretical curve as the flatness deviation was increased. Nearly half of the data of Series 6_A is already within 50% of the theoretical values which account only for the macroscopic constriction effect. As conditions became more favorable for the dominance of the macroscopic constriction resistance, which occurred at large values of d_t, the agreement was invariably better. The foregoing observation suggests that besides macroscopic constriction resistance, the film and/or the microscopic constriction resistance are operative at the smooth aluminum surfaces.

By considering Figure 35, it can be seen that the conductance initially increases as d_t is increased. However, at the larger values of d_t a decrease takes place and the shape of the experimental curve again resembles the theoretical prediction. The dominance of R_L is again seen.

The following arguments seem to indicate that the additional resistance of importance in Series 3_A, 4_A, 5_A and 6_A was mainly the film resistance:

i) Comparing similar values of d_t and p_a, this additional resistance is more predominant for aluminum than for stainless steel. If microscopic constriction resistance was important, the dominance should be very similar for both materials, since, as was shown in Section 4.2, the ratio R_L/R_s is approximately the same. On the other hand, film resistance could be greater for aluminum since its film eliminates conduction by the quantum mechanical tunnel effect, which according to Mott [48] is possible if the film thickness is less than about 40 Å.

Stainless steel should still conduct by this mechanism.

ii) The magnitude of the additional resistance seems too large to be attributed to R_s. For example, in Series 3_A the contact resistance was almost 100 times larger than the theoretical value. On the other hand, the analysis given in Section 4.2 indicates R_L/R_s is of the order of 100. Thus, the model from which R_s was calculated would have to be in error by over a factor of 1000 to account for the large resistance obtained in Series 3_A.

iii) The decrease in the contact resistance for the rough surfaces of Series 7_A as compared to the smooth surfaces of Series 6_A cannot be attributed to microscopic constriction resistance. This resistance should increase with an increase in roughness. However, rougher surfaces should result in more plastic deformation and, consequently, greater film damage. It was observed in figures 34 and 36 that much better agreement with theory was obtained for rough surfaces than for smooth surfaces.

iv) The improvement of conductance with a reduction in the macroscopic contact area appears logical if film resistance were the dominant portion of this additional resistance. A greater concentration of the load causes a larger amount of plastic deformation; hence a greater amount of film damage occurs. The microscopic contact areas also become more intimate when the microscopic contact pressure p_s, is increased. More intimate contact could reduce the film resistance by: a) causing a reduction in the tunnel resistivity, b) causing an increase in the contact area on a submicroscopic level and c) causing a decrease in any transition resistance which may be present.

6.1.5 Comparison of Materials Tested and Further Discussion of Results

Obviously, since the model proposed only includes the effects of macroscopic constriction resistance, it will always fail if the contacting members are sufficiently flat. Because the value of d_t at which R_L is no longer dominating and also the magnitude and nature of the quantity $(R_s + R_o)$ which then becomes important are of interest, very flat surfaces were investigated in this study. With the exception of the brass surfaces that were tested early in the program, the surfaces studied were generally flatter than engineering surfaces and those investigated in the literature (see Section 7.2). The total flatness deviation in the later tests ranged from 20 to 230 microinches. This means that the average flatness deviation per specimen ranged from 10 to 115 microinches. In many of the tests the diameter of the macroscopic contact region was less than half the diameter of the specimen. In this region of the contact plane, the total flatness deviation was never greater than 60 microinches, which is an average of only 30 microinches per specimen. Thus, macroscopic constriction resistance probably dominates the thermal contact resistance of engineering surfaces and those studied in the literature even more completely than the surfaces studied in this analysis of macroscopic effects.

The value of the total flatness deviation at which the macroscopic constriction resistance is no longer dominating will now be considered. The experimental results have shown the following:

i) Brass: R_L was the dominating resistance at a value of $d_t = 780$ microinches. Smaller values of d_t were not studied for this material.

ii) Magnesium: R_L was the dominating resistance for $d_t > 80$ microinches for freshly polished interfaces. One value of d_t

less than 80 microinches was investigated; however, the test surfaces were covered with a visible surface film which caused an appreciable amount of film resistance. R_L may still dominate the thermal contact resistance for values of d_t < 80 microinches if the surfaces are freshly polished.

iii) Stainless Steel: R_L was beginning to dominate at d_t = 40 microinches. For this material and surface finish, 40 microinches seems to be the limiting value of d_t. The extent of the dominance of R_L for this case can be seen in Figure 32.

iv) Aluminum: The aluminum interfaces tested were dominated by another resistance until a value of d_t of 220 microinches was reached, at which point R_L again began to dominate the contact resistance. Rougher surfaces resulted in better agreement with theoretical predictions than smooth surfaces, as can be seen in Figures 34 and 36.

Before further considering the limit of the range of the dominance of R_L, let us consider what resistance becomes important in the case of these flat contacting surfaces. The discussion which was given for aluminum in Section 6.1.4 indicates that for this material the additional resistance was probably composed mainly of film resistance. Many of these arguments can also be applied to magnesium and stainless steel.

Aluminum and stainless steel surfaces in the presence of oxygen form films very rapidly up to thicknesses of about 100 and 15 Å, respectively (see Ref. 31,

pp. 30 and 109). At these film thicknesses the growth at room temperature virtually stops. Consequently, no data with a known difference in the film thickness were obtained for stainless steel or aluminum; hence, the importance of these films was difficult to ascertain. However, magnesium interfaces with known differences in the surface film were tested. Let us consider these results.

The magnesium specimens of Series 1_M had visible films on the test surfaces. The conductance was very low for this condition; however, when these surfaces were repolished, the conductance of the interface increased approximately ten-fold (see Series 2_M). Since the surface finishes were practically identical for both Series 1_M and 2_M, it seems logical to conclude that the additional resistance of the interface in Series 1_M is due to the surface film. The microscopic constriction resistance could have been affected by repolishing only if this resistance were a function of the macroscopic contact pressure, p_L ($p_L = p_a/x_L^2$). However, consider the data of Table 5 which compares tests from Series 1_M and 2_M with approximately equal values of p_L. Both the load and the macroscopic contact area of the test of Series 2_M are less than half of those of Series 1_M.

Series	p_a (psi)	p_L (psi)	x_L	h (BTU/hr ft^2 $^\circ$F)
1_M (visible film)	157	272	0.76	344
2_M	67	290	0.48	1450

Table 5

A Comparison of Series 1_M and Series 2_M at Equal Values of p_L

Both of these effects should cause the conductance of the test of Series 2_M to be smaller; however, the interface conductance is over four times higher than

that of the test of Series 1_M. This, in the writer's opinion, is conclusive evidence that the additional resistance present in Series 1_M is composed predominantly of film resistance.

With the present understanding of the effects of films and microscopic constriction resistance, a definite range for the dominance of R_L cannot be given. If the surface films were sufficiently thick, they could dominate the thermal contact resistance of an interface even at extremely large values of flatness deviation. For freshly polished surfaces, the data given in the previous sections give an indication of the range of the dominance of R_L.

By comparing the results for the various materials, creep was found to cause, with time, a discernible decrease in the contact resistance only for magnesium. This combined with its low modulus of elasticity results in relatively high conductance interfaces for magnesium. For example, in Series 2_M a conductance of 900 BTU/hr ft^2 ^oF was obtained at an apparent contact pressure of 28 psi. This value is over five times greater than any value reported by Fried [24] at this apparent contact pressure including his data for silicone grease filled interfaces. These data demonstrate that with an understanding of the mechanisms, high conductance interfaces can be rationally produced.

Since both contacting members in these experiments were made from the same material, the change of the macroscopic contact area due to the effects of thermal strain should be small; however, for dissimilar materials this may no longer be true. (If the thermal and mechanical properties of both specimens are the same and independent of temperature, symmetry with respect to the contact plane would cause the axial thermal strains to cancel.) An analytical investigation of the influence of thermal strain on the contact area is currently being performed under the direction of Professor A. P. Boresi in the Department of

Theoretical and Applied Mechanics. Thermal strain may be a reason for the direction of heat flow affecting the thermal contact resistance in contacts between dissimilar metals.

The data for all the materials investigated are compared on a single dimensionless plot in Figure 37. The ranges of d_t/b_L for the data given in this plot are included in the figure. For spherical contacting surfaces, macroscopic constriction resistance was shown, both theoretically and experimentally, to be significant if the elastic conformity modulus, ζ, is less than approximately 0.2. For geometries other than spherical surfaces, this resistance still may be significant for considerably higher values of ζ.

6.2 CONDUCTIVE-LIQUID ANALOG MEASUREMENTS

The objective of pursuing a conductive-liquid analog study was stated in Section 5.6. To ascertain its accuracy, the constriction resistance of a circular contact area of radius a_L, concentric with the apparent contact area of radius b_L was measured. This simple geometry was chosen to enable a comparison with the theoretical results given by Roess [50] (see Equation 4.9). Figure 38 shows such a comparison. The dimensionless resistance, $\Delta L_m/b_L = k_m/h\ b_L$, is employed for the ordinate, and the constriction ratio, x_L, is employed for the abscissa. The agreement between the theoretical curve and the experimental data was very good. This lends support to the validity of the assumption used by Roess in his analysis (see Section 4.1.1). The deviation between the data and the theoretical predictions is less than 5%.

Assured of the accuracy and feasibility of the analog measurements, the effect of the eccentricity of the macroscopic contact area on the constriction resistance was studied. Such knowledge is of value in interpreting the results

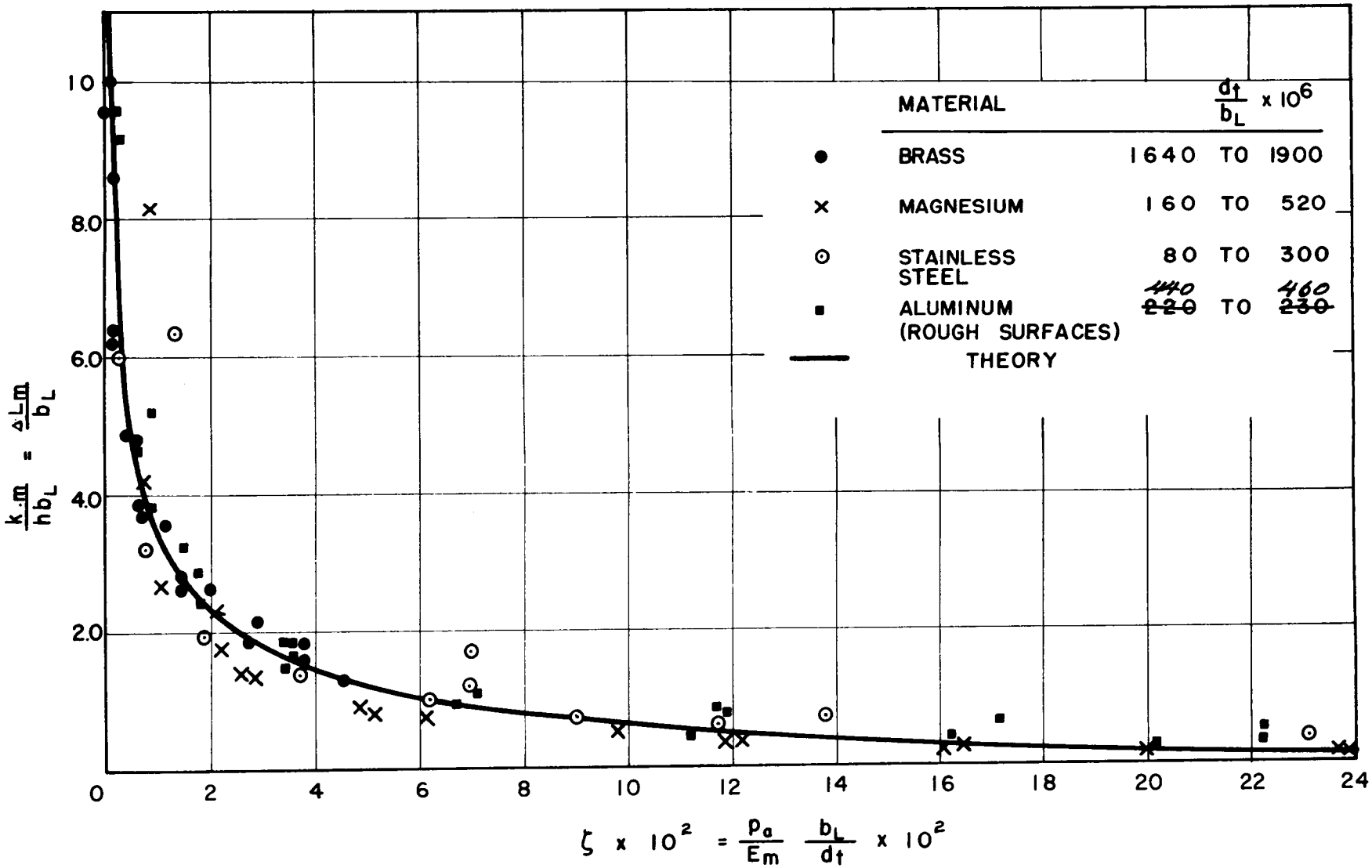

FIG. 37 COMPARISON OF RESULTS FROM ALL MATERIALS INVESTIGATED WITH THEORY

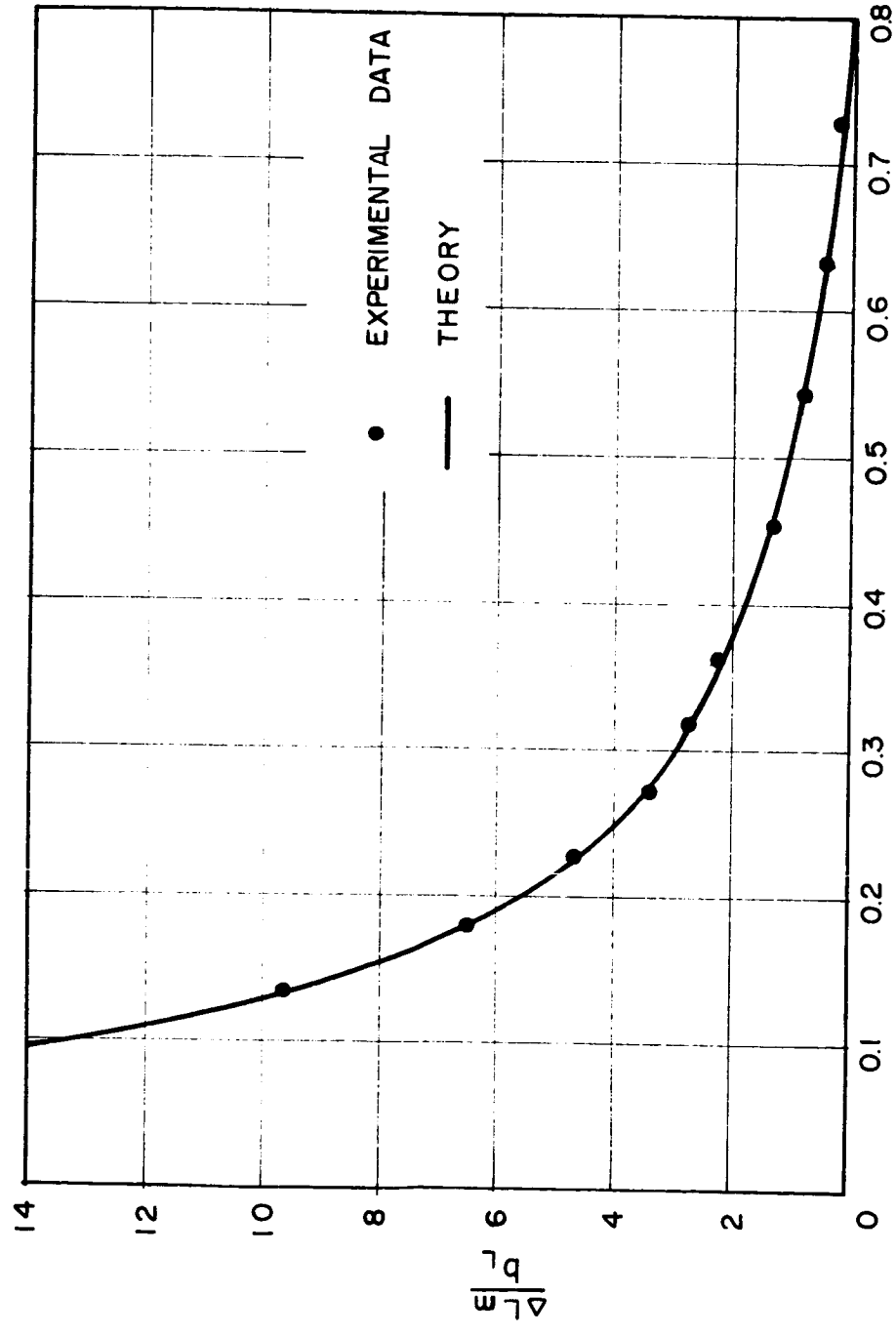

FIG. 38 DEMONSTRATION OF THE ACCURACY OF THE CONDUCTIVE - LIQUID ANALOG

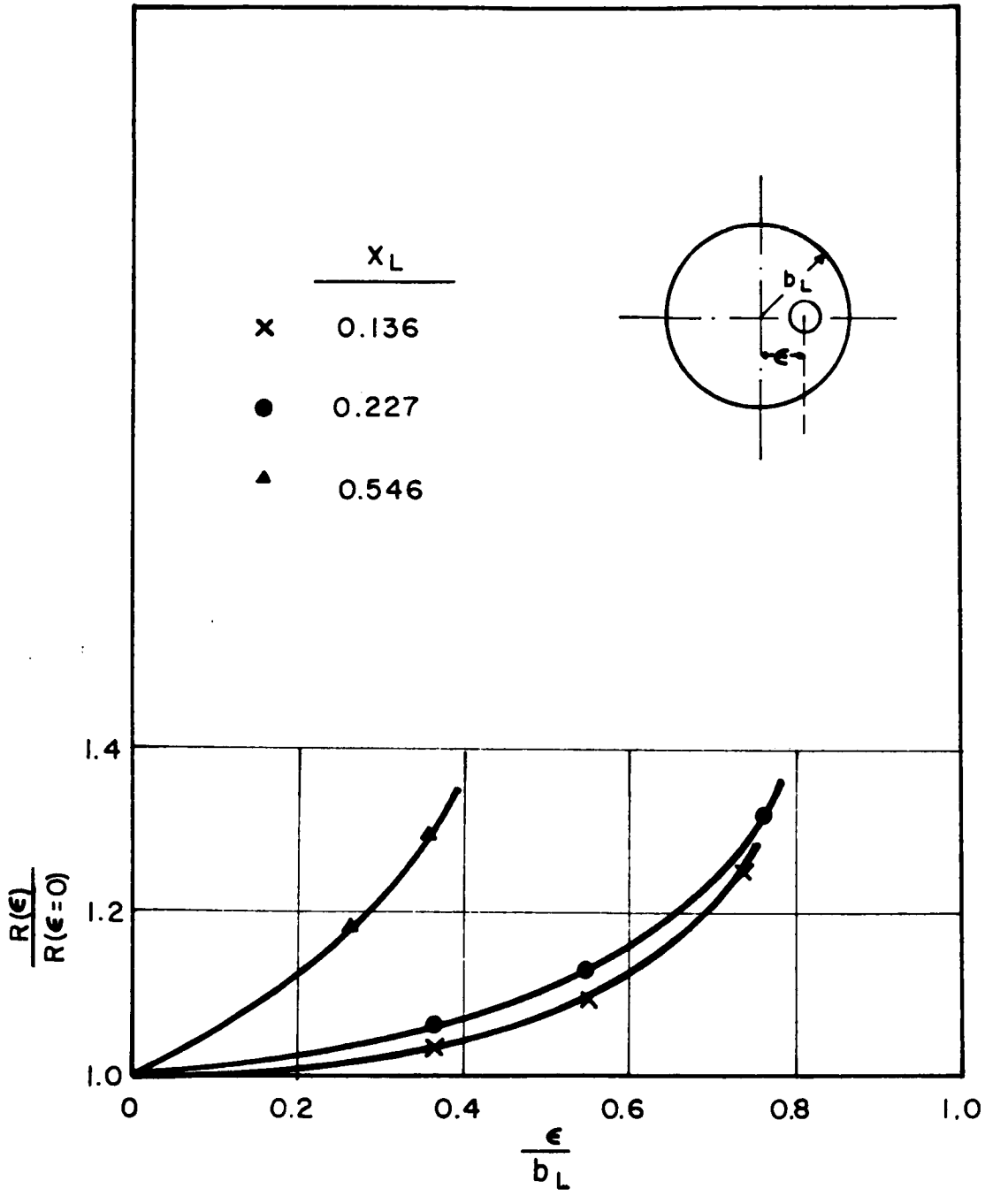

FIG. 39 THE INFLUENCE OF ECCENTRICITY ON THE CONSTRICTION RESISTANCE

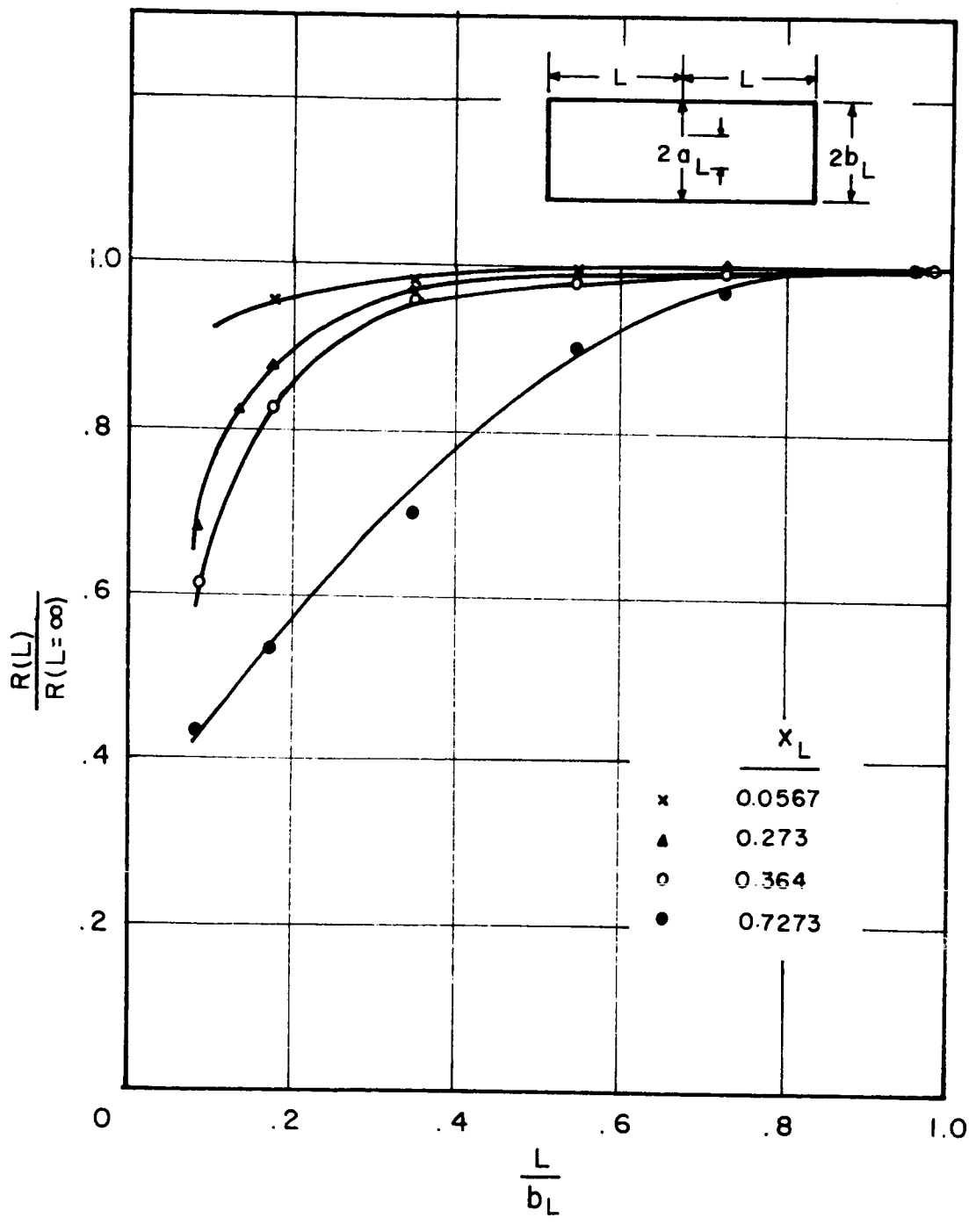

FIG. 40 THE INFLUENCE OF SPECIMEN LENGTH ON THE CONSTRICTION RESISTANCE

of the thermal constriction resistance measurements. The results of this study are shown in Figure 39. Data are given for several different values of the constriction ratio, x_L. In general, the influence of the eccentricity on the constriction resistance is not very large. At small values of x_L a large amount of eccentricity is possible; however, its influence on the constriction resistance is small (as x_L goes to zero, it becomes independent of the eccentricity). It has a greater influence when x_L is large, but the maximum possible amount of eccentricity is then small.

In the study of the physical nature of thermal contact resistance, it is the local phenomenon at the interface which is of interest. Therefore, the geometry of the test specimens and the imposed thermal boundary condition should be such that the experimental data can be correctly interpreted. Therefore, the influence of the length of the cylindrical specimens used in this investigation on the macroscopic constriction resistance was of interest. The conductive-liquid analog offered a convenient means for such study. The results are shown in Figure 40. It can be seen that when L/b_L was greater than approximately 0.6, the macroscopic constriction resistance was virtually unaffected by the specimen length. It can also be seen that the influence of the length was more pronounced when the constriction ratio was large. As the length, L, goes to zero, the macroscopic constriction resistance also goes to zero (this can also be shown theoretically). Thus, if the constant temperature boundary condition at $z = L$ could be maintained, this would be a means of eliminating the macroscopic constriction resistance in order to enable an experimental study of the remaining resistances. The effect of the specimen geometry on the measured thermal contact resistance has not received the attention it deserves by many investigators. It oftentimes has lead to a misinterpretation of data, or data which could not be analyzed.

6.3 DISCUSSION AND ANALYSIS OF EXPERIMENTAL ACCURACY

The accuracy of the primary measurements was discussed in detail in Chapter 5. Here, the overall accuracy of the measured conductance, h, which is a function of the apparent contact pressure, p_a, will be considered. Since the dimensionless parameters, $\Delta L_m/b_L$ and the elastic conformity modulus, ζ, are employed in the comparison of theory with experimental data, the accuracy with which these parameters can be determined will also be analyzed.

Experimentally the interface conductance, h, is determined from the temperature drop, ΔT, across the interface and the heat flux, q, through the specimen. Its accuracy at low contact pressures is limited by that of determining q and at high pressures by that of determining ΔT. The accuracy of determining q, as explained in Section 5.3, is approximately 8% for the worst conditions. Thus for low values of contact pressure, the accuracy of h is within 8 percent. At high values of the contact pressure, the experimental error can become so large that the results would cease to be meaningful. As an example we cite Reference 1 in which negative temperature drops were reported. In the present investigation, contact pressures higher than those which resulted in a temperature drop less than $3^{\circ}F$ were not studied. A ΔT of $3^{\circ}F$ was equivalent to a resistance in terms of ΔL_m of less than 0.1 inches for the conditions of these tests.

As discussed in Section 5.4, the absolute experimental error in the determination of ΔT is not believed to exceed $2^{\circ}F$. (Some of the early tests, which are listed in Section 5.4, may have had errors as large as $3^{\circ}F$.) The relative error is less than $2^{\circ}F$. By comparing the thermocouple millivolt readings, relative changes of 0.1 to $0.2^{\circ}F$ in the temperature drop across the interface can be detected. This procedure was often employed to determine variations in contact resistance: i) during loading and unloading, ii) during

an individual test, and iii) between relatively large loads.

If the dimensionless conductance or resistance is considered, error in the determination of the harmonic mean thermal conductivity, k_m, must be included. From the measured values of the thermal conductivity and the values reported in the literature, it was ascertained that the error in k_m could be as large as 5%.

The interface conductance is highly dependent on the applied load. The accuracy of the determination of the apparent contact pressure was discussed in Section 5.2. At low loads, p_a is accurate to within 2 psi. This would be an error of 20% at 10 psi. At high loads the error in p_a is less than 2%. If one considers the elastic conformity modulus, $(p_a/E_m)(b_L/d_t)$, two additional sources of error arise. First, let us consider the harmonic mean modulus of elasticity, E_m. In this analysis values for the modulus of elasticity were taken from the literature. From the information available, which is discussed in Appendix A, it was estimated that the error in E_m could be as large as 5%. The major source of error in the determination of ζ was probably due to error in the determination of d_t. The error in d_t varied from approximately 25% at small values of d_t to 10% at large values of d_t. These values include the effect of non-sphericity of the contacting surface.

The percentage error in several of the measured quantities may seem large; however, considering the nature of the problem and our understanding of it at the present time, the overall measurement accuracy achieved is satisfactory. The most irritating error is that present in ΔT when the contact resistance is very low; however, from a practical standpoint, extremely low contact resistances are of no interest since they can be ignored in many applications. It is pertinent that the errors in many instances are much less than their cited

values, and they are not at random. Very small changes can often be determined with good reliability during a given test or test series.

7. A CRITICAL COMPARISON BETWEEN PUBLISHED STUDIES AND THE PRESENT ANALYSIS

7.1 THEORETICAL MODELS

To the writer's knowledge, all published analysis on thermal contact resistance assumed that the actual areas of contact were uniformly distributed over the entire apparent contact area. The total actual contact area was determined from an equation similar to Equation 4.13, i.e., by assuming some type of relationship between the hardness of the material, the load, and the actual contact area (the microscopic contact area, A_s). Examples are the models presented by Cetinkale and Fishenden [4], Boeschoten and van der Held [12], Fenech and Rohsenow [20] and Laming [40]. They have been briefly discussed in Chapter 2. Fenech and Rohsenow considered surfaces of two types of roughness with different frequencies. As a sample situation they gave the case of one type of irregularity resulting from the shearing action of a cutting tool (high frequency irregularities) and the other due to low frequency vibrations in the machine tool or workshop structure. Both irregularities were assumed to be uniformly distributed over the contact surface. For the longer wavelength irregularities, they suggested that elastic deformation theory be employed until the onset of plasticity, at which time the procedure employed for surface roughness is applicable. However, no further development on this aspect of the problem was reported in the later work done at M.I.T. (see reference 1, 21, 30, 41, 42). Their emphasis was placed on the development of analog and statistical methods for the analysis of the geometric parameters associated with surface roughness. The comparison made between experimental data and their theory was based on a single type of irregularity. In their experimental studies only surface roughness values were reported. The possible flatness deviation of the specimens was not given.

Thus, it appears that the elastic deformation of the contacting members and the macroscopic constriction resistance has been grossly overlooked by investigators in the analysis of thermal contact resistance. However, evidence has been obtained in this investigation that such resistance is of importance and, in many instances, is dominating, especially for engineering surfaces.

Since the various models postulated in the literature consider only the microscopic effects, their application should be limited to extremely flat surfaces or mating surfaces of ideal conformity. For interfaces in air under these circumstances, the conductances are usually very high. For example, if film resistance is neglected and only fluid conduction is considered, the equivalent length of this contact resistance would be:

$$\Delta L_m = \frac{k_m \delta}{k_f}$$

where δ is the effective fluid thickness defined in Section 3.2. Some representative lengths of this resistance are given in Table 6.

δ	ΔL_m Stainless Steel	ΔL_m Aluminum
10 μin.	0.006"	0.046"
200 μin.	0.12"	0.9"

Table 6

The Equivalent Contact Resistance
Considering Only Fluid Conduction

$$\left(k_{s.s.} = 10;\ k_{AL} = 80;\ k_{air} = 0.017 \text{ - units: } \frac{BTU}{hr\ ft\ ^oF}\right)$$

First consider the agreement between the theory and experimental data presented by Fenech and Rohsenow for interfaces in air. To the writer's knowledge, only two sets of data from nonidealized metallic surfaces in contact have been compared with their theory. Reference 20 gave a comparison for an armco-iron/aluminum interface. The contacting surfaces were roughly machined with a fly-cutter. Both surfaces had a reported roughness of 150 microinches rms, maximum. No value of the possible flatness deviation of these surfaces was mentioned. Macroscopic effects must have been of importance at their lower values of contact pressure. The contact resistance was low; the corresponding equivalent length, ΔL_m, varied from approximately 0.037 inches to 0.54 inches. At the high values of contact pressure, their calculations show that only 4% of the heat flows through the voids. In the light of the analysis and experimental results presented in the present study, this small contribution of the conducting fluid seems to be a direct consequence of the idealized model of the contacting surfaces they employed.

A more recent publication [30] gave a comparison with theory for a stainless steel interface. A definite attempt was made to obtain flat surfaces; however, again no value of the possible flatness deviation was given. The surfaces were ground to a mirror finish by Blanchard Machine Company in order to assure "flatness." They were treated later by blasting with glass spheres to produce surface roughnesses of 45 and 65 microinches rms. The reported conductance ranged from approximately 10^3 to 10^4 BTU/hr ft^2 ^oF. This represents resistances in terms of ΔL_m ranging from 0.018 to 0.18 inches. Thus the contact resistance for these relatively flat surfaces under the conditions of their tests was extremely small. It is questionable if such a resistance is of practical interest. Good agreement was reported between the data and the theoretical predictions. In this writer's opinion, the agreement was surprising

considering the unavoidable error in these high conductance measurements.

In the model used by Fenech and Rohsenow, the contact areas were assumed to be formed between cylindrical asperities of radius a_s and length δ. For clean surfaces in the absence of a conducting fluid, their theoretical expression for the joint conductance becomes:

$$h = \frac{\frac{p_a}{H}\frac{k_m}{a_s}\frac{1}{(1 - p_a/H)}}{\frac{\delta_1}{a_s}\frac{k_m}{k_1} + \frac{\delta_2}{a_s}\frac{k_m}{k_2} + 0.81} .$$

If $\delta_1 = \delta_2 = \delta$, $k_1 = k_2 = k_m$, the equation simplifies to:

$$h = \frac{\frac{p_a}{H}\frac{k_m}{a_s}\frac{1}{(1 - p_a/H)}}{\frac{\delta}{a_s} + 0.81} \qquad (7.1)$$

The ratio of $\frac{p_a}{H}$ has been employed in this equation, as they suggested, for the ratio of the actual contact area to the apparent contact area. In view of the discussion in Section 4.1.1, the validity of this assumption is subject to serious question. The dependence of the microscopic constriction resistance on δ, as indicated by Equation 7.1, is a consequence of their model. Considering the small reported asperity slopes, it is difficult to physically justify this dependence. Under large loads, δ/a_s becomes small compared to 0.81. Equation 7.1 then becomes:

$$h \cong 1.2 \frac{p_a}{H}\frac{k_m}{a_s}\frac{1}{(1 - \frac{p_a}{H})} . \qquad (7.2)$$

A comparison with Equation 4.14 shows that the quantity $(1 - \frac{p_a}{H})$ accounts for the constriction alleviation which is described in our model by $g(\dot{x}_s)$. For the polished surfaces employed in the present study, δ/a_s is probably small, and for the pressure range of interest $\frac{p_a}{H} \cong 0$. Thus, Equation 7.1 becomes:

$$h \cong 1.2 \frac{p_a}{H} \frac{k_m}{a_s} .$$

This is equivalent to Equation 4.14 if $(\xi)[g(x_s)] = 0.5$. On the basis of the assumptions inherent in the Fenech-Rohsenow model, the feasibility of predicting thermal contact resistance of the majority of engineering surfaces seems unlikely.

A comparison was not given by Cetinkale and Fishenden [16] for their theoretical prediction and experimental results, nor were their experimental data reported. However, good agreement was reported when their theoretical equation was fitted to the experimental data by the use of undetermined parameters. The flatness deviation of the specimens was not mentioned. In all cases one member was a lapped chromium steel surface. The other consisted of a steel, aluminum or brass specimen with surface roughness ranging from 12 to 570 microinches. The interface conductance ranged from 550 to 12,500 BTU/hr ft^2 ^oF. Since chromium steel has a relatively low conductivity, the contact resistance in terms of the equivalent length, ΔL_m, was again small.

Wheeler [63] stated, "The theory of thermal contact joints as developed by Holm, Cetinkale and Fishenden shows the number of points of contact per unit area of joint and the harmonic mean thermal conductivity of the joint materials to effect the conductance. An attempt to evaluate these factors quantatively produced results that had no statistical significance." Wheeler also found that the equivalent thickness δ of the gas layer determined from the conductance measurements was relatively independent of surface roughness. He suggested that a constant value gave a better approximation than some constant times the surface roughness. Wheeler's discussion clearly demonstrates

the inadequacy of the current theories that do not take into account the macroscopic constriction resistance.

Boeschoten and van der Held [12] employed an expression very similar to Equation 4.14 for the calculation of heat conducted through the metallic contact points. These circular microscopic contact areas were assumed to be uniformly distributed across the entire apparent contact area. The unknown radius, a_s, of the contact was determined from thermal conductance measurements. The average diameter of these areas was calculated to be about 60 micrometers. It was found to be independent of the material and contact pressure over the range of pressures studied. Since the roughness of their surfaces as estimated from profilometer measurements was about 10 μ , a diameter of 60 μ for the microscopic contact areas seems unlikely. This is especially true considering the fact that the distance between contact areas was reported to be very much greater than their diameter.

This unrealistic size of the calculated contact area may very well be a direct consequence of the neglect of the macroscopic constriction resistance in their model. From Equation 4.14, one sees that R_s is proportional to a_s; thus, if R_s includes the macroscopic effects, the value of a_s calculated from that equation would be too large.

In Chapter 2, a discussion of Laming's model [40] was presented. It is essentially the same as the one employed by Boeschoten and van der Held; thus, it also leads to an expression similar to Equation 4.14. Accordingly, the microscopic constriction resistance is proportional to the product of the hardness, H, and the radius of the microscopic contact areas, a_s. Boeschoten and van der Held obtained correlation by employing an artificially large value of a_s. Laming also had difficulty in obtaining correlation between his model and

theory. In an effort to correlate his data, he obtained hardness values which were, in his words, "fabulously high." He stated: "The only claim made for the 'super hardness' hypothesis in this paper is its value in correlating the heat transfer data." Again, since R_s in Laming's experiments includes the macroscopic constriction resistance, the "fabulously high" value of H is a natural consequence.

It is thus concluded that the models presented in the literature have generally had little success in correlating the heat transfer data and hold little promise of successful application to interfaces in a vacuum environment.

7.2 EXPERIMENTAL PROCEDURES AND RESULTS

Much of the experimental data reported in the literature failed to include information on flatness deviation. This probably was a result of overlooking this parameter, but perhaps also a consequence of the difficulty of obtaining reliable measurements, particularly for rough surfaces. Table 7 lists the references which gave data for the flatness deviation along with the

Investigator	Total Flatness Deviation
Barzelay et al. [7]	800
Barzelay et al. [6]	300 - 1900
Fried and Costello [22]	1500 - 4500
Jacob and Starr [33]	"Approximately Optical Flatness"
Rogers [51]	300 (or less)
Weils and Ryder [61]	400 (or less)

Table 7

Flatness Deviations Reported in the Literature

range reported. The values shown in this table are converted as close as possible from the reported data to the total maximum flatness deviation between the contacting surfaces at zero load. No description of the macroscopic surface contour could be found in the literature. From Table 7 it is seen that surfaces with total flatness deviations larger than those employed in this investigation have been used by many investigators; thus, macroscopic effects must have been of importance in their studies. However, several investigators employed "lapped" specimens. In this case macroscopic effects were probably not completely dominant.

The importance of the macroscopic constriction resistance for many of the interfaces tested by the numerous investigators also manifests itself by the reported presence of temperature gradients in planes parallel to the interface. Such temperature gradients have been observed by: Sanderson [53], Fried [23], Weils and Ryder [61], Barzelay, et al. [7], and perhaps others. It is difficult to see how surfaces with uniformly distributed microscopic contact areas could give rise to such temperature gradients.

When macroscopic constrictions are present, the axial gradient* in a region outside of the influence of interfacial disturbances must be projected to the plane of contact in order to determine the contact resistance. Otherwise, erroneous results will be obtained. Hence, a procedure like that employed by Fried [22] is subject to serious question. The procedure used by Barzelay, et al. [7], is better but still suffers from a similar criticism. While two to six thermocouples were installed in a plane parallel to that of contact, they were only at either 0.100" or 0.050" from the interface. Also, they were all located in the center third of the apparent contact area; thus, the averaged value was

* Refers to temperature gradient in the direction of heat flow.

not a good representation of the average temperature of that plane. Other investigators (see References 1 and 18) employed only two or three thermocouples for the determination of the axial temperature gradient. It is clear that if one of these thermocouples were in the disturbed area, the experimental error could be very large.

Several investigators studied the effects of metallic foil and other sandwich materials on the thermal contact resistance. Brunot and Buckland [14] presented data for steel specimens in air with 5, 10 and 15 sheets of aluminum foil placed between the interfaces under an apparent contact pressure of 200 psi. The thermal contact resistance was found to be almost unchanged for all three tests, even though the number of interfaces varied from 6 to 16. In other investigations [7, 24], a decrease in contact resistance was experienced with the inclusion of sandwich materials. Many of these reported effects are difficult to explain unless the presence of macroscopic constrictions are admitted.

Now consider the results reported by Mikesell and Scott [44] for the flow of heat through a stack of thin metallic plates in a vacuum. For example, they reported that the conduction through a stack of 0.0008 inch thick stainless steel plates under an apparent contact pressure of 1000 psi was found to be approximately 2% of the conduction of a solid member of equivalent length. Considering a stack of thin plates from the macroscopic view point, one would conclude that the resistance of any given interface would be small. If the equivalent length of the resistance of each interface in the above example is calculated, it is found to be very small, less than 0.05 inches. All three component resistances could be of importance in this case. A thin layer of manganese dioxide dust on these surfaces was shown to greatly increase the contact resistance of a stack of such plates.

Several investigators [7, 51] have reported experimental data showing that the contact resistance of a steel-aluminum contact depends on the direction of heat flow. Williams [64] attributed this phenomenon to surface contamination, whereas Moon and Keeler [46] applied the theory of heat conduction in the solid state to explain this asymmetric behavior. None of the models for the prediction of thermal contact resistance include a means of explaining this directional effect. A recent report from Massachusetts Institute of Technology [30] stated that this effect is presently believed to be negligible. However, Barzelay, et al. [7], found the interface conductance for heat flow from aluminum to steel was, in some instances, over five times higher than when heat was flowing in the other direction. A very significant observation of their study was the presence of large radial gradients only when heat flowed from steel to aluminum. This seems to indicate that changes in the macroscopic contact occured during the reversal of heat flow and thus created the directional effect.

The properties of most metals and fluids are such that, according to the models presented in the literature, an increase in the mean interface temperature should cause a decrease in the contact resistance. Several reported observations have shown just the contrary. Examples are the steel-aluminum interface studied by Barzelay, et al. [7], and the interface examined by Kouwenhoven and Potter [39]. Since the sink temperature was relatively constant in both of these experiments, a change in the mean interface temperature was effected by a change in the heat flux. This caused a change in the amount of thermal strain, hence, a change in the macroscopic contact area. The effects of thermal strain on the macroscopic contact area are presently being studied.

Generally, rough engineering surfaces are less flat than smooth surfaces. This is believed to be the main reason for the general trend of an increase in thermal contact resistance with an increase in surface roughness, which is again readily understood from the macroscopic theory presented here. Some of the data obtained in the literature show exceptions to this trend (see, e.g., References 22 and 39). This is probably the consequence of the rough surfaces being flatter than the smooth surfaces with which they were compared.

Summarizing, we note that many of the apparent discrepancies and observations in the literature, heretofore unexplainable, are now understandable. The present analysis, admittedly approximate and perhaps somewhat oversimplified, has thrown considerable light on the mechanism of thermal contact resistance.

8. SUMMARY AND CONCLUSIONS

A survey of literature on thermal contact resistance reveals that: i) there exists considerable discrepancy between experimental data and proposed theories and oftentimes even contradictions and ii) the amount of data on thermal contact resistance in a vacuum environment is extremely meager.

Thermal radiation and interstitial conduction were shown to be unimportant for the conditions that are of interest in this investigation. Attention was thus focused on the study of the metal-to-metal conduction. The total resistance of the interface was conceived to consist of three resistances in series: the macroscopic constriction resistance, the microscopic constriction resistance, and the film resistance. They were each examined; however, a quantitative analysis is presented only for the situation wherein the macroscopic constriction is dominating. It is demonstrated that the agreement between theoretical prediction and experimental data is good for surfaces which satisfy the said condition.

The following major conclusions could be drawn based upon conditions within the limits of this investigation:

1. The macroscopic constriction effect is of importance and dominates the thermal contact resistance of a majority of engineering surfaces. This fact has been grossly overlooked in many previous investigations.

2. An analysis based on a model of macroscopic elastic contact between mating members has been carried out, which makes possible a satisfactory prediction of thermal contact resistance whenever the macroscopic constriction is dominating. It naturally leads to a pair of dimensionless parameters for correlating data.

They are: the Biot modulus, $\frac{h\, b_L}{k_m}$,

and the elastic conformity modulus $\zeta = (\frac{p_a}{E_m})(\frac{b_L}{d_t})$.

Experimental evidence is given to establish the validity of the theory.

3. The relative importance of the macroscopic constriction resistance for clean surfaces can be ascertained from the expression:

$$\frac{R_L}{R_s} = \frac{\frac{2}{\pi}(\frac{p_a}{H})(\frac{b_L}{a_s})\frac{1}{g(x_s)}}{g'(\zeta)}$$

Calculations have indicated that microscopic constriction resistance is not of importance for many engineering surfaces.

4. Film resistance can be of considerable importance for heavily oxidized surfaces; however, it also has been shown that for freshly machined surfaces with a realistic value of flatness deviation, film resistance is only of secondary importance.

5. Using the model put forth in this investigation, many phenomena associated with thermal contact resistance, which previously resisted explanation, are now understandable.

6. High conductance interfaces, thermal switches, etc., can now be designed more rationally. By judiciously choosing E_m, k_m and d_t, a wide range of contact resistance can be obtained for any given load.

Other specific conclusions are:

7. An appreciable decrease of the macroscopic contact resistance can occur,

with time, due to creep of the contact members. For the temperature level of these experiments, creep was only significant for magnesium.

8. With heat treated alloys, an appreciable change in the thermal contact resistance can occur as a consequence of property changes caused by aging or annealing effects at elevated temperatures.

9. The size of the macroscopic contact area is affected by thermal strain. It could be of considerable importance in contacts between dissimilar materials.

10. The improvement of the conductance with the addition of a conducting fluid can be appreciable, even at large loads.

9. RECOMMENDATIONS FOR FUTURE EXTENSIONS

The present investigation has provided a better understanding of the mechanism of thermal contact resistance. It has revealed the importance of macroscopic effects and has been successful in predicting this resistance. In spite of the assumptions and approximations used, the present analysis provides a basis from which a detailed and refined study can be effected. A few recommended extensions follow.

The Hertz equation which was employed for the calculation of the macroscopic contact area is only applicable if the dimensions of this area are small compared with those of the contact members. The experimental results obtained indicated that the Hertz equation was applicable for X_L less than approximately 0.65. Thus, the macroscopic constriction resistance for the model employed cannot be accurately predicted if X_L becomes larger than this value. The ability to predict the macroscopic resistance when X_L is greater than 0.65 would be an asset for the study of interfaces with low resistance and for the analysis of film and microscopic constriction resistances. The variation of contact area with load for geometries other than spheres would also be of interest.

The effects of thermal strain on the macroscopic contact area are not clear at the present time. A theoretical study of this problem has begun in the Department of Theoretical and Applied Mechanics under the direction of Professor A. P. Boresi. The temperature gradients due to the macroscopic constrictions produce thermal strains which result in a change of the macroscopic contact area. While these effects do not seem to be significant for contacts between similar materials, they could become appreciable for dis-

similar metals. It would be interesting and enlightening to find out if the variation of thermal contact resistance between dissimilar metals with the direction of heat flow is a consequence of thermal strain or of other causes.

This study is mainly concerned with the macroscopic constriction resistance; thus the physical nature of the film and microscopic constriction resistances must be examined further. The knowledge and experience gained in this study should prove to be useful in planning the experiments and interpreting the data.

Several possible methods of reducing film resistance should be investigated. For example, plating the contacting surfaces with a noble metal such as gold or silver may provide a means of reducing film resistance. Also, the film resistance could be mechanically reduced by treatment inside the vacuum chamber. A soft metallic plating of suitable material and thickness would be a possible means of reducing both the microscopic and film resistances by increasing the microscopic contact area. Film resistance also could be studied by varying the film thickness; however, the control and measurement of the film thickness would be difficult, particularly for thin films.

The influence of surface roughness on the effective macroscopic contact area and the variation of this area with loading and unloading should also be examined. The problem of film damage as affected by roughness and manner of loading warrants a careful and systematic study for surfaces with both large and small flatness deviations.

A more complete investigation of the effect of the geometry of the contacting members and the thermal boundary conditions should be made. The conductive-liquid analog would be a valuable tool for such studies. A problem of definite interest would be to examine further the influence of the manner in which the macroscopic contact areas are distributed.

An interesting and possibly rewarding extension of the present model would be the inclusion of an interfacial fluid. Qualitatively, the effects of an interfacial fluid have been discussed, but at this time no quantitative prediction has been attempted. Possible technological applications are obvious.

NOMENCLATURE

A	contact area
a	radius of a contact area
b	radius of constriction region
C	conductance, $C = \frac{1}{R}$
d	equivalent flatness deviation
E	modulus of elasticity
$g(x)$	defined by Equation 4.10
h	interface conductance, $h = \frac{1}{A_a R}$
k	thermal conductivity
L	length of specimen
ΔL	equivalent length of contact resistance
n	number of contact points
P	load
p	contact pressure
q	heat flux
R	resistance
r	radius of spherical cap or radial coordinate
s	film thickness
T	temperature
ΔT	a temperature difference
x	constriction ratio
y	dimensionless radial coordinate, r/a_L
z	axial coordinate
α	accommodation coefficient
γ	ratio of specific heats

δ	equivalent distance between contacting surfaces
ε	emissivity of surface
ζ	elastic conformity modulus
λ	mean free path
υ	Poisson's ratio
ξ	proportionality constant between p_s and H
ρ	resistance across a unit area of surface film
σ	Stefan-Boltzmann's constant
$\phi(\zeta)$	defined by Equation 4.33

Subscripts

1	surface or specimen 1
2	surface or specimen 2
a	apparent contact area
c	metal-to-metal conduction mode
f	interstitial conduction mode
L	macroscopic constrictions or contact regions
m	a mean value as defined in text
o	surface film property or contribution
r	radiation mode
s	microscopic constrictions or contact areas
t	total

36. W.D. Kimmel, Personal Correspondence, L. D. Caulk Company, September 1962.

37. W. Köster, "Die Temperaturabhängigkeit des Elastizitätsmoduls reiner Metalle," Zeitschrift Für Metallkunde, Vol. 39, 1948, pp. 1-9.

38. W. Köster, "Über die Konzentrations-und Temperaturabhängigkeit des Elastizitätsmoduls," Zeitschrift Für Metallkunde, Vol. 32, 1940 pp. 160-162.

39. W.B. Kouwenhoven and J.H. Potter, "Thermal Resistance of Metal Contacts," J. Am. Weld. Soc., Vol. 27, Part 2, 1948, pp.515-520.

40. L.C. Laming, "Thermal Conductance of Machined Metal Contacts," 1961 International Heat Transfer Conference, Part 1, No. 8, Boulder, Colorado, September 1961, pp. 65-76.

41. Massachusetts Institute of Technology, Progress Report, "Description of Method for Determining Geometric Parameters of Surfaces In Contact," AEC Report NYO-9456, May 1961.

42. Massachusetts Institute of Technology, Progress Report, "Some Methods of Surface Analysis for the Prediction of Thermal Resistance of Metal Contacts," AEC Report NYO-9457, November 1961.

43. Metals Handbook, Vol. 1, Eighth Edition, American Society for Metals, 1961, p. 1024.

44. R.P. Mikesell and R.B. Scott, "Heat Conduction Through Insulating Supports in Very Low Temperature Equipment," Journal of Research of the National Bureau of Standards, Vol. 57, 1956, pp. 371-378.

45. T. Mizushina, S. Iuchi, T. Sasano, and H. Tamurs, "Thermal Contact Resistance Between Mercury and a Metal Surface," Int. J. Heat Mass Transfer, Vol. 1, 1960, pp. 139-146.

46. J.S. Moon and R.N. Keeler, "A Theoretical Consideration of Asymmetric Heat Flow at the Interface of Two Dissimilar Metals," University of California, Lawrence Radiation Laboratory Report No. 9885, October 1961.

47. A.J.W. Moore, "Deformation of Metals in Static and in Sliding Contact," Proc. Rog. Soc. Series A, Vol. 195, 1948, pp. 231-244.

48. M.F. Mott, "The Theory of the Formation of Protective Oxide Films on Metals-III," Trans. Faraday Soc., Vol. 43, 1947, pp. 429-434.

49. D.J. Nourie, Personal Correspondence, Field Engineer, Leeds and Northrup Company, February 1962.

50. L.C. Roess, "Theory of Spreading Conductance," Appendix A of an unpublished report of the Beacon Laboratories of Texas Company, Beacon, New York.

51. G.F.C. Rogers, "Heat Transfer at the Interface of Dissimilar Metals," Int. J. Heat Mass Transfer, Vol. 2, 1961, pp. 150-154.

52. Ryerson Data Book, Joseph T. Ryerson and Sens Incorporated, 1960, p. 360.

53. P.D. Sanderson, "Heat Transfer From the Uranium Fuel to the Magnox Can in a Gas-Cooled Reactor," 1961 International Heat Transfer Conference, Part 1, Number 8, Boulder, Colorado, September 1961.

54. E.H.W. Schmidt and E. Jung, "Measurement of the Thermal Contact Resistance from Stainless Steel to Liquid Sodium," Modern Developments in Heat Transfer, Academic Press, New York, 1963, pp. 251-263.

55. R.S.G. Skipper and K.J. Wooton, "Thermal Resistance Between Uranium and Can," International Conference on Peaceful Uses of Atomic Energy, Proceedings, Vol. 7, 1958, pp. 684-690.

56. D. Tabor, The Hardness of Metals, Oxford University Press, London, 1951, p. 63.

57. C.L. Taylor, Personal Correspondence, Dow Corning Corporation, October 1962.

58. C. Timms, "The Measurement of Finely Finished Surfaces by Optical Interference," J. Sci. Instruments, Vol. 22, No. 12, 1945, pp. 245-246.

59. S. Timoshenko and J.N. Goodier, Theory of Elasticity, McGraw-Hill Book, New York, 1951, p. 375.

60. United States Steel Company Brochure, "Steel For Elevated Temperature Services," 1949.

61. N.D. Weills and E.A. Ryder, "Thermal Resistance Measurements of Joints Formed Between Stationary Metal Surfaces," Trans. ASME, Vol. 71, 1949, pp. 259-267.

62. R.G. Wheeler, "Thermal Contact Conductance," AEC Report No. HW-53598, November 1957.

63. R.G. Wheeler, "Thermal Conductance of Fuel Element Materials," AEC Report No. HW-60343, 1959.

64. A. Williams, "Comment on Rogers' Paper 'Heat Transfer at the Interface of Dissimilar Metals,'" Int. J. Heat Mass Transfer, Vol. 3, 1961, p. 159.

BIBLIOGRAPHY

1. A. Adamantiades, "Experimental Determination of Contact Conductance for Some Stainless Steel Contacts," AEC Report No. NYO-9458, July 1962.

2. Alcoa Aluminum Handbook, Aluminum Company of America, Pittsburgh, 1962 pp. 20 and 28.

3. Alcoa Structural Handbook, Aluminum Company of America, Pittsburgh, 1960, p. 11.

4. J.F. Archard, "Elastic Deformation and Laws of Friction," Proc. Roy. Soc. (London), Series A, Vol. 243, 1957, pp. 190-205.

5. H. Baker, Personal Correspondence, Dow Metal Products Company, May 1963.

6. M.E. Barzelay, K.N. Tong, and G.F. Holloway, "Thermal Conductance of Contacts in Aircraft Joints," NACA TN-3167, March 1954.

7. M.E. Barzelay, K.N. Tong, and G.F. Holloway, "Effect of Pressure on Thermal Conductance of Contact Joints," NACA TN-3295, May 1955.

8. M.E. Barzelay and G.F. Holloway, "Effect of an Interface on Transient Temperature Distribution in Composite Aircraft Joints," NACA TN-3824, April 1957.

9. M.E. Barzelay and G.F. Holloway, "Interface Conductance of Twenty-Seven Riveted Aircraft Joints," NACA TN-3991, July 1957.

10. M.E. Barzelay, "Range of Interface Thermal Conductance for Aircraft Joints," NACA TN D-426, May 1960.

11. R. Berman, "Some Experiments on Thermal Contact at Low Temperatures," Journal of Applied Physics, Vol. 27, No. 4, April 1956, pp. 318-323.

12. F. Boeschoten and E. Van der Held, "The Thermal Conductance of Contacts Between Aluminum and Other Metals," Physica, Vol. 23, 1957, pp. 37-44.

13. F.P. Bowden and D. Tabor, The Friction and Lubrication of Solids, Oxford University Press, 1950, pp. 10-32.

14. A.W. Brunot and F.F. Buckland, "Thermal Contact Resistance of Laminated and Machined Joints," Trans. ASME, Vol. 71, 1949, pp. 253-257.

15. P.M. Budge, Personal Correspondence, Technical Manager, Anaconda Aluminum Company, April 1963.

16. T.N. Cetinkale and M. Fishenden, "Thermal Conductance of Metal Surfaces in Contact," General Discussion on Heat Transfer, Conference of Institution of Mech. Eng. and ASME, September 1951.

17. Dow Metal Products Company Brochure, Form No. 141-76-1057.

18. J. Dyson and W. Hirst, "The True Contact Area Between Solids," Proceedings of the Physical Society, Section B, Vol. 67, 1954, pp. 309-312.

19. E.R. G. Eckert and R.M. Drake, Heat and Mass Transfer, McGraw-Hill, New York, 1959, p. 403.

20. H. Fenech and W.M. Rohsenow, "Thermal Conductance of Metallic Surfaces in Contact," U.S. AEC Report NYO-2136, May 1959.

21. H. Fenech and W.M. Rohsenow, "Prediction of Thermal Conductance of Metallic Surfaces in Contact," ASME Paper No. 62-HT-32, August 1962.

22. E. Fried and F.A. Costello, "Interface Thermal Contact Resistance Problem in Space Vehicles," American Rocket Society Conference, Palm Springs, California, April 1961 (See also ARS Journal, Vol. 32, 1962, pp. 237-243).

23. E. Fried, "The Thermal Conductance of Space Vehicle Interfaces - Experimental Results," General Electric Report No. 61GL65, March 1961.

24. E. Fried, "Thermal Joint Conductance in a Vacuum," ASME Paper No. AHGT-18, Aviation and Space Hydraulic and Gas Turbine Conference, Los Angeles, California, March 1963.

25. Goldsmith, Waterman, and Hirschhorn, Handbook of Thermophysical Properties of Solid Materials, Vol. II, Macmillan, New York, 1961.

26. W.J. Graff, "Thermal Conductance Across Metal Joints," Machine Design, Vol. 32, 1960, pp. 166-172.

27. M.E. Haine and W. Hirst, "The Adaptation of an Electron Microscope for Reflexion and Some Observations on Image Formation," Brit J. Applied Physics, Vol. 4, 1953, pp. 239-244.

28. J.S. Halliday, "Surface Examination by Reflection Electron Microscopy," Institution of Mech. Eng. Proceedings, Vol. 169, 1955, pp. 777-781.

29. J.P. Hartnett, "A Survey of Thermal Accommodation Coefficients," Advances in Applied Mechanics Supplement 1, Rarefied Gas Dynamics, Academic Press, New York, 1961, pp. 1-28.

30. J.J. Henry, "Thermal Conductance of Metallic Surfaces in Contact," AEC Report NYO-9459, February 1963.

31. R. Holm, Electrical Contacts, Springer Verlag, Berlin, 3rd Ed., 1958.

32. W.W. Hough, "Torque Limits for Spacecraft Structural Fasteners," JPL-NASA Process Specification No. 20503, May 1961.

33. R.B. Jacobs and C. Starr, "Thermal Conductance of Metallic Contacts," Rev. of Scientific Instruments, Vol. 10, 1939, pp. 140-141.

34. J.D. Keller, "Heat Transmission in Strip-Coil Annealing," Iron and Steel Engineer, Vol. 25, 1948, pp. 60-67.

35. E.H. Kennard, Kinetic Theory of Gases, McGraw-Hill, New York, 1938, pp. 315-318.

APPENDICES

A. MATERIAL PROPERTIES

1) Modulus of Elasticity

The modulus of elasticity of metals is a function of the temperature. Generally, this variation with temperature cannot be neglected. For example, the modulus of some magnesium alloys at 500°F is only half of its value at room temperature. Some excellent work on the variation of the modulus of elasticity with temperature has been done by Köster [37, 38]. He reported data for 32 pure metals for temperatures ranging from -180°C to the melting point or 1000°C. Data on various alloys also were reported. In Reference [38] data for copper-zinc alloys are given. The percentage of copper was varied from 63% to 95%. The variation of the magnitude of the modulus between alloys was large; however, the slope of these curves, $\frac{dE}{dT}$, at a given temperature was approximately the same for all the copper-zinc alloys. Using Köster's slopes and the room temperature value of the modulus for leaded brass reported by Reference 43, the data for brass given in Figure 41 were calculated.

Alcoa [2] reported that the compression modulus for aluminum was about 2% greater than the tension modulus. They also reported no variation in this modulus with the heat treatment. For example, 2024-O, -T4, and -T6 were reported to have the same modulus of elasticity. Their structural handbook [3] listed the percentage variation of the modulus with temperature. From these data and the room temperature value for 2024-T4, the variation of the modulus with temperature given in Figure 41 was calculated. The data given for stainless steel and magnesium were obtained from References 60 and 17, respectively.

In this investigation the possible variation of the modulus of elasticity with temper and the difference between the compression and tension moduli were

neglected. These effects apparently were small. Sufficient data were not available to justify their inclusion.

ii) Hardness Data

Indentor Load (Kilograms)	Diamond Pyramid Hardness Number *			
	Magnesium (AZ 31B)	Brass (Anaconda) (271)	Aluminum (2024T4)	Stainless Steel (303)
0.1	74	170	150	-
1.0	60	135	143	260
2.0	59	130	140	254
3.0	-	-	-	240

iii) Thermal Conductivity Measurements

In Figures 41 and 42 the experimentally determined thermal conductivities of the materials employed in this investigation are compared with the data taken from the literature. Much of the deviation and scatter shown is due to slightly different compositions or heat treatments.

* This number represents the load in kilograms divided by the projected area of the indentation in square millimeters. A Tukon microhardness testing machine was employed to determine the above hardness numbers.

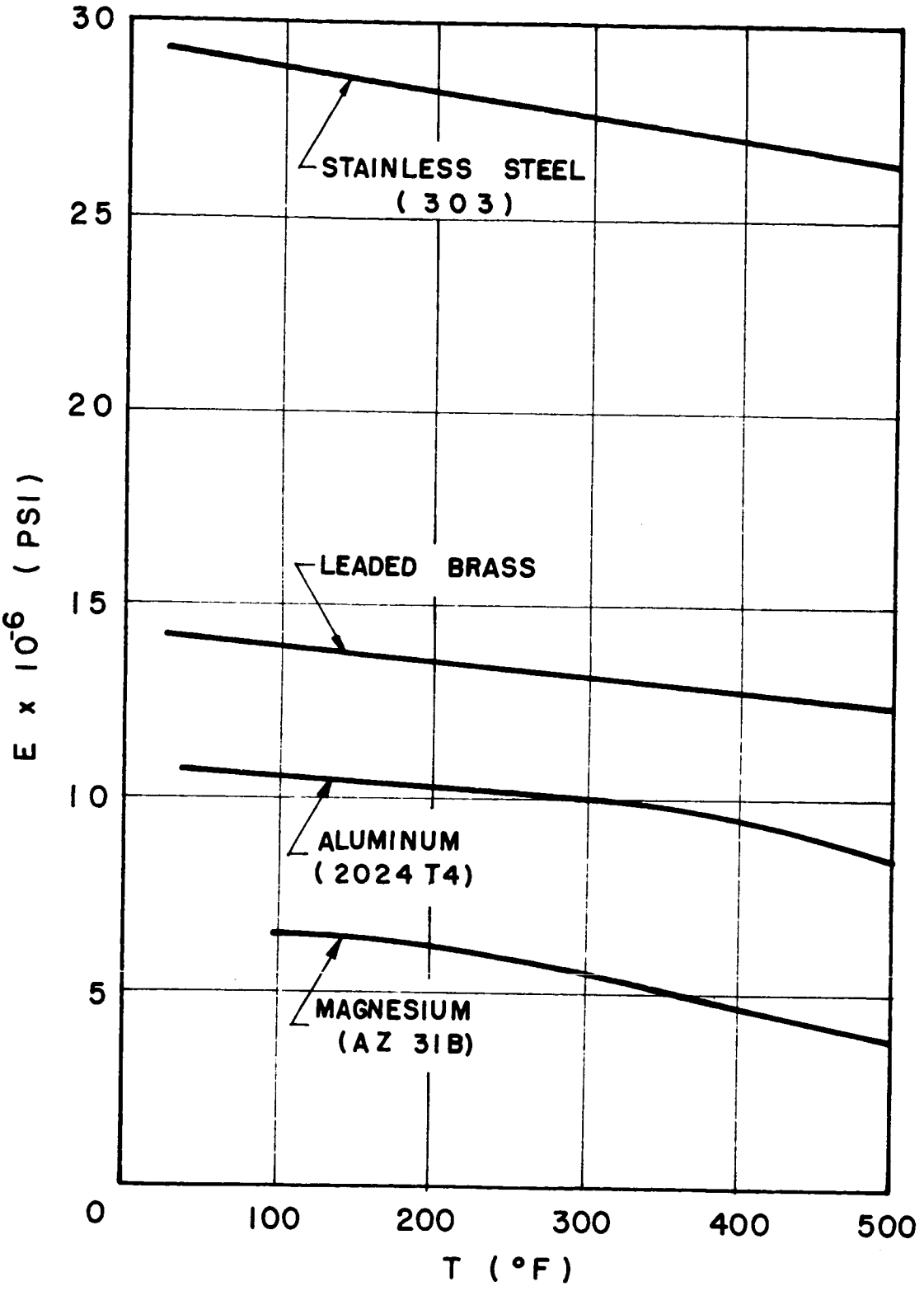

FIG. 41 THE INFLUENCE OF TEMPERATURE ON THE ELASTIC MODULUS

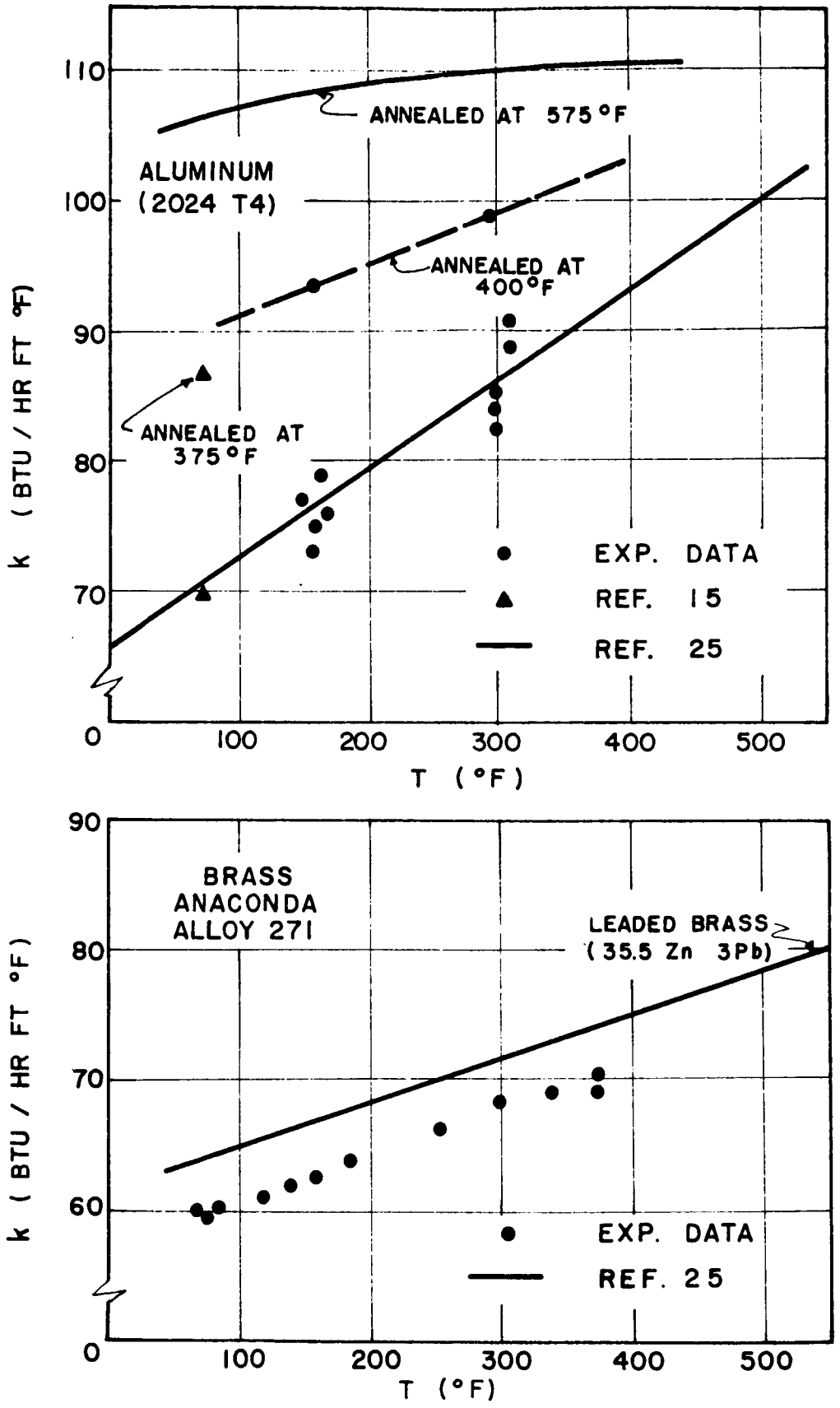

FIG. 42 THERMAL CONDUCTIVITY DATA

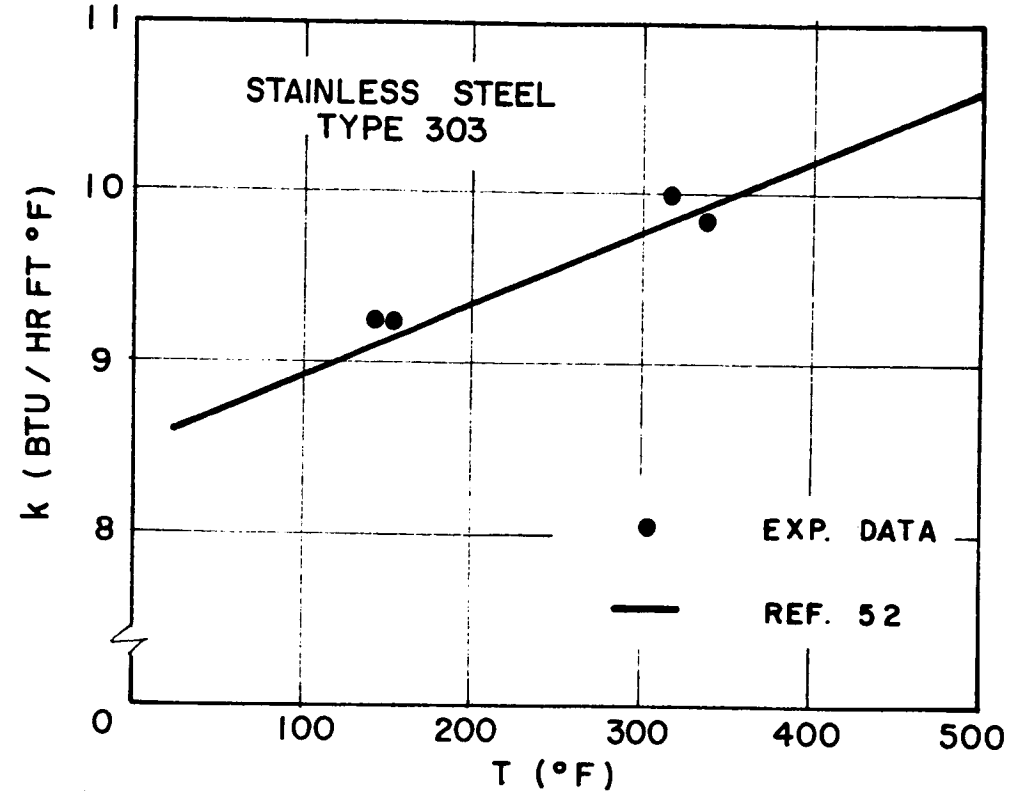

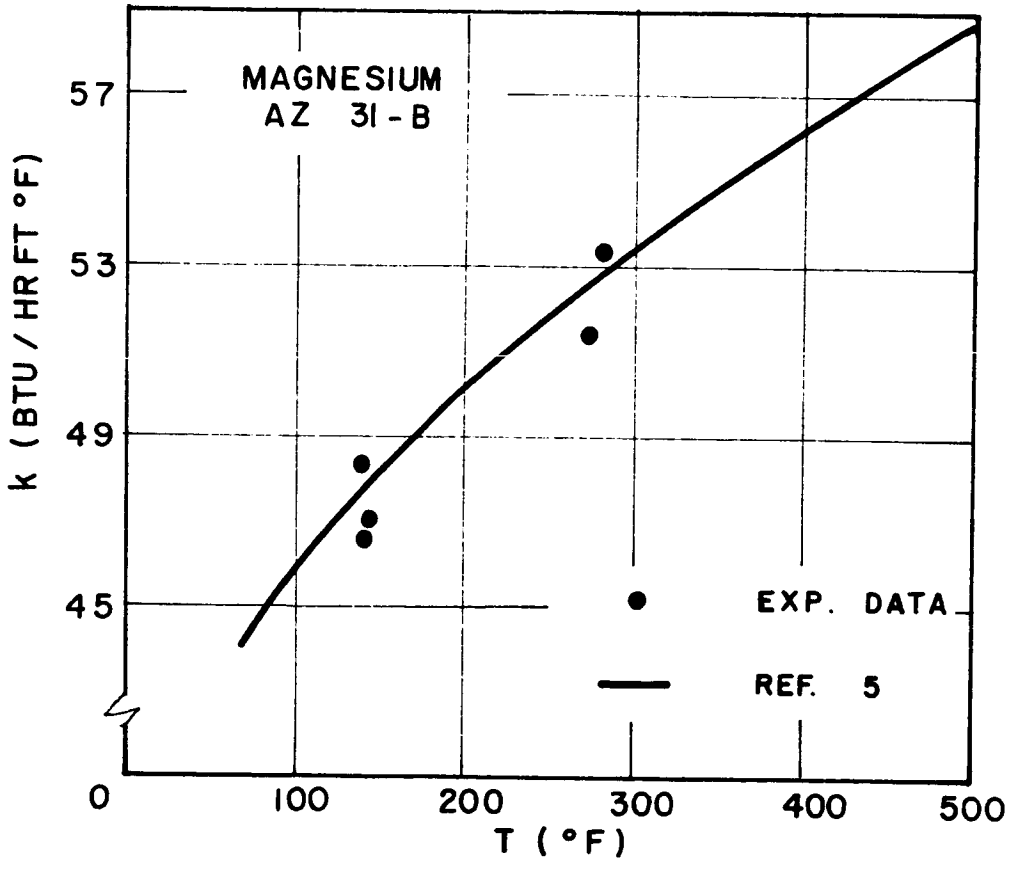

FIG. 43 THERMAL CONDUCTIVITY DATA

B. TEST SCHEDULE AND DESCRIPTION OF SPECIMENS

Series	Specimens	Material	Total Equivalent Flatness Deviation		Surface Roughness*	Notes
			Initial (μ in.)	Final (μ in.)		
1_B	$1_B - 2_B$	Brass Anaconda Alloy 271	-	820	12 - 14	all brass specimens 1" long
2_B	$3_B - 4_B$		-	780	14 - 14	
3_B	$5_B - 6_B$		-	950	14 - 18	
4_B	$3_B - 4_B$		-	780	14 - 14	same assembly as 2_B-upper specimen rotated 90^0
5_B	$1_B - 2_B$		-	820	12 - 14	same assembly as 1_B with silicone grease
6_B	$5_B - 6_B$		-	950	14 - 18	same assembly as 3_B with silicone grease
7_B	$3_B - 4_B$		-	780	14 - 14	chamber gas pressure varied
1_M	$1_M - 2_M$	Magnesium AZ 31B	35	80	3 - 3	
2_M	$1_M - 2_M$		130	80	3 - 3	same specimens as 1_M-repolished
3_M	$1_M - 4_M$		260	210	3 - 3	
1_S	$1_S - 3_S$	Stainless Steel 303	25	25	3 - 3	
2_S	$1_S - 3_S$		40	40	3 - 3	same specimens as 1_S-repolished
3_S	$3_S - 4_S$		150	150	3 - 3	

Series	Specimens	Material	Total Equivalent Flatness Deviation		Surface Roughness*	Notes
			Initial ($\frac{1}{4}$ in.)	Final ($\frac{1}{4}$ in.)		
4_S	3_S - 4_S		150	150	3 - 3	same assembly as 3_S-thermal strain effects studied
1_A	1_A - 2_A	Aluminum 2024T4	-	230	12 - 12	
2_A	1_A - 2_A		-	230	12 - 12	same specimens as 1_A-upper specimen rotated 90^0
3_A	4_A - 5_A		15	15	3 - 3	
4_A	4_A - 5_A		40	40	3 - 3	same specimens as 3_A-repolished
5_A	4_A - 6_A		120	120	3 - 3	
6_A	1_A - 6_A		220	220	3 - 3	
7_A	1_A - 6_A		220	220	45 - 80	same specimens as 6_A-surfaces etched
8_A	1_A - 6_A		220	220	45 - 80	same specimens as 7_A-annealed for 7 hours at 400^0F

* Roughness measurements were made on a type Q profilometer for roughness values greater than 5 microinches. These values are rms values. Roughness values below 5 microinches were determined optically. Numerous large scratches often present were overlooked.

C. TABULATED EXPERIMENTAL RESULTS

Units of tabulated quantities:

p_a(psi); $\Delta T(^{\circ}F)$; $h\left(\frac{BTU}{hr\ ft^2\ ^{\circ}F}\right)$;

E_m(psi); $T_m(^{\circ}F)$; $k_m\left(\frac{BTU}{hr\ ft\ ^{\circ}F}\right)$

Series	p_a	h	ΔT	Other Parameters
1_B	11.1	172	65	
	29.2	245	64	$T_m \simeq 340$
	44.6	259	64	
	87	346	57	$k_m \simeq 69$
	157	465	50	
	311	652	41	$E_m \simeq 13.1 \times 10^6$
	519	918	33	
	760	1126	29	
	954	1327	26	
2_B	11.1	126	86	
	29.2	220	70	$T_m \simeq 265$
	44.6	257	63	
	87	334	58	$k_m \simeq 66.5$
	157	432	53	
	311	590	44.5	$E_m \simeq 13.35 \times 10^6$
	519	830	36	
	760	1045	30.9	
	954	1260	27	
3_B	11.1	93.5	118	
	29.2	148	103	$T_m \simeq 160$
	44.6	174	92.5	
	87	238	81	$k_m \simeq 62.5$
	157	316	72	
	311	422	62	$E_m \simeq 13.7 \times 10^6$
	519	579	51.5	
	760	706	45.5	
	954	849	40	
4_B	11.1	158	134	
	29.2	253	98.0	$T_m \simeq 260$
	44.6	289	91.8	
	86.9	370	78.1	$k_m \simeq 66.5$
	157	472	67.8	
	311	647	54.1	$E_m \simeq 13.4 \times 10^6$
	519	881	42.5	
	760	1182	33.2	
	954	1390	28.9	

Series	p_a	h	ΔT	Other Parameters
5_B	11.1	1940	11.1	
	29.2	2360	10.6	$T_m \simeq 340$
	44.6	2630	10.2	
	86.9	2980	9.8	$k_m \simeq 69$
	157	3260	9.9	
	311	4190	8.4	$E_m \simeq 13.1 \times 10^6$
	519	5100	7.4	
	760	6700	5.9	
	954	6860	5.9	
6_B	11.1	538	39	
	29.2	629	39.1	$T_m \simeq 165$
	44.6	718	36.7	
	86.9	985	29.2	$k_m \simeq 62.5$
	157	1440	22.1	
	311	2370	14.8	$E_m \simeq 13.7 \times 10^6$
	519	3190	11.7	
	760	3730	10.5	
	954	4080	9.8	

Series	Chamber Pressure (mm of Hg)	h	ΔT	Other Parameters
7_B	10^{-3}	428	46.0	
	3×10^{-2}	437	45.1	$T_m \simeq 180$
	8×10^{-2}	437	45.2	
	5×10^{-1}	436	45.1	$k_m \simeq 63$
	2	452	43.4	
	760	1022	20.6	$E_m \simeq 13.8 \times 10^6$
	3×10^{-2}	442	45.5	

		Loading		Unloading		
Series	p_a	h	T	h	ΔT	Other Parameters
1_M	10.2	35.0	201	-	-	
	28.4	85.3	142	108	140	$T_m \simeq 215$
	67	152	105	229	86.9	
	157	344	61.4	500	48.0	$k_m \simeq 50.8$
	310	816	31.7	1200	22.7	
	518	1540	18.0	2200	12.9	$E_m \simeq 6.1 \times 10^6$
	759	2270	12.6	2910	9.9	
	986	3200	9.0	-	-	

Series	p_a	Loading h	Loading ΔT	Unloading h	Unloading ΔT	Other Parameters
2_M	10.2	283	68.7	-	-	
	28.4	687	33.6	898	26.2	$T_m \simeq 210$
	67	1450	17.4	-	-	
	157	3570	7.5	4900	5.5	$k_m \simeq 49.6$
	311	9100	3.0	-	-	
						$E_m \simeq 6.1 \times 10^6$
3_M	10.2	61	170	-	-	
	28.4	145	107	440	48.0	$T_m \simeq 210$
	67	511	43	830	28.6	
	157	1250	20	1600	16.2	$k_m \simeq 49.3$
	310	2320	11	3070	8.8	
	518	5050	5.4	6400	4.3	$E_m \simeq 6.1 \times 10^6$
	759	8700	3.2	-	-	
1_S	11.1	17.2	180	20.9	164	
	29.2	28.3	139	37.7	118	$T_m \simeq 230$
	67.7	48.5	98.4	78.2	69.2	
	157	108	53.8	187	33.6	$k_m \simeq 9.45$
	311	223	27.7	464	14.1	
	519	695	9.5	993	6.8	$E_m \simeq 28 \times 10^6$
	760	1700	4	2140	3.2	
	987	2300	3	-	-	
2_S	29.2	20.3	174	36.3	125	$T_m \simeq 245$
	157	139	44.1	199	32.3	
	311	341	19.5	-	-	$k_m \simeq 9.53$
	519	740	9.3	-	-	
						$E_m \simeq 28 \times 10^6$
3_S	29.2	38.4	122	45.4	109	
	67.7	71.7	77.2	-	-	$T_m \simeq 245$
	157	120	51.2	118	53	
	311	168	37.9	-	-	$k_m \simeq 9.53$
	519	244	27.9	243	27.2	
	760	321	21.2	-	-	$E_m \simeq 28 \times 10^6$
	987	396	17.4	-	-	

Series	Time (Hours)	h	ΔT	Q(BTU/hr)	Other Parameters
4_S	9.33	35.1	91.5	17.5	
	10	38.4	85.9	18	
	10.33	38.0	87.4	17.9	$T_m \simeq 193$
	10.67	36.3	88.7	17.6	
	11	35.3	89.9	17.3	$k_m \simeq 9.30$
	11.33	36.0	89.1	17.45	
	11.67	37.3	87.5	17.8	$E_m \simeq 28 \times 10^6$
	12	35.1	89.8	17.2	
	12.33	35.3	89.9	17.3	
	12.67	35.9	89.6	17.35	$\Delta T(ave.) \simeq 88.7$
	13	35.9	89.5	17.35	
	16	35.2	90.7	17.4	$h(ave.) \simeq 36.3$
	16.3	36.7	88.9	17.8	
	16.6	38.1	86.9	18.0	$p_a = 29.2$
	16.9	37.8	86.9	17.9	
	17.5	35.0	90.3	17.2	
	21.5	41.5	80.5	18.2	
	22	39.8	81.9	17.8	
	22.33	34.7	88.3	16.7	
	22.58	36.6	86.4	17.25	
	23.5	43.5	78.0	18.5	
	34.33	35.0	88.5	16.9	
	34.67	35.7	88.0	17.1	
	36.84	35.2	89.5	17.2	
	37.16	37.4	87.7	17.9	
	37.5	35.4	89.5	17.25	
	37.9	35.7	89.1	17.35	
	38	36.3	88.7	17.6	
	38.4	36.5	88.1	17.55	
	38.74	37.0	87.4	17.65	
	39.05	35.7	89.1	17.35	
	39.38	36.2	88.3	17.45	
	39.8	37.7	86.6	17.8	
	40.15	37.3	87.2	17.75	

Series	p_a	h	ΔT	Other Parameters
1_A	10.4	88	164	
	28.4	191	109	$T_m \simeq 220$
	44.0	365	71.5	
	86.2	660	46.7	$k_m \simeq 79$
	157	1030	33.8	
	310	2080	19.1	$E_m \simeq 10^7$
	518	4090	10.6	
	759	5310	8.6	
	986	7960	5.9	

Series	p_a	Loading h	Loading ΔT	Unloading h	Unloading ΔT	Other Parameters
2_A	10.4	219	113	238	115	
	44.0	513	65.8	518	68.3	$T_m \simeq 238$
	86.2	821	44.9	-	-	
	157	1330	30.9	1320	33.1	$k_m \simeq 82$
	310	2300	19.4	2400	20.0	
	518	4520	10.6	4130	11.9	$E_m \simeq 10^7$
	759	5670	8.8	6500	7.8	
	986	7940	6.4	-	-	
3_A	10.4	32	274	-	-	
	28.4	68	220	94	193	$T_m \simeq 238$
	67	138	162	228	122	
	157	428	80	623	60.6	$k_m \simeq 81.8$
	310	1140	36.4	1480	28.8	
	518	2270	19.9	3300	14.0	$E_m \simeq 10^7$
	759	3850	12.2	4650	10.3	
	986	5240	9.2	-	-	
4_A	10.4	46	237	-	-	
	28.4	98.5	184	140.8	156	$T_m \simeq 238$
	67	224	119	-	-	
	157	695	52.9	1010	39.4	$k_m \simeq 82.0$
	310	1860	23.1	-	-	
	518	3150	14.6	4470	10.4	$E_m \simeq 10^7$
	759	5000	9.5	-	-	
	986	6700	7.1	-	-	
5_A	10.4	38.2	253	-	-	
	28.4	133	161	214	118	$T_m \simeq 240$
	67	476	69.3	-	-	
	157	1220	32.5	1260	32.4	$k_m \simeq 82.0$
	310	2450	17.6	-	-	
	518	4160	10.7	4700	9.8	$E_m \simeq 10^7$
	759	6500	6.9	-	-	
	986	9500	5.0	-	-	
6_A	10.4	54	238	-	-	
	28.4	213	128	218	127	$T_m \simeq 235$
	67	440	78.8	-	-	
	157	762	52.5	786	51.5	$k_m \simeq 82$
	310	1270	34.5	-	-	
	518	1970	23.4	1950	23.8	$E_m \simeq 10^7$
	759	2780	17.0	-	-	
	986	3740	12.9	-	-	

Series	p_a	Loading h	Loading ΔT	Unloading h	Unloading ΔT	Other Parameters
7_A	10.4	212	90	-	-	
	28.4	452	63	527	61.1	T_m - 235
	67	632	51.4	-	-	
	157	1120	33.3	1220	32.7	k_m - 85
	310	1880	22.0	-	-	
	518	2640	16.6	2790	16.2	E_m - 10^7
	759	3380	13.6	-	-	
	986	4280	11.0	-	-	
8_A	157	1440	30.7	1350	33.7	T_m - 225
	518	3260	15.1	-	-	
	986	6580	8.0	-	-	k_m - 96
						E_m - 10^7